
Analysis of Cosmological models through Dynamical System

Thesis submitted

by

Santanu Das

Index No: 38/18/Maths./25

for the degree of Doctor of Philosophy (Ph.D.)

in Science



Department of Mathematics

Jadavpur University

Kolkata, India

August, 2025

Certificate from the Supervisor

This is to certify that the thesis entitled “**Analysis of Cosmological models through Dynamical System**” submitted by **Santanu Das**, who got his name registered on February 12, 2018 (Index No.: 38/18/Maths./25) for the award of Ph.D. (Science) degree of Jadavpur University, is absolutely based upon his own work under my supervision and that neither this thesis nor any part of it has been submitted for either any degree/ diploma or any other academic award anywhere before.

Nilanjana Mahata
07.08.2025

Dr. Nilanjana Mahata

Department of Mathematics

Jadavpur University

Kolkata-700032, India

Associate Professor
Department of Mathematics
Jadavpur University
Kolkata - 700032
West Bengal

Declaration from the Author

I solemnly declare that this thesis is the product of my independent research, conducted at the Department of Mathematics, Jadavpur University, Kolkata - 700032, India. I further affirm that no part of this work has been submitted for the attainment of any degree, diploma or academic qualification at any other institution.

The author has meticulously crafted all figures in this thesis using MatLab and Mathematica software. The manuscript has undergone rigorous scrutiny to eliminate discrepancies and typographical errors. However, despite these diligent efforts, astute readers may identify inadvertent mistakes and certain sections may appear unwarranted or imprecise. The author assumes full responsibility for any such errors arising from lapses in subject knowledge or inadvertent oversight.

Finally, I affirm that, to the best of my knowledge, all assistance utilized in the preparation of this thesis has been duly cited and acknowledged with the utmost integrity.

Santanu Das
07.08.2025

Santanu Das

This thesis is dedicated to my parents
Biplab Bijayee Das, Kalyani Das
and my elder sister
Gitashree Chanda

Acknowledgements

Completing this thesis, the result of several years of dedication, fills me with deep gratitude to all those who have inspired and supported me throughout my Ph.D. journey at Jadavpur University and at my work place, Institute of Engineering & Management, Kolkata. Writing a doctoral thesis presents a distinct set of challenges that can truly be understood only by those who have embarked on this journey themselves. Initially, I did not fully grasp the significance of the ‘Acknowledgments’ section. However, as I now reflect on this journey, I feel deeply compelled to express my sincere gratitude to all those who have extended their support and encouragement along the way.

Though a Ph.D. thesis is often viewed as a solitary endeavor, the list of individuals I mention here proves otherwise.

First and foremost, I would like to express my deepest gratitude to my respected supervisor, Dr. Nilanjana Mahata, for her invaluable guidance, unwavering support, immense patience and exceptional mentorship throughout the course of my doctoral work. Her knowledge and encouragement have been a constant source of inspiration in both my academic and personal life. There were times when I couldn’t attend our scheduled discussions and tasks, yet she always understood the situation and offered her support. Throughout my Ph.D. journey, I always felt comfortable asking her anything—no matter how trivial it might have seemed. Truly, she was more than just a teacher to me; she was a friend, a philosopher and a guide.

I am indebted to Prof. Subenoy Chakraborty of Jadavpur University and Dr. Atreyee Biswas of Maulana Abul Kalam Azad University of Technology, West Bengal for providing their invaluable inputs as the Research Advisory Committee members. I would also like to extend my sincere gratitude to Ms. Priyanka Ray, my fellow research scholar under the same supervisor, for her collaboration on a research paper. I would like to convey my heartfelt appreciation to Mr. Goutam Mandal of North Bengal University, Mr. Shriton Hembrom and Mr. Azizur Rahaman of Jadavpur University for their valuable support and assistance.

I am deeply thankful to my family—my parents, elder sister, brother-in-law and niece for their unwavering support, love and affection throughout this journey. I would like to thank my late grandfather, who was my first teacher and sadly, could not witness the completion of my Ph.D.

I am deeply grateful to Dibyasree Guha for her unwavering support, both at my workplace and during my time at Jadavpur University, particularly during the difficult and stressful phases of my Ph.D. journey. I am also grateful to Dr. Tina De and Dr. Ruchira Mukherjee, whose support has been as heartfelt as that of close relatives. Their warmth and care made me feel as if they were part of my own family. I would like to express my sincere gratitude to Dr. Satyajit Chakrabarti, Founder of IEM and Dr. Satyajit Chakrabarti, Director of IEM for welcoming me into their esteemed institution as a faculty member and considering me a part of their academic community. I am profoundly thankful to Dr. Prabir Kumar Das, Dr. Samapika Das Biswas, Dr. Anubhab Ray, Dr. Jeet Sen, Dr. Sharmistha Ghosh, Dr. Biswadip Basu Mallik, Dr. Satavisha Dey, Dr. Emona Datta, Dr. Arnab Basu, Paramita Sengupta and Dr. Ayan Panja for their valuable guidance, motivation and consistent support at my workplace. I would like to acknowledge the encouragement and motivation kindly provided to me by Dr. Kamakhya Prasad Ghatak and Dr. Saktipada Nanda of IEM.

I am deeply grateful to all my teachers throughout my secondary, higher secondary, college and university education whose guidance and wisdom have been instrumental in bringing me to where I am today.

I would also like to acknowledge the support I received from my friends Kalyan, Barun and Arka as well as my cousins Shuvam and Agniva during difficult times and challenging phases. Furthermore, I extend my heartfelt gratitude to all my relatives, friends and everyone around me whose names I could not mention explicitly.

“Imagination is more important than knowledge. For knowledge is limited whereas imagination embraces the entire world.”

–Dr. Albert Einstein

“Man needs his difficulties because they are necessary to enjoy success.”

–Dr. A. P. J. Abdul Kalam

“Arise, awake and stop not till the goal is reached.”

–Swami Vivekananda

Abstract

In this thesis, we have considered a flat homogeneous and isotropic FLRW model of universe. We have investigated here the qualitative behavior of cosmological models by deploying dynamical system tools. To study the cosmological models, one needs to solve the field equations pertaining to the respective cosmological models which are not always possible analytically as the field equations form a complex system of non linear differential equations. Therefore, by deploying dynamical system method, we have converted the field equations obtained from respective cosmological models into a system of autonomous differential equations. Critical points from an autonomous system of differential equations have been computed in order to study the qualitative nature of the system around those points. Stability of the hyperbolic critical points are thoroughly analyzed with special attention to stable critical points as the nature of the cosmological models around those points depicts our universe as global attractor.

In chapter-1, we have discussed key cosmological components as well as various theoretical models which have been developed earlier to explain the observational evidences.

In chapter-2, we have reviewed the components of dynamical system method briefly along with various techniques, used to analyze the stability of the critical points. We have showed how autonomous system of differential equations can be framed from the field equations pertaining to a cosmological model.

In chapter-3, we have considered a conformally coupled massless scalar field in semi-classical gravity where matter is represented by a quantum field in curved spacetime, while gravity is described by the classical spacetime metric, governed by Einstein's field equations. Here, matter content in the gravitational field equations is expressed as the expected value of the energy-momentum tensor operator in a given quantum state, thereby incorporating quantum effects of matter on the classical geometry. The dark energy component is modeled as a massless, conformally coupled scalar field. By employing this setup, evolution equations have been derived and reformulated into an autonomous system through the introduction of appropriate dimensionless variables. Subsequently, by performing a dynamical systems analysis, stability properties of the universe near the critical points have been analyzed. The cosmological implications around these critical points have been explored.

In chapter-4, we have considered non-minimally coupled $f(Q)$ gravity model. Some challenges have been observed in the framework of General Relativity to address the late time acceleration of the universe. To address this issue, geometric components of general gravity have been modified. One such approach is to change the geometric components of general gravity where gravitational interaction is denoted by Q , Q being the non metricity. Here, we have considered the linear combination of two functions of Q , namely $f_1(Q) = \alpha Q^n$, $n \neq 1$ and $f_2(Q) = Q$ where α is a constant. Forming the autonomous system, we have analyzed stable state of universe using dynamical system tools. These techniques help us to study the behavior of the universe under several circumstances. We have studied the stability around critical points and considering the recent observational data available for some cosmological parameters, feasible solutions are noted.

Lastly, we have studied Rényi holographic dark energy model where a new idea of dark energy has been studied depending on the holographic principle of quantum gravity, called as the holographic dark energy(HDE). Later on modifying Bekenstein-Hawking entropy, different generalized entropies have been proposed, one of them being Rényi entropy which leads to Rényi holographic dark energy model (RHDE). We have considered RHDE model with Hubble horizon as the IR cut off and have studied the cosmological behaviour under non interacting, linear and non-linear interacting scenarios with the help of dynamical systems analysis. We have also investigated the stability of the system around hyperbolic critical points along with the type of fluid description, evolution of equation of state parameter as well as matter and energy density parameters.

List of Publications

The work of this thesis has been carried out at the Department of Mathematics, Jadavpur University, Kolkata-700032, India. This thesis is based on the following published papers.

- **Cosmological implications of non-minimally coupled $f(Q)$ gravity**
Santanu Das, Nilanjana Mahata, and Priyanka Ray
Modern Physics Letters A, Vol. 39, No. 12, 2450017 (2024)
doi:<https://doi.org/10.1142/S0217732324500172>
arXiv:2410.02318 (gr-qc)
- **Conformally coupled massless scalar field in semi-classical gravity and its cosmological consequences**
Santanu Das and Nilanjana Mahata
EPJ Web of Conferences, Volume 325 (2025)
doi:<https://doi.org/10.1051/epjconf/202532501013>
- **Phase space analysis of Rényi Holographic dark energy model**
Santanu Das and Nilanjana Mahata
General Relativity and Gravitation, Vol. 57, No. 120 (2025)
doi:<https://doi.org/10.1007/s10714-025-03454-6>
arXiv:2507.21549 (gr-qc)

List of Figures

2.1	Figure in the left shows that C_1 is an unstable node, C_2 is a stable node and C_3 is a saddle while the figure in the right shows that P_1 is a stable focus/spiral.	45
3.1	Phase plot corresponding to the critical point $A_1(1, 0)$ and $B_1(-1, 0)$ in (\bar{H}, \bar{Y}) plane	61
3.2	Phase plot corresponding to the critical point A and B with $\omega = -0.85$ in $(\bar{H}, \bar{\rho})$ plane	61
3.3	Phase plot corresponding to the critical point A and B with $\omega = -1.25$ in $(\bar{H}, \bar{\rho})$ plane	62
4.1	Phase plot corresponding to the point $(0, 0)$ for $q = -0.53$, $n = 20$, $\omega = -0.4$ which shows that for the choices of aforesaid values of q , ω and n , $(0, 0)$ is locally stable node	72
4.2	Phase plot corresponding to the point $(0, 0)$ for $q = -0.48$, $n = 3$, $\omega = -0.87$ (P_6 in table 4.2) which shows that for the choices of aforesaid values of q , ω and n , $(0, 0)$ is locally unstable node.	73
4.3	Phase plot corresponding to the point $(-0.1305, 0)$ (P_{11} in table 4.3) for $q = -0.53$, $n = 2$, $\omega = -0.8$ which shows that for the choices of aforesaid values of q , ω and n , $(-0.1305, 0)$ is a saddle node.	74
4.4	Phase plot corresponding to the point $(0.2695, 0)$ for $q = -0.48$, $n = 10$, $\omega = -0.87$ which shows that for the choices of aforesaid values of q , ω and n , $(0.2056, 0)$ is locally stable node.	75
4.5	Phase plot corresponding to the point $(0, -0.4194)$ (P_{24} in table 4.4) for $q = -0.53$, $n = 5$, $\omega = -0.7$ which shows that for the choices of aforesaid values of q , ω and n , $(0, -0.4194)$ is an unstable node.	76
4.6	Phase plot corresponding to the point $(0, 0.4748)$ (P_{25} in table 4.4) for $q = -0.48$, $n = 2$, $\omega = -0.75$ which shows that for the choices of aforesaid values of q , ω and n , $(0, 0.4748)$ is locally stable node.	77
4.7	Phase plot presenting the behaviour of the trajectories for the model when $n = 2$ and $q_0 = -0.55$ which shows that A is unstable, B is stable and C is a saddle node for the aforesaid values of the parameter.	79
4.8	Phase plot presenting the behaviour of the trajectories for the model as $n = 3$ and $q_0 = -0.55$ which shows that A is unstable, B is stable and C is stable node for the aforesaid values of the parameter.	80

5.1	Phase plot corresponding to the point $(0, 1)$ for $\alpha = 0.2, \beta = -0.1$. .	91
5.2	Phase plot corresponding to the point $(0, 1)$ for $\alpha = 0.02, \beta = 0.5$. .	91
5.3	Phase plot corresponding to the point $(0, 1)$ for $\alpha = -0.2, \beta = -2.5$.	92
5.4	Phase plot corresponding to the point $(0, 1)$ for $\alpha = -0.02, \beta = -0.75$	93
5.5	Evolution of cosmological parameters corresponding to the point $(0, 1)$ for $\alpha = 0.2, \beta = -0.25$	93
5.6	Phase plot corresponding to the point $(0, 1)$ for $\alpha = 2, \beta = 1$	95
5.7	Phase plot corresponding to the point $(0, 1)$ for $\alpha = 0.25, \beta = -0.75$	95
5.8	Evolution of cosmological parameters corresponding to the point $(0, 1)$ for $\alpha = 0.25, \beta = -0.75$	96
5.9	Phase plot corresponding to the point $(1, 0)$ for $\alpha = 4, \beta = 0.25$. . .	99
5.10	Phase plot corresponding to the point $D_1(\frac{3}{2}, -\frac{1}{2})$ and $D_2(\frac{3}{7}, \frac{4}{7})$ for $\alpha = \frac{2}{3}, \beta = 3$	100
5.11	Phase plot corresponding to the point $D_1(-\frac{3}{2}, \frac{5}{2})$ and $D_2(\frac{1}{3}, \frac{2}{3})$ for $\alpha = 5, \beta = 2$	100
5.12	Phase plot corresponding to the point $E_1(-1, 2)$ and $E_2(\frac{1}{3}, \frac{2}{3})$ for $\alpha =$ $4.5, \beta = 0$	103
5.13	Phase plot corresponding to the point $E_1(-\frac{1}{2}, \frac{3}{2})$ and $E_2(\frac{3}{8}, \frac{5}{8})$ for $\alpha = 6, \beta = -2$	104
5.14	Phase plot corresponding to the point $F_1(0, 0)$ for $\alpha = 2, \beta = -3$. .	106
5.15	Phase plot corresponding to the point $F_2(0, 1)$ for $\alpha = -1, \beta = 4$. .	107
5.16	Phase plot corresponding to the point $F_2(0, 1)$ for $\alpha = -1, \beta = -1$.	107
5.17	Evolution of cosmological parameters near $F_2(0, 1)$ for $\alpha = -1, \beta = 0.2$	108
5.18	Phase plot corresponding to the point $G(\frac{4}{3}, -\frac{16}{3})$ for $\alpha = 4, \beta = 1$. .	111
5.19	Phase plot corresponding to the point $G(\frac{3}{2}, -\frac{9}{2})$ for $\alpha = -6, \beta = -2$.	111

List of Tables

1.1	Classification of Future Singularities in FLRW Universe	34
3.1	Critical points and their corresponding eigenvalues for the autonomous system (3.11).	59
3.2	Critical points and their corresponding eigenvalues for the autonomous system (3.13).	60
4.1	Set of critical points and corresponding eigenvalues.	71
4.2	For $q = -0.53$, $q = -0.48$ and for $n=2, 3, 4, 5, 6$, this table shows eigenvalues corresponding to the critical point $(0, 0)$	71
4.3	For $q = -0.53$, $q = -0.48$ and for $n=2, 3, 4, 5, 6$, this table shows the eigenvalues corresponding to the critical point $(\frac{1.22\epsilon+\omega}{\omega}, 0)$	73
4.4	For $q = -0.53$, $q = -0.48$ and for $n=2, 3, 4, 5, 6$, this table shows the eigenvalues corresponding to the critical point $(0, 0.33\epsilon - 0.67\epsilon n + 1)$	76
4.5	Critical points corresponding to autonomous system (4.29), (4.30).	78
4.6	Eigenvalues corresponding to critical points A, B and C and the respective value of ω at those points.	79
5.1	Set of critical points and their coordinates.	90
5.2	Critical points and their corresponding eigenvalues, obtained from the linearized Jacobian matrix.	90
5.3	Set of critical points and their coordinates.	94
5.4	Critical points and their corresponding eigenvalues, obtained from the linearized Jacobian matrix.	94
5.5	Set of critical points and their coordinates.	98
5.6	Eigenvalues and the value of other cosmological parameters corresponding to D_1 for different choices of α and β	98
5.7	Eigenvalues and the value of other cosmological parameters corresponding to D_2 for different choices of α and β	99
5.8	Set of critical points and their coordinates.	102
5.9	Eigenvalues and the values of other cosmological parameters corresponding to E_1 for different choices of α and β	102
5.10	Eigenvalues and the values of other cosmological parameters corresponding to E_2 for different choices of α and β	103

5.11	Set of critical points and their coordinates.	105
5.12	Eigenvalues pertaining to all critical points of autonomous system (5.58).	106
5.13	Set of critical points and their coordinates.	110
5.14	Eigenvalues corresponding to G for different choices of α and β	110

Contents

Certificate from the Supervisor	i
Declaration From the Author	ii
Acknowledgements	iv
Abstract	vii
List of Publications	ix
List of Figures	x
List of Tables	xii
Contents	xiv
1 Introduction to cosmology and various cosmological models	1
1.1 Cosmology	1
1.1.1 Observational evidences and Big Bang theory	2
1.1.2 Cosmological Principle	5
1.1.3 Friedmann–Lemaitre–Robertson–Walker(FLRW) Cosmology and corresponding evolution equations	6
1.1.4 Dynamics of the universe with a perfect fluid	9
1.2 Cosmological models and key cosmological components	11
1.2.1 Semiclassical gravity	11
1.2.2 Ordinary matter and dark matter	12
1.2.3 Dark Energy	13
1.2.4 Cosmological Constant	14
1.2.4.1 Fine-tuning problem	14
1.2.4.2 Coincidence Problem	15
1.2.5 Modified matter model	15
1.2.5.1 Quintessence	16
1.2.5.2 k-essence	17
1.2.5.3 Phantom dark energy	18

1.2.5.4	Dilatonic dark energy	19
1.2.5.5	Unified dark energy and matter: Chaplygin gas . . .	19
1.2.5.6	Coupled dark energy and matter	20
1.2.6	Holographic dark energy	21
1.2.6.1	Kaniadakis holographic dark energy	22
1.2.6.2	Barrow holographic dark energy	22
1.2.6.3	Tsallis holographic dark energy	23
1.2.6.4	Rényi holographic dark energy	24
1.2.6.5	Sharma-Mittal holographic dark energy	25
1.2.7	Modified Gravity Theory	26
1.2.7.1	$f(R)$ Gravity	27
1.2.7.2	$f(R, T)$ gravity.	28
1.2.7.3	Gauss-Bonnet gravity.	29
1.2.7.4	Scalar tensor Gravity Theory	30
1.2.7.5	$f(T)$ Gravity	31
1.2.7.6	$f(Q)$ gravity theory	31
1.2.7.7	$f(Q, T)$ gravity theory	32
1.2.8	Future singularities and the fate of the universe	33
2	Dynamical system analysis in cosmology	36
2.1	Introduction	36
2.2	Dynamical system: Basic framework	38
2.2.1	Methods of stability analysis around critical points	40
2.2.2	Linear stability method and Hartman-Grobman theorem . . .	40
2.2.3	Classification of critical points	43
2.2.4	Stable, unstable and center manifold	45
2.2.5	Lyapunov's stability method	46
2.2.6	Center manifold theory	47
2.2.7	Asymptotic behaviour in plane	50
2.2.8	Asymptotic behaviour in higher dimension	51
2.3	Formulation of an Autonomous Dynamical System: An Example . . .	52
3	Dynamical system analysis on conformally coupled massless scalar field in semiclassical gravity	55
3.1	Introduction	55
3.2	Semiclassical dynamical equations in conformally coupled massless scalar field	57
3.3	Dynamical system analysis in semiclassical gravity for a conformally coupled massless scalar field	58
3.4	Summary and discussion	62
4	Dynamical system analysis on non-minimally coupled $f(Q)$ gravity	64

4.1	Introduction	64
4.2	Basic tools of $f(Q)$ gravity	66
4.3	Implementation of $f(Q)$ gravity in FLRW spacetime	68
4.4	Formation of autonomous system and stability analysis by dynamical system approach	69
4.4.1	Autonomous system with equation of state parameter	70
4.4.2	Autonomous system with equation of state parameter in terms of dimensionless variables	77
4.5	Summary and discussion	80
5	Dynamical system analysis on Rényi holographic dark energy	82
5.1	Introduction	82
5.2	Introduction of Rényi entropy in holographic dark energy	84
5.3	Basic equations	85
5.4	Rényi holographic dark energy model with Hubble horizon as IR cut off (without interaction)	87
5.4.1	Analysis of non-interacting Rényi HDE with $\lambda(x, y) = \alpha x + \beta y$	89
5.4.2	Analysis of non-interacting Rényi HDE with $\lambda(x, y) = e^{\alpha x + \beta y}$	93
5.5	Rényi holographic dark energy model with Hubble horizon as IR cut off (with interaction)	96
5.5.1	Analysis of interacting Rényi HDE with linear interaction $Q = 3H(\rho_m + \rho_d)$	97
5.5.2	Analysis of interacting Rényi HDE with linear interaction $Q = 3H\rho_d$	101
5.5.3	Analysis of interacting Rényi HDE with linear interaction $Q = 3H\rho_m$	104
5.5.4	Analysis of interacting Rényi HDE with non-linear interaction $Q = 3H\frac{\rho_d}{\rho_m + \rho_d}$	108
5.6	Summary and discussion	112
6	Discussion and future direction	115
	Bibliography	118

Chapter 1

Introduction to cosmology and various cosmological models

1.1 Cosmology

Cosmology is derived from the Greek word *cosmos* meaning the study of the universe. Cosmology involves the scientific investigation of the universe's large-scale features with a central aim of understanding its overall structure, origin and long-term evolution across vast cosmic distances and timescales. Since the dawn of human civilization, there has been an enduring curiosity about the origin of the universe and its further evolution. For centuries, our understanding was limited to some basic facts. However, over the past few decades, a revolution has occurred—thanks to precise astronomical observations, scientists have been able to measure key cosmological parameters with increasing accuracy. As a result, a range of theoretical models have emerged that agree with these measurements, helping to unify and deepen our understanding of the universe's origin, structure and evolution [1, 2].

Einstein's General Theory of Relativity [3] forms the cornerstone of theoretical cosmology. Proposed by Albert Einstein and Willem de Sitter in 1917, it provides the fundamental framework for understanding the dynamics of the universe, where gravity plays the dominant role in shaping its evolution [4, 5, 6].

Our contemporary comprehension of the universe is predominantly shaped by the hot Big Bang theory, which elucidates the cosmic evolution from its origin to the

present epoch. Contrary to the earlier steady state hypothesis which posited a static and eternal universe, the Big Bang framework asserts that the universe is dynamic and continuously evolving. The discovery of the universe's expansion stands out as one of the most profound and influential achievements in modern cosmology.

1.1.1 Observational evidences and Big Bang theory

The universe, as we observe it, is made up of stars, galaxies and larger structures such as galaxy clusters and super clusters. For much of human history, our understanding of these cosmic elements relied solely on visible light. However, a transformative development in the 20th century enabled researchers to investigate the universe across the entire electromagnetic spectrum. Modern observational tools now permit the detection of various forms of electromagnetic radiation—ranging from radio waves and microwaves to infrared, ultraviolet, X-rays and gamma rays. Each type of radiation offers unique insights, allowing us to construct a far more comprehensive view of the cosmos than what was possible using visible light alone.

Observational evidences have laid the foundation for the modern study of cosmology. The following discoveries serve as its guiding pillars.

- **Expansion of Space:** Galaxies are observed to be receding from one another through the redshift of light wave and velocities are increasing with distance which is an effect, first documented by Edwin Hubble in 1929 [7], establishing the concept of an expanding universe.
- **Cosmic Microwave Background (CMB):** A uniform microwave radiation field detected in 1965 by A. Penzias [8] across the sky, represents the leftover light from the universe's early, hot and dense phase.
- **Primordial Nucleosynthesis:** Light elements like hydrogen, helium and trace amounts of lithium formed within minutes after the Big Bang. The predicted abundances align well with current measurements. It was first explained by George Gamow in 1940 [9].
- **Formation of Structure:** Initial little irregularities in matter density grew under gravity over billions of years, giving rise to galaxies, clusters and cosmic filaments observed today.

These series of observations established hot Big Bang as the preferred cosmological model of the universe from an initial state of extreme density and temperature [10]. The redshift which was observed, considered as the reason of recession of the cosmic objects, paved the path to conclude that the universe is expanding [11]. The concept of an expanding universe was first rigorously introduced by physicist Alexander Friedmann [12] and Georges Lemaître [13] in 1920s which gained strong observational support after Hubble's observations [7] of galaxies in 1930s which showed a systematic increase of redshift with distance. Later on, in the late 20 century, a series of observational evidences [14, 15, 16, 17, 18, 19, 20, 21, 22, 23, 24, 25, 26, 27, 28] have rigorously vouched for a universe with accelerated expansion.

Owing to the concept of expanding nature of the universe, history of universe has been studied in different epochs starting from a hot dense phase to expansion till it reached to a space time singularity where all the laws of classical physics become invalid. This singularity is termed as "Big Bang".

- **Planck Time** ($t < 10^{-43}s$): In the first phase of cosmic history, the universe was so dense and hot that our current physics breaks down. All known forces are believed to have been unified during this phase. Describing this period requires a theory of quantum gravity, which remains elusive.
- **Era of Grand Unification** ($10^{-43}s$ to $10^{-36}s$): As the universe cooled slightly, gravity likely split from the other interactions. Soon after, the strong nuclear force emerged as a distinct entity, marking a key phase transition in the early universe.
- **Epoch of Inflation** ($10^{-36}s$ to $10^{-32}s$): A rapid burst of expansion dramatically increased the universe's size in an instant. This inflationary process helped to address key cosmological puzzles, like the horizon and flatness problems.
- **Electroweak Phase** ($10^{-32}s$ to $10^{-12}s$): Further cooling led to the separation of the electroweak interaction into the weak nuclear force and electromagnetism. The elementary particles that define the standard model started becoming prominent.

- **Quark-Dominated Stage** ($10^{-12}s$ to $10^{-6}s$): The universe was filled with high-energy particles including free quarks and gluons. It was too hot for these quarks to form stable particles like protons or neutrons.
- **Hadron Formation Phase** ($10^{-6}s$ to $1s$): As temperatures dropped, quarks combined to form hadrons such as protons and neutrons. Matter-antimatter collisions were frequent but a slight imbalance left a residue of ordinary matter.
- **Lepton-Dominated Interval** ($1s$ to $10s$): With most hadrons annihilated, light particles such as electrons and neutrinos took center stage. Around this time, neutrinos stopped interacting significantly with other particles and began free-streaming.
- **Photon Era** ($10s$ to $\sim 380,000$ years): The universe was a glowing plasma where photons were constantly scattered by electrons and ions, keeping the cosmos opaque.
- **Recombination** ($\sim 380,000$ years): Atoms began forming as electrons attached to nuclei, allowing photons to travel freely. These ancient photons form the Cosmic Microwave Background we observe today.
- **Cosmic Dark Ages** ($\sim 380,000$ to ~ 150 million years): In the absence of stars, the universe was filled with neutral hydrogen and no sources of visible light. This era lasted until the first luminous objects formed.
- **Epoch of Reionization** (~ 150 million to 1 billion years): Radiation from the first stars and galaxies reionized the neutral hydrogen, ending the cosmic dark ages and making the universe transparent once more.
- **Development of Stars and Galaxies** (1 billion years to present): Stars and galaxies evolved into complex systems. Gravity sculpted large-scale structures from earlier matter distributions, forming the observable universe.
- **Dark Energy Era** (~ 5 billion years ago to now and beyond): The influence of dark energy is considered as one of the important factor for universe's accelerating expansion.

These epochs can be divided in four groups :

- **Quantum gravity epoch:** This epoch is considered to be present during plank time. In this phase all fundamental forces - gravity, electromagnetism, the weak nuclear force and the strong nuclear force were unified into a single fundamental force. The energy of the universe was around 10^{19} *Gev*. At such high energy all laws of physics broke down and quantum effects of gravity became significant. Classical General Relativity may no longer be valid during this time.
- **Inflationary epoch:** Previously discussed era of grand unification, epoch of inflation, electroweak phase can be clustered as the inflationary epoch. In this epoch, gravity separated from unified forces and emerged as a very strong force. Semi classical theory of gravity can explain this epoch where matter source is considered as quantum field and gravity as classical. We have discussed such type of cosmological model in our thesis.
- **Pregalactic epoch:** Quark dominated stage, hadron formation phase, lepton dominated interval, photon era, recombination, cosmic dark ages, epoch of reionization can be grouped into this epoch. In this epoch there were two phases. One is pre-decoupling period when matter is ionized as well as it is strongly interacting with radiation through Thompson scattering and another is post-decoupling period when matter and radiation evolve independently.
- **Postgalactic epoch:** This epoch consists of development of stars and galaxies and dark energy era.

The physics of these last two epochs is relatively well understood and together they provide us the core of hot Big Bang model which provides us a direction towards explaining various facts [29] about our own universe and scope of thorough analysis of observational data. At the same time two earlier epochs are under robust study though the physics at those times are not well understood.

1.1.2 Cosmological Principle

It is usually assumed that the evolution of universe is governed by the Einstein field equations during Post-galactic, Pre-galactic and Inflationary epoch. When

Friedman, Lemaitre and others had studied the expanding nature of the universe in 1920s and 1930s [12, 13], they assumed their mathematical models as simple as possible. They had considered the space time geometry as homogeneous and isotropic in large scale structure. These assumptions called as *Cosmological Principle*, characterizes the Robertson, Walker [30, 31] geometry which collectively with Einstein field equations leads to *Friedman-Lemaitre-Robertson-Walker(FLRW)* cosmological models. This cosmological principle is the basis of Big Bang cosmology.

Homogeneity and Isotropy: In modern physical cosmology, the cosmological principle posits that the Universe is homogeneous and isotropic on a large scale. “Homogeneous” signifies that the Universe lacks any preferred or distinguished location, meaning it appears uniform regardless of observer’s position. “Isotropic” indicates that no particular direction is favoured, implying that the Universe looks the same in every direction. The phrase “large scales” refers to vast distances of approximately 100 megaparsecs (Mpc) or greater, where these principles hold true [32, 33]. On smaller scales, the Universe exhibits neither uniformity nor directional symmetry. It is also important to note that homogeneity does not inherently imply isotropy. There are adequate evidences for the isotropy and homogeneity for the observable universe. The conclusive probe for the isotropy is the uniformity of the temperature of CMBR. Similarly, inhomogeneities in the density of the universe would lead to temperature anisotropies (In this regard, CMBR is a very powerful tool).

1.1.3 Friedmann–Lemaitre–Robertson–Walker(FLRW) Cosmology and corresponding evolution equations

The evolution of the Universe is governed by the Einstein field equations which are in general complicated non-linear equations that establish a connection between the geometry of space time and distribution of matter within the universe. They possess a simple analytical solution under the assumption of symmetry. Friedmann-Lemaitre-Robertson-Walker(FLRW) metric which describes the space time geometry, is based upon the cosmological principle on large scale structure. If we observe our nearby environment, we see stars, galaxies, cluster of galaxies which represent the highly inhomogeneity in the universe that is ignored at large scales. The FLRW metric can

be written in terms of invariant geodesic as

$$ds^2 = g_{\mu\nu} dx^\mu dx^\nu \quad (1.1)$$

where $\mu, \nu = 0, 1, 2, 3$ in four dimensions. In spherical coordinate system (r, θ, ϕ) (1.1) can be explicitly written as

$$ds^2 = -dt^2 + a^2(t) \left[\frac{dr^2}{1 - \kappa r^2} + r^2(d\theta^2 + \sin^2\theta d\phi^2) \right] \quad (1.2)$$

There are only two variables in the above metric, namely, $a(t)$ which represents the scale factor that measures the size of the universe, while κ symbolizes the scalar curvature. κ describes the spatial geometry of the universe. $\kappa = 1$ corresponds to a closed Universe, $\kappa = -1$ characterizes an open Universe and $\kappa = 0$ signifies a flat Universe. Depending on the dynamics, evolution of the universe may vary. Universe may expand forever when $\kappa < 0$, re-collapses in future when $\kappa > 0$ or approach in between asymptotically while $\kappa = 0$.

Einstein's field equation takes the form

$$G_{\mu\nu} = \kappa T_{\mu\nu} \quad (1.3)$$

where

$$G_{\mu\nu} = R_{\mu\nu} - \frac{1}{2}g_{\mu\nu}R \quad (1.4)$$

Here, $R_{\mu\nu}$ is the Ricci tensor which depends on the metric, $T_{\mu\nu}$ is the energy momentum tensor which describes the matter distribution. Here, R represents the Ricci scalar, a fundamental quantity that describes the curvature of space-time, defined through the contraction of the Ricci tensor.

$$R = R_{\mu\nu}g^{\mu\nu} \quad (1.5)$$

So, in (1.3), left hand part describes the geometry connected to gravity and right hand part describes the matter, energy distribution.

Hubble's parameter H which is a very essential cosmological parameter describes the rate of expansion of the universe. It is denoted in terms of scale factor as

$$H = \frac{\dot{a}}{a} \quad (1.6)$$

where \dot{a} is the change of scale factor with respect to time.

Another important parameter is also used in place of scale factor which is denoted by z and defined as

$$z = \frac{\lambda_0}{\lambda_e} - 1 = \frac{a_0}{a_e} - 1 \quad (1.7)$$

where λ_e is the wavelength of a photon emitted at time t_e when the scale factor is $a(t_e) = a_e$ and is observed today ($t = t_0$) with the present scale factor $a_0 = a(t_0)$ at wavelength λ_0 . A longer wavelength refers to redshift.

According to Weyl's postulate, the matter distribution in the universe is modeled as a perfect fluid, characterized by an energy-momentum tensor of the form:

$$T_{\mu\nu} = (\rho + p)u_\mu u_\nu + pg_{\mu\nu} \quad (1.8)$$

where u_μ is fluid velocity in space time, ρ and p are density and pressure of the fluid respectively. Einstein field equation in (1.3) provides two independent equations for a non flat model ($\kappa \neq 0$):

$$3H^2 + \frac{3\kappa}{a^2} = 8\pi G\rho, \quad (1.9)$$

$$2\dot{H} + 3H^2 + \frac{\kappa}{a^2} = -8\pi Gp. \quad (1.10)$$

where H is the Hubble parameter, G is the Newton's gravitational constant, ρ and p denote the total energy density and thermodynamic pressure. These equations are known as Friedmann equations. The conservation of the energy-momentum tensor gives rise to the continuity equation

$$\nabla_\mu T^\mu_\nu = 0. \quad (1.11)$$

From above equation, we derive

$$\dot{\rho} + 3H(p + \rho) = 0. \quad (1.12)$$

From (1.12), we can understand that the Hubble's parameter which stands for expansion of the universe can change energy density. (1.12) can also be derived from (1.9) and (1.10), which indicates that out of three equations (1.9), (1.10) and (1.12), any two are independent. By eliminating $\frac{\kappa}{a^2}$ from equations (1.9) and (1.10), we

obtain the following result.

$$\frac{\ddot{a}}{a} = -\frac{4\pi G}{3}(3p + \rho) . \quad (1.13)$$

The term $\frac{\ddot{a}}{a}$ denotes the acceleration of the expansion.

If $(3p + \rho) > 0$, then $\frac{\ddot{a}}{a} < 0$, indicating that the universe is decelerating . Conversely, if $(3p + \rho) < 0$, then $\frac{\ddot{a}}{a} > 0$, signifying that the universe is accelerating.

Matter for which $(3p + \rho) > 0$, satisfies the strong energy condition, is classified as normal matter. Conversely, matter that violates the strong energy condition is referred to as exotic matter.

The first Friedmann equation (1.9) can be expressed as follows

$$\Omega(t) = 1 + \frac{\kappa}{a^2 H^2} , \quad (1.14)$$

Here $\Omega(t) \equiv \frac{\rho}{\rho_c}$ is defined as the dimensionless density parameter, where $\rho_c = \frac{3H^2}{8\pi G}$ is the critical density.

From the equation (1.14), we can conclude:

$$\begin{aligned} \Omega(t) > 1 &= \rho > \rho_c \implies \kappa = +1 , \\ \Omega(t) < 1 &= \rho < \rho_c \implies \kappa = -1 , \\ \Omega(t) = 1 &= \rho = \rho_c \implies \kappa = 0 . \end{aligned} \quad (1.15)$$

Thus, we can categorize the geometry of the Universe based on the distribution of matter.

$$q = - \left(1 + \frac{\dot{H}}{H^2} \right) . \quad (1.16)$$

The deceleration parameter, denoted as q , is a dimensionless quantity. A negative value of q ($q < 0$) signifies that the universe is accelerating, while a positive value ($q > 0$) indicates that the universe is decelerating.

1.1.4 Dynamics of the universe with a perfect fluid

Assuming that the universe is filled with a perfect fluid, we consider pressure as a single valued function of density, i.e., $p = p(\rho)$. Equation of state parameter is

defined as

$$\omega = \frac{p}{\rho} \quad (1.17)$$

where, the equation of state parameter ω is assumed to be constant. It is directly related to the evolution of the energy density and consequently, to the expansion of the universe.

Using the equation of state parameter from equation (1.17) into the Friedmann equations (1.9) and (1.10), one can obtain the following results.

$$H = \frac{2}{3(1+\omega)(t-t_0)}, \text{ when } \kappa = 0 \quad (1.18)$$

$$a(t) \propto (t-t_0)^{\frac{2}{3(1+\omega)}} . \quad (1.19)$$

$$\rho \propto a^{-3(1+\omega)} . \quad (1.20)$$

Here t_0 is the integrating constant. The above solution is valid for $\omega \neq -1$.

For a universe dominated by radiation, where the equation of state parameter $\omega = \frac{1}{3}$, the evolution of the universe is fundamentally governed by radiation pressure.

$$\begin{aligned} \rho &\propto a^{-4} , \\ a &\propto (t-t_0)^{\frac{1}{2}} . \end{aligned} \quad (1.21)$$

For a universe dominated by dust, where the equation of state parameter $\omega = 0$, the evolution is primarily driven by matter, with gravitational attraction playing a dominant role in shaping the expansion during this phase as pressure becomes negligible.

$$\begin{aligned} \rho &\propto a^{-3} , \\ a &\propto (t-t_0)^{\frac{2}{3}} . \end{aligned} \quad (1.22)$$

In the stiff fluid era, equation of state parameter $\omega = 1$, the dynamics are dominated by an extremely rigid equation of state, where the pressure equals the energy density, resulting in the most intense and non-relativistic behaviour possible for any

cosmological fluid.

$$\begin{aligned}\rho &\propto a^{-6}, \\ a &\propto (t - t_0)^{\frac{1}{3}}.\end{aligned}\tag{1.23}$$

1.2 Cosmological models and key cosmological components

After considering Big Bang model as the viable option to explain the expansion of universe, different theoretical models have been proposed to study the evolution of universe and different cosmological phenomena. Within the framework of FLRW geometry and using Einstein field equations, derived Friedmann equations helped scientists to propose different theoretical cosmological models [34, 35, 36].

1.2.1 Semiclassical gravity

To study the evolution of universe before plank time, quantum gravity [37, 38, 39] is considered to be the most useful tool. One approach to incorporate quantum gravity is introduction of canonical quantum gravity which can be imposed by applying normal quantization methods to Einstein field equations but this approach suffers from both the technical and conceptual point of view. As a result, it is common to adopt a semiclassical approach [40, 41, 42, 43, 44, 45, 46, 47] in which gravity is described by classical general relativity while matter fields are treated using quantum theory. This method offers a more tractable framework that still captures certain aspects of quantum gravitational effects. Though semiclassical gravity theory is complicated and also is not applicable near Plank time but it can be widely applied in explaining the inflation era and future singularity [48, 49]. It is believed to be essential in early stages of black hole evaporation [50, 51] in the semiclassical regime of quantum gravity.

Semiclassical gravity theory has two parts: quantum field theory in spacetime and semiclassical Einstein equation. Semiclassical theory describes the effect of quantum field as the source of gravity. Matter part in the Einstein field equation feels the effect

of quantum field theory which propagates in spacetime and impacts the classical Einstein equation through the expected value of the stress energy tensor. As a result, Einstein field equation in semiclassical gravity is transformed into

$$G_{\mu\nu} = 8\pi G \langle T_{\mu\nu} \rangle \quad (1.24)$$

where $G_{\mu\nu}$ is the Einstein tensor, G is the Newton gravitational constant, $\langle T_{\mu\nu} \rangle$ denotes the expected value of stress-energy tensor.

The manner in which the matter sector is treated leads to a modification of equation (1.24). For example, if the matter part is considered as quantized scalar field [52] in which the state vector is considered as $\psi(\phi)$ where ψ is the quantum state and ϕ is the scalar field, satisfies the Schrödinger equation

$$i\partial_t\psi(\phi, t) = \hat{H}\psi(\phi, t) \quad (1.25)$$

where the Hamiltonian operator \hat{H} depends on the spacetime metric g and the metric satisfies Einstein field equation

$$G_{\mu\nu}(g) = 8\pi G \langle \psi | T_{\mu\nu}(\phi, g) | \psi \rangle \quad (1.26)$$

Semiclassical gravity provides accurate predictions as long as the stress-energy tensor's quantum fluctuations [53] remain modest—that is, when deviations from its expectation value are sufficiently small. Under such conditions, the influence of these fluctuations on the classical spacetime geometry is minimal, allowing the semiclassical Einstein equations to hold effectively. Mathematically when,

$$\langle T_{\mu\nu}(x)T_{\gamma\delta}(y) \rangle = \langle T_{\mu\nu}(x) \rangle \langle T_{\gamma\delta}(y) \rangle \quad (1.27)$$

1.2.2 Ordinary matter and dark matter

Matter component of the universe can be classified into two parts, namely ordinary baryonic matter and dark matter. Baryonic matter is the type of matter which are strongly interactive carrying a conserved quantum number which is known as baryon number. This type of matter made up with protons, neutrons and electrons. In universe, stars, planets, gas, dusts which are visible or otherwise are referred to

as baryonic matter where baryons include protons, neutrons and electrons which are most important part of ordinary matter but negligible in terms of mass compared to protons and neutrons. Current estimate of baryonic matter density is $\Omega_b = 0.04$ [54, 55]. This estimate comes from CMB power spectrum [22, 28] and Big-Bang nucleosynthesis [9, 56] from which we also came to know that all the baryons in the universe can not provide us the observed amount of matter.

As a matter of fact, most of the matter must be in the form of non-baryonic dark matter which is simply called as dark matter [2, 57, 58] due to its gravitational pull. It is non-interacting and does not emit or reflect light. There are two types of dark matter; hot relativistic and cold non relativistic. Between them there is another type of dark matter which is called as warm dark matter. Cold dark matter(CDM) is most important in forming the large scale structure of universe such as galaxies or cluster of galaxies.

1.2.3 Dark Energy

An equally mysterious and important cosmological component like dark matter is dark energy. Numerous observational evidences like large scale structure(LSS) [59, 60, 61], cosmic microwave background radiation(CMBR) [21, 28, 62, 63], type Ia supernova [14, 15, 20, 64, 65] suggest that our universe is experiencing an accelerated expansion. The matter density of the universe accounts for approximately one-third of the critical density required for a spatially flat universe. To combat with this situation two schools of thoughts are there. One of which is the modification of the matter part in Einstein equation by incorporating an exotic matter known as dark energy.

The nature of the dark energy is characterized by negative pressure which is very puzzling and still unknown to us. Unlike baryonic and cold dark matter, at all scales, dark energy remains unclustered. Later on, different models of dark energy [66, 67, 68, 69, 70, 71] will be discussed in this literature.

1.2.4 Cosmological Constant

The cosmological constant, Λ [66, 72] and the cold dark matter (Λ CDM) model are frequently employed as candidates for dark energy (DE) [69, 72, 73, 74, 75, 76]. It was first introduced by Einstein while he was interested to find a static solution. So, he modified (1.3) as

$$R_{\mu\nu} - \frac{1}{2}g_{\mu\nu}R + \Lambda g_{\mu\nu} = 8\pi G T_{\mu\nu} \quad (1.28)$$

here Λ , a new parameter, is termed as the cosmological constant. With this modification the Friedmann equations (1.9) and (1.10) are transformed into

$$\begin{aligned} H^2 &= \frac{8\pi G}{3}\rho - \frac{K}{a^2} + \frac{\Lambda}{3} \\ \frac{\ddot{a}}{a} &= -\frac{4\pi G}{3}(3p + \rho) + \frac{\Lambda}{3} \end{aligned} \quad (1.29)$$

After Edwin Hubble's groundbreaking observation that the universe is expanding, the importance of introducing Λ for static model of universe was postponed. Later on, it was again introduced to explain late time acceleration [66, 72, 77]. The cosmological constant was assumed to be the vacuum energy density. The vacuum was considered as a perfect fluid with equation of state $\frac{p_\Lambda}{\rho_\Lambda} = -1$. Here

$$\rho_\Lambda = \frac{\Lambda}{8\pi G} \quad \text{and} \quad p_\Lambda = \frac{-\Lambda}{8\pi G} \quad (1.30)$$

Besides being the basic standard dark energy model, known as Λ CDM (cold dark matter) with very significant alignment with observational data, it suffers from two significant limitations and the cosmological constant is not widely accepted as a robust model for dark energy. These two major issues are the (i) fine-tuning problem [78, 79] and (ii) the coincidence problem [78, 80, 81].

1.2.4.1 Fine-tuning problem

Recent cosmological observations have confirmed that the cosmological constant is a non-zero quantity, with its measured value

$$\rho_\Lambda = \frac{\Lambda}{8\pi G} = 10^{-47} \text{GeV}^4. \quad (1.31)$$

According to quantum field theory, the expected value of the cosmological constant is extraordinarily large, approximately $10^{74} GeV^4$. However, this theoretical estimate widely deviates from observed value, creating a major discrepancy. This mismatch represents one of the most critical and unresolved issues with the cosmological constant.

1.2.4.2 Coincidence Problem

Recent observational evidence suggests that the energy density of the cosmological constant i.e., vacuum energy density and matter density are comparable. Specifically, if the energy density of the cosmological constant is denoted as ρ_Λ and that of matter as ρ_m , we find that $\rho_\Lambda \propto \rho_m$. This implies we are in a unique epoch of the universe's evolution, where the energy densities of both matter and the cosmological constant are approximately equal. This phenomenon is referred to as the Coincidence Problem, prompting the question of why these densities coincide precisely at this particular moment in cosmic history.

1.2.5 Modified matter model

To address the challenges faced by the Λ CDM model in explaining the late-time acceleration of the Universe, some physicists have proposed modifications in the matter part of Einstein's field equations, i.e., introducing exotic matter and modification in the energy momentum tensor $T_{\mu\nu}$ in General Relativity and this modified matter part serves as a possible source of dark energy.

The simplest choice of matter source has been considered as the scalar fields which naturally arise in particle physics including string theory. These can act as the source of dark energy and help in developing dynamical dark energy models.

In the literature, a variety of such models has been discussed which include quintessence [73, 82, 83, 84, 85, 86, 87, 88, 89], k-essence [90, 91, 92, 93, 94, 95], phantom [96, 97, 98, 99, 100, 101], dilatonic dark energy [102], unified dark energy and matter model like chaplygin gases [103, 104, 105, 106], coupled dark energy and matter model [107, 108, 109, 110, 111, 112, 113, 114, 115, 116, 117, 118, 119, 120, 121, 122].

1.2.5.1 Quintessence

Quintessence refers to a dynamic form of dark energy, modelled as a time-dependent scalar field that gradually evolves by slowly rolling down its potential towards a minimum. It is described by a scalar field ϕ , which is minimally coupled to gravity. Action of quintessence is given by

$$S = \int d^4x \sqrt{-g} \left[\frac{1}{16\pi G} R - \frac{1}{2} (\nabla\phi)^2 - V(\phi) \right] \quad (1.32)$$

Varying the action (1.32) with respect to ϕ in FLRW flat spacetime, the equation of motion in an expanding universe is given by

$$\ddot{\phi} + 3H\dot{\phi} + \frac{dV}{d\phi} = 0 \quad (1.33)$$

The energy density of the scalar field is denoted as the sum of kinetic, gradient and potential energies

$$\rho_\phi = \frac{1}{2}\dot{\phi}^2 + V(\phi) + \frac{1}{2}(\nabla\phi)^2 \quad (1.34)$$

where $\frac{1}{2}\dot{\phi}^2$ is the kinetic energy and $V(\phi)$ is the potential energy. The energy momentum tensor is obtained by varying (1.32) with respect to $g^{\mu\nu}$ as

$$T_{\mu\nu} = -\frac{2}{\sqrt{-g}} \frac{\delta S}{\delta g^{\mu\nu}} \quad (1.35)$$

Assuming a homogeneous field ($\nabla\phi \approx 0$) for simplicity, the energy density and pressure corresponding to scalar field becomes

$$\begin{aligned} \rho_\phi &= \frac{1}{2}\dot{\phi}^2 + V(\phi) \\ p_\phi &= \frac{1}{2}\dot{\phi}^2 - V(\phi) \end{aligned} \quad (1.36)$$

The equation of state parameter is denoted by

$$\omega_\phi = \frac{p_\phi}{\rho_\phi} = \frac{\frac{1}{2}\dot{\phi}^2 - V(\phi)}{\frac{1}{2}\dot{\phi}^2 + V(\phi)} \quad (1.37)$$

(1.37) always implies that the equation of state for the scalar field lies in between $(-1, 1)$, i.e., $-1 < \omega_\phi < 1$. For late time acceleration, $\omega_\phi < -\frac{1}{3}$. This in turn implies

$\dot{\phi}^2 < V(\phi)$. Hence, the scalar potential should be flat enough for the scalar field to undergo slow-roll evolution. It is same as the case in inflationary cosmology. During the radiation or matter dominated epochs, the energy density of matter significantly exceeds that of dark energy, i.e., $\rho_m \gg \rho_\phi$. For dark energy to become dominant at late times, its energy density must evolve in a manner that tracks that of radiation or matter during earlier epochs. The existence of such a tracking solution critically depends on the specific form of the scalar potential $V(\phi)$.

Quintessence models are broadly classified into two categories. The first is known as the freezing model [84, 89], in which the equation of state parameter gradually decreases towards -1 . The second category is referred to as the thawing model [123, 124, 125, 126] where the equation of state parameter starts close to -1 initially and increases at late times but remains below $-\frac{1}{3}$ to drive acceleration.

1.2.5.2 k-essence

The quintessence model is based on a canonical scalar field characterized by the standard kinetic energy term $\frac{1}{2}\dot{\phi}^2$ and a potential energy $V(\phi)$ in the action. However, by modifying the canonical kinetic term to a non-canonical form, one can account for the effects of exotic matter with negative pressure without necessarily invoking a potential term [90, 91, 92, 93].

The action is defined here as

$$S = \int d^4x \sqrt{-g} \left[\frac{1}{16\pi G} R + p(\phi, X) \right] \quad (1.38)$$

where $X = -\frac{1}{2}(\nabla\phi)^2$ is the canonical kinetic energy of the field ϕ and Lagrangian density $p(\phi, X)$ corresponds to a pressure. In most of the k-essence models $p(\phi, X)$ takes the form $p(\phi, X) = f(\phi)p(\hat{X})$, primarily motivated by insights from string theory.

For certain choices of the kinetic and potential functions, k-essence models can naturally track the evolution of the total radiation energy density during the radiation-dominated epoch. Then it transits to an approximately constant behaviour as the matter-dominated era begins. However, achieving desirable evolution generally requires a finely tuned kinetic term.

1.2.5.3 Phantom dark energy

Recent observational evidences suggest that, the current value of equation of state parameter nearly varies around -1 [127, 128, 129, 130, 131]. In previously discussed scalar field models, equation of state parameter is greater than -1, i.e., $\omega > -1$. But the dark energy model which violets weak energy condition with $\omega < -1$ is termed as phantom dark energy. Specific models in braneworld [132] or Brans-Dicke gravity can lead to phantom energy. Phantom fields were originally proposed within Hoyle's formulation [133] of the steady-state cosmological model. To comply with the cosmological principle and maintain a uniform matter density despite the universe's expansion, Hoyle introduced a "creation field" responsible for continuously generating matter in the regions, left empty by cosmic expansion. It was further modified and reconstructed in Hoyle and Narlikar theory of gravity [134].

Here, action is defined by simply considering a scalar field with negative kinetic energy.

$$S = \int d^4x \sqrt{-g} \left[\frac{1}{16\pi G} R + \frac{1}{2} (\nabla\phi)^2 - V(\phi) \right] \quad (1.39)$$

Here, sign of the kinetic term is opposite compared to (1.32). Energy and pressure density is defined by

$$\begin{aligned} \rho_\phi &= -\frac{1}{2} \dot{\phi}^2 + V(\phi) \\ p_\phi &= -\frac{1}{2} \dot{\phi}^2 - V(\phi) \end{aligned} \quad (1.40)$$

The equation of state parameter is denoted by

$$\omega_\phi = \frac{p_\phi}{\rho_\phi} = \frac{\frac{1}{2} \dot{\phi}^2 + V(\phi)}{\frac{1}{2} \dot{\phi}^2 - V(\phi)} \quad (1.41)$$

Hence, we get $\omega_\phi < -1$ for $\dot{\phi}^2 < V(\phi)$. A universe filled with phantom dark energy shows some interesting properties [135, 136, 137, 138, 139]. In a universe dominated by phantom energy, the curvature becomes infinitely large within a finite duration. This scenario is accompanied by a divergence in the Hubble parameter, indicating that the expansion rate of the universe becomes infinite in finite time. Such a divergence stems from the unbounded growth of the phantom energy density which approaches a singularity in a limited time span. This culminates in a catastrophic

event known as the Big Rip, where spacetime curvature becomes singular, signaling the breakdown of classical General Relativity. Phantom fields typically suffer from significant ultraviolet (UV) instabilities at the quantum level. Due to the fact that their energy density is unbounded below, the vacuum becomes unstable, allowing spontaneous production of ghost particles along with conventional energy fields [136].

1.2.5.4 Dilatonic dark energy

Phantom fields which involve a negative kinetic term, are often associated with significant quantum instabilities. Since our primary interest lies in ultraviolet (UV) vacuum instabilities, it is reasonable to adopt a Minkowski background when examining quantum fluctuations as UV effects are dominant at high energies and short distances. In this context, the dilatonic ghost condensate model [102] serves as a useful framework for analysis where we assume pressure

$$p = -X + ce^{\lambda\phi} X^2 \quad (1.42)$$

where X is kinetic term, c is positive constant. This framework is inspired by dilatonic higher-order corrections to the tree-level action found in the low-energy effective theory of string theory [140]. It is typically assumed that, in the relevant limit $\phi \rightarrow \infty$, the dilaton effectively decouples from the gravitational sector.

1.2.5.5 Unified dark energy and matter: Chaplygin gas

Up to this point, we have explored various scalar field models. Another compelling approach involves a unified framework in which both dark matter and dark energy are described simultaneously at the background level. Kamenshchik. et. al [103] has proposed the chaplygin gas model wherein the pressure p of the perfect fluid is related to its energy density by

$$p = -\frac{A}{\rho^\alpha} \quad (1.43)$$

where A is a positive constant. When $\alpha > 0$, the pressure remains negligible compared to the energy density during the early stages of cosmic evolution. However, at later times, the negative pressure becomes significant, enabling the onset of cosmic

acceleration. Thus, a fluid obeying the Chaplygin gas equation of state effectively transitions from behaving like pressureless matter in the early universe to exhibiting dark energy-like properties in the late universe.

1.2.5.6 Coupled dark energy and matter

An alternative approach to address the coincidence problem involves introducing an interaction between dark matter and dark energy. Given that their energy densities are of the same order in the current epoch, it is plausible to explore possible couplings between these two dark components. Numerous investigations have been conducted in this context [107, 108, 109, 110, 111, 112, 113, 114, 115, 116, 117, 118, 119, 120, 121, 122, 141, 142]. One of the noteworthy features of interacting dark energy models is the possibility of achieving a scaling solution that can also support accelerated cosmic expansion.

Currently, the Universe is predominantly governed by dark matter and dark energy whereas the ordinary (baryonic) matter contributes only a minor fraction. As dark energy exhibits repulsive gravitational effects in contrast to the attractive nature of other matter components, any interaction between dark matter and dark energy is generally assumed to be weak. However, observational evidences such as data from the Cosmic Microwave Background (CMB) and large-scale matter distribution support the viability of models incorporating such interactions [143, 144, 145, 146, 147, 148, 149].

With the involvement of interactions, continuity equations become

$$\begin{aligned}\dot{\rho}_m + 3H(1 + \omega_m)\rho_m &= Q \\ \dot{\rho}_\phi + 3H(1 + \omega_\phi)\rho_\phi &= -Q\end{aligned}\tag{1.44}$$

Here ρ_m and ρ_ϕ are the dark matter and dark energy density respectively. ω_m and ω_ϕ are the equation of state parameters corresponding to dark matter and dark energy respectively. Dot denotes the derivative with cosmic time and Q is the parameter, denoting interchange between dark matter and dark energy. $Q > 0$ indicates a flow from dark energy to dark matter and $Q < 0$, a flow from dark matter to dark energy. For different dark energy models, a comparative study can be done between

a model having interaction and one without interaction between dark matter and dark energy by choosing different forms of Q .

1.2.6 Holographic dark energy

The holographic dark energy (HDE) models [150, 151, 152, 153, 154, 155, 156, 157] present an alternative framework for addressing the challenges associated with dark energy. It is derived from the holographic principle [158] in quantum gravity, which asserts that the physical degrees of freedom within a system are determined by its boundary area rather than its volume. This concept leads to a connection in quantum field theory between a short-distance (ultraviolet) cutoff and a long-distance (infrared) cutoff.

When extended to cosmology, this IR cutoff is interpreted as a characteristic cosmological length scale and the holographic principle then implies that the energy contained in a region must not exceed that of a black hole with the same volume. Mathematically

$$\rho_d \leq M_p^2 L^{-2} \quad (1.45)$$

where ρ_d is the energy density of dark energy, M_p is reduced plank mass, L is the size of the region, i.e., IR cut off. Usually from effective field theory the energy density can be written as [151, 154]

$$\rho_d = \frac{3M_p^2 c^2}{L^2} \quad (1.46)$$

c being the dimensionless parameter. Therefore, the selection of the IR cutoff is pivotal in defining the holographic energy density. Multiple choices of IR cut offs have been considered in different HDE models including the Hubble radius ($L = H^{-1}$), particle horizon ($L = R_p = a \int_0^t \frac{dt'}{a(t')}$), future event horizon ($L = R_h = a \int_t^\infty \frac{dt'}{a(t')}$), the Granda–Oliveros (GO) cutoff ($L^{-2} = \alpha H^2 + \beta \dot{H}$), and the Ricci scalar curvature cutoff ($L^{-2} \propto R$ where $R = -6(\dot{H} + 2H^2)$).

In this present literature, we discuss several HDE models such as the Kaniadakis, Tsallis, Barrow and Rényi HDE models. These models can be studied under both non-interacting scenarios and scenarios involving interactions between dark energy and dark matter, providing a broad perspective on their dynamical behaviours and implications for late-time cosmic acceleration.

1.2.6.1 Kaniadakis holographic dark energy

The basic idea behind Kaniadakis holographic dark energy [159, 160, 161, 162] is the introduction of Kaniadakis entropy which is nothing but one parameter generalized classical entropy which is defined by Kaniadakis [163, 164] as

$$S_K = -k_B \sum_i p_i \ln_{\{k\}}(p_i) \quad (1.47)$$

where k_B is the Boltzman constant and $\ln_{\{k\}}(x) = \frac{x^k - x^{-k}}{2k}$. This entropy is distinguished by dimensionless parameter K where $-1 < k < 1$ where $\lim k \rightarrow 0$ gives back the classical entropy. Kaniadakis entropy can be redefined by

$$S_K = -k_B \sum_i^w \frac{p_i^{1+k} - p_i^{1-k}}{2k} \quad (1.48)$$

where p_i and w are the probability of a specific microstate of the system and the total number of possible configurations respectively. When applied within the black hole framework, it leads to

$$S_k = \frac{1}{k} \text{Sinh}(k) S_{BH} \quad (1.49)$$

where S_{BH} is the standard Bekenstein-Hawking entropy. By considering future event horizon R_E as the IR cut off from the essence of basic holographic dark energy inequality (1.45), Kaniadakis holographic dark energy density can be defined as

$$\rho_d = \frac{3M_p^2 c^2}{R_h^2} + k^2 M_p^6 R_h^2 \quad (1.50)$$

1.2.6.2 Barrow holographic dark energy

Barrow holographic dark energy model [165, 166, 167, 168, 169, 170, 171, 172] is dependent on Barrow entropy which was proposed by Barrow where he introduced a new form of entropy with quantum gravitational effect. This can exhibit intricate and fractal features of black hole and therefore this complex structure provides finite volume with finite or infinite area and hence a deformed expression of black-hole

entropy. Modified entropy defined by Barrow [173] is

$$S_B = \frac{A^{1+\frac{\Delta}{2}}}{A_0} \quad (1.51)$$

where A and A_0 are the standard horizon area and Plank area respectively. Δ is a new parameter which is introduced here to define quantum gravitational deformation with $\Delta = 0$ giving back the usual Bekenstein-Hawking entropy and $\Delta = 1$ corresponds to most intricate and fractal structure. Hence the range of the parameter Δ is in between 0 and 1. By using inequality (1.45) and (1.51), Barrow holographic dark energy density can be written as

$$\rho_d = CL^{\Delta-2} \quad (1.52)$$

where C is a parameter with dimension $L^{-2-\Delta}$. With future event horizon as the IR cut off (1.52) can be rewritten as

$$\rho_d = CR_h^{\Delta-2} \quad (1.53)$$

1.2.6.3 Tsallis holographic dark energy

Tsallis holographic dark energy [174, 175, 176, 177] is a different form of holographic dark energy which relies on Tsallis entropy [178, 179]. The conventional Boltzmann–Gibbs additive entropy, founded on the hypothesis of weak probabilistic correlations and their connection to ergodicity, has been extended to a non-additive entropy formalism. This generalization is known as Tsallis entropy. It satisfies the property that the entropy of the whole system is not necessarily the sum of the entropies of its subsystems.

$$S_T = k \frac{1 - \sum_{i=1}^w p_i^q}{q - 1} \quad (1.54)$$

where w is the total number of configuration, p_i is the associate probabilities, q is any real constant and k is any positive constant. $\lim_{q \rightarrow 1}$ gives back the conventional Boltzmann-Gibbs entropy.

The non extensive entropy [180] can be expressed as

$$S_T = \gamma A^\delta \quad (1.55)$$

where $A \propto L^2$ is the area of the system with length L , the parameter γ is a constant and δ is the non additivity parameter associated to the dimension of the system d with one important choice of the d being $\delta = \frac{d}{d-1}$ for $d > 1$ as defined in [181]. Bekenstein entropy can be obtained from (1.55) for $\delta = 1$. By using inequality (1.45) and (1.55), Tsallis holographic dark energy density can be expressed as

$$\rho_d = BL^{2\delta-4} \quad (1.56)$$

where B is a parameter with dimension $L^{-2\delta}$.

By considering Hubble radius as the IR cut off (1.56) can be re written as

$$\rho_d = BH^{-2\delta+4} \quad (1.57)$$

1.2.6.4 Rényi holographic dark energy

Rényi holographic energy model [177, 182] is connected to Rényi entropy [183, 184]. For a system of w discrete states, it is defined by

$$S_R = k \frac{\ln \sum_{i=1}^w p_i^q}{1-q} \quad (1.58)$$

where q is a non extensive parameter [181, 185], k is a positive constant and p_i is the probability for i th state. Rényi entropy reduces to standard Boltzmann- Gibbs entropy for $\lim q \rightarrow 1$. Using Tsallis entropy defined in (1.54) and (1.58), we obtain a relation between Tsallis entropy and Rényi entropy as

$$S_R = \frac{1}{\delta} \ln(1 + \delta S_T) \quad (1.59)$$

where $\delta = 1 - q$ is a parameter which measures whether the system is non-additive [178] or not. By deducing (1.59) by Biro et al. [186], it was shown that when formal logarithmic transformations are applied to generalized thermodynamic quantities,

the resulting expressions exhibit additive behaviour. These transformed forms continue to follow the conventional laws and relationships of standard thermodynamics. To calculate the Rényi entropy related to black hole [187, 188, 189, 190], Tsallis entropy is considered as formal Bekenstein-Hawking entropy. As a result (1.59) is redefined as

$$S_R = \frac{1}{\delta} \ln(1 + \delta S_{BH}) \quad (1.60)$$

where S_{BH} is Bekenstein-Hawking entropy which is denoted as

$$S_{BH} = \frac{k_B c^3 A}{4\hbar G} \quad (1.61)$$

where k_B , c , A , \hbar , G are respectively Boltzmann constant, speed of light, area of the black hole horizon, reduced plank constant and Newton's gravitational constant. By considering in natural units where $k_B = \hbar = c = G = 1$, it simplifies to:

$$S_{BH} = \frac{A}{4} \quad (1.62)$$

By assuming $A = 4\pi L^2$, where L is the IR cut off and using (1.62), (1.60) is rewritten as

$$S_R = \frac{1}{\delta} \ln(1 + \pi\delta L^2) \quad (1.63)$$

Now, by using the thermodynamic relation

$$TdS_R \propto \rho_d dV \quad (1.64)$$

$$\rho_d = \frac{3d^2}{8\pi L^2} (1 + \pi\delta L^2)^{-1} \quad (1.65)$$

where d is a constant, δ is the non-extensive Rényi parameter and L is the IR cutoff. By considering Hubble horizon as the IR cut off, (1.65) can be redefined as

$$\rho_d = \frac{3d^2 H^4}{8\pi(\pi\delta + H^2)} \quad (1.66)$$

1.2.6.5 Sharma-Mittal holographic dark energy

A new form of entropy was developed by Sharma and Mittal [191, 192] which is nothing but the generalization of Tsallis and Rényi entropy. Using this, a new

holographic dark energy model was proposed which is known as Sharma-Mittal holographic dark energy [193, 194]. Sharma-Mittal entropy [190, 195] is defined as

$$S_{SM} = k \frac{(\sum_{i=1}^w p_i^{1-\delta})^{\frac{1-r}{\delta}} - 1}{1-r} \quad (1.67)$$

where r is a free parameter. Tsallis and Rényi entropies defined in (1.54) and in (1.58) can be obtained from (1.67) by considering $\lim r \rightarrow 1 - \delta$ where $\delta = 1 - q$ and $\lim r \rightarrow 1$ respectively.

The relation between Tsallis and Sharma-Mittal entropy can be written as

$$S_{SM} = \frac{1}{R} ((1 + \delta S_T)^{\frac{R}{\delta}} - 1) \quad (1.68)$$

where R is a parameter defined as $R = 1 - r$. Now, for black hole we consider Tsallis entropy as Bekenstein-Hawking entropy S_{BH} and as a result (1.68) changes to

$$S_{SM} = \frac{1}{R} ((1 + \delta S_{BH})^{\frac{R}{\delta}} - 1) \quad (1.69)$$

Now by assuming (1.62), $A = 4\pi L^2$, where L is the IR cut off, (1.69) modifies to

$$S_{SM} = \frac{1}{R} ((1 + \delta \pi L^2)^{\frac{R}{\delta}} - 1) \quad (1.70)$$

By using thermodynamic relation in (1.64), inequality in (1.45) and Hubble horizon as IR cut off Sharma-Mittal dark energy density can be written as

$$\rho_d = \frac{3C^2 H^4}{8\pi R} ((1 + \frac{\delta \pi}{H^2})^{\frac{R}{\delta}} - 1) \quad (1.71)$$

C^2 is a free parameter. Original HDE model can be recovered when $\lim R \rightarrow \delta$.

1.2.7 Modified Gravity Theory

General Relativity theory being the backbone of gravity theory, explains the geometric description of gravity theory. General Relativity theory is governed by the fundamental Einstein field equations which lead to Friedmann equations under the framework of FLRW spacetime. The standard Big Bang theory explains the earlier evolution of universe which was matter and radiation dominated. Afterwards, to

explain the accelerated expansion of universe, simplest Λ CDM model was proposed which faced two major problems which encouraged the scientists to modify the right hand side of Einstein field equation i.e., the matter part by introducing exotic matter with negative pressure, termed as dark energy. Another group of scientists thought of modifying the left hand side of Einstein field equation which describes the gravity part by modifying gravity [196, 197, 198, 199, 200, 201, 202, 203, 204] itself. They have tried to change the Einstein–Hilbert action term by introducing higher order curvature invariants. In general, Einstein field equation is of 2nd order but by introducing higher order curvature invariants, Einstein field equations involve higher order derivatives. As a result, extra degrees of freedom do involve in the evolution equations.

In this literature, we will discuss a few of modified gravity models namely $f(R)$ gravity [200, 205, 206, 207, 208, 209, 210], $f(R, T)$ gravity [211, 212, 213, 214, 215], $f(T)$ gravity [216, 217, 218, 219, 220], Gauss-Bonnet gravity [221, 222, 223, 224, 225, 226, 227, 228, 229, 230], Scalar-Tensor gravity theory [231, 232, 233, 234, 235], $f(Q)$ gravity [236, 237, 238, 239, 240, 241, 242], $f(Q, T)$ gravity [243, 244, 245, 246] etc.

1.2.7.1 $f(R)$ Gravity

$f(R)$ gravity is nothing but an extension of General Relativity. Instead of Ricci scalar R , a function of R is considered in the Einstein-Hilbert action. So, to recover General Relativity, in $f(R)$ gravity, function of R should be equal to the Ricci scalar itself. This variable function introduces the possibility of accounting for the accelerated expansion and structure formation of the universe without considering dark energy or dark matter [200, 206, 207, 208, 209, 210, 247]. Certain functions in this framework may be inspired by modifications, arising from quantum gravity theories. First introduced by Hans Adolph Buchdahl in 1970 [205], $f(R)$ gravity has advanced considerably over time, with significant progress driven by Starobinsky's [248] influential work on cosmic inflation.

The Einstein-Hilbert action which serves as the core of General Relativity from which the Einstein field equations are derived through the principle of least action,

gets modified as

$$S_{f(R)} = \frac{1}{16\pi G} \int f(R) \sqrt{-g} d^4x + \int \sqrt{-g} d^4x \mathcal{L}_m \quad (1.72)$$

Here, g represents the determinant of the metric tensor $g_{\mu\nu}$, R , the Ricci scalar which is obtained through the contraction of Ricci tensor $R_{\mu\nu}$ ($R = R_{\mu\nu} g^{\mu\nu}$). The term \mathcal{L}_m denotes the Lagrangian matter density. G represents the universal gravitational constant and c signifies the speed of light in vacuum.

$f(R)$ gravity theory is widely regarded as a well established framework among modified gravity theories, used to explain the current phase of cosmic acceleration.

1.2.7.2 $f(R, T)$ gravity.

$f(R, T)$ gravity model which is proposed by [211], where, in Einstein-Hilbert action, instead of Ricci scalar R , a function of Ricci scalar R and the trace of energy-momentum tensor T is considered. Einstein-Hilbert action for $f(R, T)$ gravity is modified to

$$S_{f(R,T)} = \frac{1}{16\pi G} \int d^4x \sqrt{-g} f(R, T) + \int \sqrt{-g} d^4x \mathcal{L}_m \quad (1.73)$$

Compared to $f(R)$ gravity, the use of the trace of the energy-momentum tensor, T , in modified $f(R, T)$ gravity theory [212, 213, 214] can be attributed to motivations such as the presence of exotic forms of matter or quantum effects like the conformal anomaly. Additionally, the unconventional coupling of matter and curvature might reflect deeper principles such as the idea that matter could emerge from geometric properties of spacetime or that physical forces may have a geometric origin. Since the inception of $f(R, T)$ gravity, a wide range of its features have been explored. These include investigations into its thermodynamic behaviour [249, 250], the validity of various energy conditions [251, 252] and solutions in both isotropic and anisotropic cosmological backgrounds [253]. Researchers have also examined wormhole configurations [215, 254], applied scalar field methods and analyzed scalar perturbations within the theory [255, 256].

1.2.7.3 Gauss-Bonnet gravity.

Among the various curvature invariants beyond the Ricci scalar, the Gauss–Bonnet term emerges as a particularly well motivated extension. It is defined as

$$\mathcal{G} = R^2 - 4R^{\mu\nu}R_{\mu\nu} + R^{\mu\nu\alpha\beta}R_{\mu\nu\alpha\beta} \quad (1.74)$$

In four dimension, the Gauss–Bonnet term is topologically invariant and thus does not contribute to the dynamics when linearly connected with the Lagrangian in the Einstein–Hilbert action. Modified gravity theory which is associated to the Gauss-Bonnet term is characterized as Gauss-Bonnet Gravity [221, 222].

To incorporate nontrivial dynamics

- Einstein-Hilbert action might be modified with some arbitrary functions of \mathcal{G} .
- In Einstein-Hilbert action, Gauss-Bonnet term might get coupled to some scalar field.

For the 1st instance, the action term is defined as

$$S_{GB} = \int d^4x \sqrt{-g} \left[\frac{R}{2} + f(\mathcal{G}) \right] + \int \sqrt{-g} d^4x \mathcal{L}_m \quad (1.75)$$

where R is Ricci scalar, f is an arbitrary function of Gauss-Bonnet invariant \mathcal{G} and \mathcal{L}_m is the Lagrangian matter density.

For the second case, usual Einstein-Hilbert action is modified into

$$S_{GB} = \int d^4x \sqrt{-g} \left[\frac{1}{16\pi G} R - \frac{\gamma}{2} \delta_\mu \phi \delta^\mu \phi - V(\phi) + f(\phi) \mathcal{G} \right] \quad (1.76)$$

Here G is the Newton's constant. $\gamma = \pm 1$ which takes the value 1 for canonical scalar field and -1 for phantom scalar field (when Gauss-Bonnet term is not included). $V(\phi)$ is the field potential. ϕ and \mathcal{G} are the scalar field and Gauss-Bonnet term respectively.

This modified gravity theory can be instrumental in studying the inflationary epoch, the transition from decelerated to accelerated expansion, passing solar system experimental constraints, enabling the crossing of the phantom divide line for various viable models [223, 224, 225, 226, 227]. This model acts as an alternative effective

theory of dark energy in explaining different cosmic hazards [228, 229, 230]. It has also proven valuable in the study of future singularities and the late-time acceleration of the universe [257, 258].

1.2.7.4 Scalar tensor Gravity Theory

The scalar-tensor theory is another prominent framework within modified gravitational theories [231, 232, 233, 234, 235]. Scalar-tensor gravity theories generalize General Relativity by introducing one or more scalar fields that couple to the metric tensor, effectively rendering the gravitational "constant" a dynamical quantity which can vary across space and time. This extension modifies the gravitational interaction, enabling richer phenomenology at both cosmological and astrophysical scales. Scalar-tensor theories preserve the geometric foundation of General Relativity while incorporating additional dynamical scalar degrees of freedom. This extension enriches the gravitational framework, offering greater flexibility in addressing phenomena that lie beyond the explanatory scope of Einstein's original theory. The Brans-Dicke theory emerges as a specific case within this framework, distinguished by its constant coupling parameter. Originally influential in cosmological studies [259], the scalar-tensor theory has recently gained renewed focus from researchers examining the current acceleration era [260]. Notably, this theory offers distinct advantages in addressing both the fine-tuning and coincidence problems in cosmology. The action integral governing this gravitational theory is expressed as

$$S_{ST} = \frac{1}{16\pi G} \int [f(\phi, R) - \xi(\phi)(\Delta\phi)^2] \sqrt{-g} d^4x + \int \sqrt{-g} d^4x \mathcal{L}_m \quad (1.77)$$

Here, f denotes an arbitrary function, dependent on both the scalar field ϕ and the Ricci scalar R . \mathcal{L}_m represents the matter Lagrangian, while ξ is a function explicitly tied to ϕ . Furthermore, G is Newton's gravitational constant.

This theory reverts back $f(R)$ gravity when $f(\phi, R) = f(R)$ and $\xi(\phi) = 0$. Likewise, it adopts the form of the Brans-Dicke (BD) theory by setting $f(\phi, R) = \phi R$ and $\xi(\phi) = \frac{\omega_{BD}}{\phi}$, where ω_{BD} represents the Brans-Dicke parameter. Subsequently, two field equations can be derived by varying the action with respect to ϕ and the metric tensor $g_{\mu\nu}$.

1.2.7.5 $f(T)$ Gravity

In the framework of $f(T)$ gravity [216, 217, 218, 219], like all torsional formulations, vierbein field e_μ^α is deployed which forms an orthonormal basis in the tangent space at each point on the manifold x^μ [220]. The metric is then expressed as $g_{\mu\nu} = \eta_{\alpha\beta} e_\mu^\alpha e_\nu^\beta$, where μ, ν refer to the coordinate space and α, β correspond to the tangent space. Instead of the the torsion-free Levi-Civita connection, the curvature-free Weitzenböck connection is implemented which is defined as $\Gamma_{\nu\mu}^\lambda = e_\alpha^\lambda \partial_\mu e_\nu^\alpha$ [261, 262]. Consequently, the gravitational field is characterized by the torsion tensor.

$$T_{\mu\nu}^\rho \equiv e_\alpha^\rho (\partial_\mu e_\nu^\alpha - \partial_\nu e_\mu^\alpha) \quad (1.78)$$

The Lagrangian for the teleparallel equivalent of general relativity, represented by the torsion scalar T , is obtained through the contractions of the torsion tensor, as established in [261, 262].

$$T \equiv \frac{1}{4} T^{\rho\mu\nu} T_{\rho\mu\nu} + \frac{1}{2} T^{\rho\mu\nu} T_{\nu\mu\rho} - T_{\rho\mu}{}^\rho T_\nu^{\nu\mu}. \quad (1.79)$$

Torsion scalar T can be extended as a function of torsion i.e., $f(T)$, henceforth the action for $f(T)$ gravity is defined as [263, 264]

$$S_{f(T)} = \frac{1}{16\pi G} \int d^4 x e (f(T)) \quad (1.80)$$

here, $e = \det(e_\mu^\alpha) = \sqrt{-g}$, and G is the gravitational constant, with units chosen such that the speed of light is set to 1. It is essential to note that the $f(T)$ gravity gives back General Relativity itself when $f(T) = T$. Additionally, general relativity with a cosmological constant is regained when $f(T) = T + \Lambda$.

1.2.7.6 $f(Q)$ gravity theory

In modified theories of gravity, geometric quantities play a central role in describing gravitational interactions. For instance, in $f(R)$ gravity, the Ricci scalar R , which encodes spacetime curvature, is generalized. Similarly, in $f(T)$ gravity, the torsion scalar T , arising from the Weitzenböck connection, governs the dynamics. More

recently, Jiménez et al. [265] introduced a modified gravity theory, called symmetric teleparallel $f(Q)$ gravity [266, 267], which is based on a geometry that is free of curvature and torsion but incorporates non-metricity Q [268, 269, 270]. This non-metricity scalar Q , constructed from a flat and torsionless connection, plays the role of gravitational interaction in this framework. Unlike General Relativity, which relies on the Levi-Civita connection in a Riemannian manifold (and is thus not curvature-free), symmetric teleparallel gravity redefines the gravitational interaction through a non-Riemannian but flat and torsion-free geometry.

The non-metricity tensor $Q_{\alpha\mu\nu} = \nabla_\alpha g_{\mu\nu}$ has two independent traces which are denoted as $Q_\alpha = Q^\mu{}_\alpha{}^\mu$ and $\tilde{Q}_\alpha = Q^\mu{}_{\alpha\mu}$. Then quadratic non-metricity scalar Q can be defined as

$$Q = -\frac{1}{4}Q_{\alpha\mu\nu}Q^{\alpha\mu\nu} + \frac{1}{2}Q_{\alpha\mu\nu}Q^{\mu\nu\alpha} + \frac{1}{4}Q_\alpha Q^\alpha - \frac{1}{2}Q_\alpha \tilde{Q}^\alpha \quad (1.81)$$

Therefore the action in symmetric teleparallel gravity can be written as

$$S_{f(Q)} = \int d^4x \sqrt{-g} \left[\frac{1}{2}f(Q) + \mathcal{L}_m \right] \quad (1.82)$$

where $f(Q)$ is any arbitrary function of non-metricity Q and \mathcal{L}_m is the Lagrangian matter density. Many cosmological facts like inflation, future singularity, late time acceleration have been studied based on this modified gravity theory [236, 237, 238, 239, 240, 241]. Harko et. al. [242] extended the symmetric teleparallel gravity by incorporating minimal coupling between Lagrangian matter and non metricity Q which leads to the non conservation of the energy momentum tensor. As a result, it incorporates an additional force term into the geodesic equation of motion.

1.2.7.7 $f(Q, T)$ gravity theory

Xu et. al. [243] further extended the symmetric teleparallel $f(Q)$ gravity by introducing a new modification that incorporates a non minimal coupling between nonmetricity Q and trace of energy-momentum tensor T and thus proposed a new modified theory of gravity, called as $f(Q, T)$ gravity. Here, due to coupling between Q and T , energy-momentum tensor is not being conserved. So, the gravitational term in Einstein-Hilbert action modifies to $f(Q, T)$, an arbitrary function of non-metricity Q and trace of energy-momentum tensor T and the action gets modified

to

$$S_{f(Q,T)} = \int d^4x \sqrt{-g} \left[\frac{1}{16\pi} f(Q, T) + \mathcal{L}_m \right] \quad (1.83)$$

here, \mathcal{L}_m is the Lagrangian matter density.

Xu et. al [243] have also shown that this modified gravity theory model can represent both decelerating and accelerating phases of universe as well as both early and late time evolution of the universe. Observational constraints, energy conditions, future singularity, dynamical behaviour and cosmological acceleration pertaining to modified $f(Q, T)$ model have been studied in few articles [244, 245, 246, 271, 272].

1.2.8 Future singularities and the fate of the universe

The effects of dark energy plays a very crucial role in determining the fate of the universe.

- If dark energy is defined by the Cosmological constant Λ (equation of state $\omega = -1$), the universe will continue to expand at an accelerating rate indefinitely [273, 274, 275] and thereby, cosmological horizon begins to expand after a given point of time.
- Alternatively, for dynamic dark energy with an equation of state in the range $-1 < w < -\frac{1}{3}$ such as in quintessence models or scenarios involving scalar fields, the current accelerated phase [276, 277] may eventually transition back into a decelerating, matter-dominated era. This behaviour also arises in certain braneworld models and in quintessence models with specific potential forms. In such cases, the universe may halt its expansion and begin to contract and tend towards a singularity where the scale factor vanishes and curvature invariants diverge.
- Phantom energy models characterized by $\omega < -1$ predict a future in which the energy density grows without bound. In this scenario, the expansion rate becomes so extreme that all bounded systems are eventually torn apart and the scale factor and curvature invariants diverge in finite time.

We now turn to the classification of future singularities in the context of FLRW universe, as discussed in [278, 279, 280]. Depending on the behaviour of key cosmological quantities—namely, the energy density ρ , pressure p , scale factor $a(t)$, Hubble parameter H , these singularities are categorized into distinct types as given in the table below.

TABLE 1.1: Classification of Future Singularities in FLRW Universe

Type	Time	Scale factor	Energy density	Pressure
O	$t \rightarrow 0$ (or ∞)	$a \rightarrow 0, H \rightarrow \infty$	$\rho \rightarrow \infty$	$p \rightarrow \infty$
I	$t \rightarrow t_s$	$a \rightarrow \infty$	$\rho \rightarrow \infty$	$ p \rightarrow \infty$
II	$t \rightarrow t_s$	$a \rightarrow a_s$	$\rho \rightarrow \rho_s$	$ p \rightarrow \infty$
III	$t \rightarrow t_s$	$a \rightarrow a_s$	$\rho \rightarrow \infty$	$ p \rightarrow \infty$
IV	$t \rightarrow t_s$	$a \rightarrow a_s$	$\rho \rightarrow 0$	$ p \rightarrow 0$
V	$t \rightarrow t_s$	$a \rightarrow \infty$	$\rho \rightarrow \rho_s$	$p \rightarrow p_s$

Here $\rho_s (\neq 0)$, $a_s (\neq 0)$, p_s and t_s are constants.

- Type-0 singularity is termed as Big Bang or Big Crunch singularity.
- Type-I singularity is called as “Big Rip” singularity [97, 278, 281, 282] which emerges from the phantom like equation of state $\omega < -1$.
- Type-II singularity is named as sudden singularity [279, 280] at which scale factor and energy density are finite but pressure diverges.
- Type-III singularity arises from the model where energy pressure relation is of the form $p = -\rho - A\rho^\alpha$ [283] which is different from the sudden future singularities as here energy density diverges is termed as Big freeze.
- Type-IV is a new type of singularity, named as Generalized sudden singularity which has been discussed elaborately by Nojiri et al. [278].
- Type-V singularity appears in brane-world models [284] which are known as quiescent singularity.

To address and potentially avoid the future singularities that arise in various dark energy models, several theoretical methodologies have been proposed. These include

the incorporation of quantum corrections such as conformal anomalies [285], the coupling of scalar fields to curvature or matter sectors [286, 287], the implementation of holographic dark energy (HDE) models with appropriate entropy formalisms and carefully chosen infrared (IR) cutoffs [288, 289]. Additionally, modifications to General Relativity through modified gravity theories [288, 290, 291, 292] have been extensively explored to regularize high-energy behaviour and eliminate or delay the occurrence of future singularities.

Chapter 2

Dynamical system analysis in cosmology

2.1 Introduction

The term “dynamical system” broadly refers to any physical system that evolves with time. Examples range from the simple motion of a pendulum, population dynamics with feedback mechanism and electrical RLC circuits to planetary motion and even the complex evolution of the universe itself. A dynamical system is classified as autonomous or non-autonomous depending on whether the governing equations explicitly depend on the time variable. If the system’s evolution equations are time-independent, it is termed autonomous; otherwise, it is non-autonomous.

There are two major components of dynamical system, namely

- A state space or phase space, which is the set of all possible states the system can occupy. Each point within this space uniquely defines the system at a given instant.
- A mathematical rule, usually formulated as a system of differential or difference equations, governs the time evolution of points within the state space. This rule dictates how the state of the system changes with time, starting from a given initial condition.

The Einstein field equations form the cornerstone of General Relativity, governing the dynamics of spacetime and the evolution of the universe. These equations constitute a highly complex system of non-linear differential equations which are often analytically impossible to characterize for many cosmological models. In such cases, dynamical system [293] techniques provide powerful methods for gaining qualitative insights into cosmic evolution. These techniques are applicable to both spatially homogeneous and inhomogeneous models and are particularly effective in analyzing the late-time behaviour of the universe.

By introducing suitable dimensionless dynamical variables, a given cosmological model can be reformulated as an autonomous system of differential equations in \mathbb{R}^n . This approach was pioneered by Collins in 1971 [294] and later developed extensively by Bogoyavlensky, Wainwright, Coley and others [295, 296, 297, 298, 299, 300]. Analyzing the structure of the resulting phase space, particularly through the identification and analysis of fixed points, specially future or past attractors, facilitates a deeper understanding of the asymptotic behaviour of cosmological solutions. The nature of these attractors, whether associated with early-time inflation, radiation-dominated epochs, matter-dominated eras or late-time accelerated expansion, provides essential insights into the global dynamical properties of the underlying cosmological model.

Such analyses are particularly important for assessing whether a cosmological model with complicated field equations is capable of reproducing key observational features such as the current accelerated expansion of the universe, matter-energy distribution of the universe, equation of state parameter, deceleration parameter etc. or not. During the transformation of the governing equations of a cosmological model into an autonomous system, independent variable is taken as dimensionless logarithmic time variable. This choice ensures the validity and applicability of the dynamical system formulation across different cosmic epochs, facilitating a unified treatment of the model's evolution. A normalized set of variables are also introduced for keeping the physically admissible state in a bounded region so that the dynamical system remains analytic within the region and over the boundary to prevail the asymptotic nature on the boundary.

2.2 Dynamical system: Basic framework

A dynamical system, connected to any system can be basically classified into two types:

- Continuous dynamical system where the evolution of the system is defined by differential equations which can be of two types:
 - If the state space X is finite dimensional, then the evolution of the system is defined by ordinary differential equations.
 - If the state space X is not finite dimensional, then the evolution of the system is defined by partial differential equations.
- Discrete dynamical system where the evolution of the system is governed by a map or difference equations.

In my current work, I have considered a system of autonomous ordinary differential equations which represents a continuous dynamical system defined in a finite dimensional phase space. Let us assume that $X \subset \mathbb{R}^n$ be a state space, $x \in X$ and $f : X \rightarrow X$. Then the usual autonomous system is defined on X as [301, 302, 303]

$$\frac{dx}{dt} = f(x) \quad (2.1)$$

At any point $x \in X$ and at any instant time t , $f(x)$ represents a vector field in X .

Definition 2.1. Critical point/Fixed point/ Equilibrium point/Singular point and Ordinary point: Let (2.1) be a system of autonomous ordinary differential equations where $x \in \mathbb{R}^n$. A point $x_0 \in \mathbb{R}^n$ is said to be a critical point or fixed point or equilibrium point of the system of autonomous ordinary differential equation $\dot{x} = f(x)$ if and only if $f(x_0) = 0$.

The point x_0 is termed as a *ordinary point* otherwise.

Definition 2.2. Stable critical point: Let x_0 be a fixed point of the system (2.1). It is called stable if for every ϵ we can find a δ such that if $\psi(t)$ is any solution of (2.1) satisfying $\|\psi(t_0) - x_0\| < \delta$, then the solution $\psi(t)$ exists $\forall t \geq t_0$ and it will satisfy $\|\psi(t) - x_0\| < \epsilon, \forall t \geq t_0$.

Definition 2.3. Asymptotically stable critical point: Let x_0 be a fixed point of the system (2.1). Then it is called asymptotically stable if \exists a δ such that for any solution $\psi(t)$ of (2.1), satisfying $\|\psi(t_0) - x_0\| < \delta$ implies $\lim_{t \rightarrow \infty} \psi(t) = x_0$.

A point is said to be asymptotically stable if it is stable and the solutions of the system approach the critical point as time progresses, for all initial conditions sufficiently close to it. In cosmology, almost all the stable critical points are asymptotically stable and therefore we shall not distinguish between them in our discussion. If a critical point is not stable then it is called an unstable critical point. A deep study of critical point allows us to understand the characteristics of time evolution of a dynamical system without explicitly knowing the solution for the given initial condition. Rather, we are able to find the qualitative behaviour of all the possible solutions.

Definition 2.4. Flow of a differential equation: Let us consider a system of autonomous ODE (2.1) and X be a open subset of \mathbb{R}^n such that $f \in C^1(X)$. For $x_0 \in X$, let $\phi(t, x_0)$ be a solution of (2.1) defined on its maximal interval of existence $I(x_0)$ such that $x(0) = x_0$. Then the set of mapping ϕ_t ($\phi_t : X \rightarrow X$) for $t \in I(x_0)$, defined by $\phi_t(x_0) = \phi(t, x_0)$ is called the flow of the differential equation (2.1). ϕ_t is also recognized as the flow of vector field $f(x)$.

The flow $\phi_t(x_0)$ provides us information about the position of the point x_0 in the phase space after a time t as it evolves under the dynamics governed by the vector field f . It describes the *trajectory or orbit* of the system passing through x_0 .

Definition 2.5. Orbit: For the given autonomous differential equation and the associated flow ϕ_t , the orbit through x_0 is defined as $\mathcal{O}(x_0) = \{x \in \mathbb{R}^n | x = \phi_t(x_0), t \in \mathbb{R}\}$.

The orbit through an equilibrium point or critical point is the point itself i.e., $\mathcal{O}(x_0) = \{x_0\}$ as the velocity at the equilibrium point is zero ($f(x_0) = 0 = \frac{dx}{dt}$), the state at x_0 does not change with time and hence x_0 remains unchanged with respect to the flow. That is the reason why equilibrium or critical point is also termed as the fixed point.

However, the orbit through an ordinary point is a smooth curve with the vector field f as a tangent, termed as ordinary orbit. There are a few special types of ordinary orbits, namely, periodic and recurrent.

Definition 2.6. Periodic orbit: Let x_0 be a ordinary point. The orbit $\mathcal{O}(x_0)$ is called a periodic orbit if \exists a $T > 0$ such that $\phi_T(x_0) = x_0$.

Definition 2.7. Recurrent orbit: Let x_0 be a ordinary point and $\mathcal{O}(x_0)$ be a non-periodic orbit. Then $\mathcal{O}(x_0)$ is called as a recurrent orbit if \forall neighbourhood $\mathcal{N}(x_0)$ and $\forall T \in \mathbb{R}, \exists$ a $t > T$ such that $\phi_t(x_0) \in \mathcal{N}(x_0)$.

If the flow ϕ_t has a periodic orbit of period T , the the physical system shows oscillatory behaviour and if recurrent then the system returns arbitrarily close to the earlier state.

Definition 2.8. Heteroclinic and Homoclinic orbit: An orbit which connects distinct equilibrium points is termed as heteroclinic orbit and an orbit which connects an equilibrium point to itself is known as a homoclinic orbit.

Definition 2.9. Invariant set: A set $S \subset \mathbb{R}^n$ is called an invariant set of the flow ϕ_t on \mathbb{R}^n (or corresponding to (2.1)) if $\forall x \in S$ and $t \in \mathbb{R}, \phi_t(x) \in S$.

If S is an invariant set and $x_0 \in S$ then the orbit $\mathcal{O}(x_0) \in S$ and henceforth an invariant set is a union of orbits. It means that if a trajectory starts from S then it remains in S for all time.

2.2.1 Methods of stability analysis around critical points

To analyze a dynamical system, at first, one has to identify the critical points of the system. After obtaining the critical points, to characterize the qualitative behaviour of the dynamical system, evolution of the system around the local neighbourhood of the critical points needs to be studied thoroughly. Therefore the stability of the system around those critical points is the essential point of attraction in dynamical system analysis. There are different techniques to study the stability of a dynamical system which have been discussed briefly.

2.2.2 Linear stability method and Hartman-Grobman theorem

One of the important ways to study the behaviour of the dynamical system around the critical point is linear stability theory, whose introduction enables us to study

the physical properties of most of the cosmological models with a very good understanding.

Here we linearize the system near the critical point for studying the dynamics of entire system near the point. The assumption here is that, the vector field $f(x) \in \mathbb{R}^n$ is sufficiently regular. Then we have $f(x) = (f_1(x), f_2(x), \dots, f_n(x))$ so that each $f_i(x_1, x_2, \dots, x_n)$ can be expanded in Taylor series near the critical point x_0 which produces,

$$f_i(x) = f_i(x_0) + \sum_{j=1}^n \frac{\partial f_i}{\partial x_j}(x_0)y_j + \frac{1}{2!} \sum_{j,k=1}^n \frac{\partial^2 f_i}{\partial x_j \partial x_k}(x_0)y_j y_k + \dots \quad (2.2)$$

where $y = x - x_0$. In linear stability it is sufficient to consider $f(x)$ as the C^1 function and considering only the first partial derivative, (2.2) can be rewritten as

$$f(x) \approx Df(x_0)(x - x_0) \quad (2.3)$$

where $Df(x_0)$ is the Jacobian of the vector field $f(x)$, evaluated at the critical point x_0 which is denoted by

$$J(x_0) = Df(x_0) = \frac{\partial f_i}{\partial x_j} = \begin{pmatrix} \frac{\partial f_1}{\partial x_1}(x_0) & \frac{\partial f_1}{\partial x_2}(x_0) & \cdots & \frac{\partial f_1}{\partial x_n}(x_0) \\ \frac{\partial f_2}{\partial x_1}(x_0) & \frac{\partial f_2}{\partial x_2}(x_0) & \cdots & \frac{\partial f_2}{\partial x_n}(x_0) \\ \vdots & \vdots & \ddots & \vdots \\ \frac{\partial f_n}{\partial x_1}(x_0) & \frac{\partial f_n}{\partial x_2}(x_0) & \cdots & \frac{\partial f_n}{\partial x_n}(x_0) \end{pmatrix} \quad (2.4)$$

The eigenvalues of this Jacobian matrix are evaluated for each critical point and through the characteristics of eigenvalues, linear stability of a dynamical system can be analyzed.

Let us consider an example of two dimensional autonomous system

$$\begin{aligned} \dot{x} &= f(x, y) \\ \dot{y} &= g(x, y) \end{aligned} \quad (2.5)$$

and assume that (x_0, y_0) is a critical point of (2.5). Critical point (x_0, y_0) is called a future attractor of the system if $(x(t), y(t)) \rightarrow ((x_0, y_0))$ when $t \rightarrow \infty$ and a past attractor if $(x(t), y(t)) \rightarrow ((x_0, y_0))$ when $t \rightarrow -\infty$. To linearize the system near the

critical point, we impose a small linear perturbation $\delta x, \delta y$ around the critical point, such that $x \rightarrow x_0 + \delta x, y \rightarrow y_0 + \delta y$. Thereafter, using the Taylor series expansion and ignoring the quadratic terms, we obtain a matrix equation corresponding to the system (2.5).

$$\frac{d}{dN} \begin{pmatrix} \delta x \\ \delta y \end{pmatrix} = \begin{pmatrix} \frac{\partial f}{\partial x} & \frac{\partial f}{\partial y} \\ \frac{\partial g}{\partial x} & \frac{\partial g}{\partial y} \end{pmatrix} \begin{pmatrix} \delta x \\ \delta y \end{pmatrix} \quad (2.6)$$

where $N = \ln(a)$ is the number of e-foldings which is used prominently in analysis of cosmological models.

The matrix

$$J = \begin{pmatrix} \frac{\partial f}{\partial x} & \frac{\partial f}{\partial y} \\ \frac{\partial g}{\partial x} & \frac{\partial g}{\partial y} \end{pmatrix}_{(x_0, y_0)} \quad (2.7)$$

(2.7) is called as a Jacobian matrix or linearized matrix evaluated at the critical points (x_0, y_0) .

Following the aforesaid process, (2.1) can be transformed to a linear differential equation

$$\dot{u} = Df(x_0)u \quad (2.8)$$

where $u = x - x_0$ is called the linearization of the original autonomous differential equation (2.1) at the critical point x_0 . It is assumed here that the solution of (2.8) will approximate the solution of (2.1) in the neighbourhood of the critical point x_0 . This assumption holds valid in qualitative sense through the idea of topological equivalence when the critical point is hyperbolic based on the Hartman- Grobman theorem [304, 305].

Definition 2.10. Hyperbolic critical point: For a given autonomous differential equation (2.1), a critical point x_0 is called a hyperbolic critical point if all the eigenvalues of $Df(x_0)$ (the linearized Jacobian matrix evaluated at x_0 corresponding to the system (2.1)) have non-zero real part.

Otherwise the critical point is termed as a non hyperbolic critical point.

Definition 2.11. Topologically equivalent flows: Two flows ϕ_t and $\tilde{\phi}_t$ on \mathbb{R}^n are called topologically equivalent if \exists a homeomorphism $h : \mathbb{R}^n \rightarrow \mathbb{R}^n$ which maps orbits of ϕ_t onto orbits of $\tilde{\phi}_t$, preserving their orientation.

Theorem 2.12. Hartman-Grobman: *Let us consider a differential equation $\dot{x} = f(x)$ in \mathbb{R}^n , where f is of C^1 with a flow ϕ_t . If x_0 is a hyperbolic critical point corresponding to the differential equation, then \exists a neighbourhood of x_0 in which ϕ_t is topologically equivalent to the flow of the linearization of the differential equation at x_0 .*

So, to study the stability of the system around the critical points, eigenvalues of the linearized matrix play a very important role for classification of the critical points. According to Hartman-Grobman theorem to study the qualitative behaviour of the original dynamical system it is sufficient to study the qualitative behaviour of the corresponding linearized system as both of them are equivalent whenever the critical point is hyperbolic.

As a result, for non hyperbolic critical points, this method fails to provide us any insight regarding the nature of the system around those critical points and in those cases some more methods can be imposed which have been discussed here briefly.

2.2.3 Classification of critical points

Let us consider a system of autonomous non linear differential equation defined in (2.1). Corresponding topologically equivalent system of linear ordinary differential equations can be written as (2.8). The linearized Jacobian matrix $A = Df(x_0)$ evaluated at the critical point x_0 , is a matrix with constant coefficients.

- If all the eigenvalues of A have positive real parts, the solutions in the neighbourhood of x_0 diverge from x_0 . In this case the critical point x_0 is termed as source.
- If all the eigenvalues of A have negative real parts, the solutions in the neighbourhood of x_0 converge to x_0 . In this case the critical point x_0 is termed as sink.
- A hyperbolic critical point which is neither a sink nor a source is termed as saddle as shown in figure 2.1.

As a result, it is obvious from the perspective of topological equivalence that a source and a sink in the linearized system will be a source and the sink respectively for the original non linear system under the same conditions, imposed on the sign of eigenvalues of the linearized Jacobian matrix $A = Df(x_0)$.

In most cases, the eigenvalues of the linearized system may have eigenvalues with both positive, negative and/or zero real parts. In such occasions, it is essential to identify the orbits that are attracted to the critical point and the one that are repelled, as the independent variable $t \rightarrow \infty$.

Now let us consider a two-dimensional system. Then definitely from the linearized matrix evaluated at a critical point, we would obtain two eigenvalues.

- If two eigenvalues are real and are of same sign, then the corresponding critical point is called as node.
 - If both eigenvalues are negative, then the node is termed as a stable node or future attractor as shown in figure 2.1.
 - If both eigenvalues are positive, the the node is denoted as an unstable node or past attractor as shown in figure 2.1
- If the matrix has a complex conjugate pair of eigenvalues in the form of $\alpha + i\beta$ with non zero real part, i.e., $\alpha \neq 0$, the corresponding critical point is called as a spiral or focus.
 - If $\alpha < 0$, the focus is termed as a stable focus or future attractor as shown in figure 2.1.
 - If $\alpha > 0$, the focus is denoted as an unstable focus or past attractor.
- Stable node or stable focus falls under the category of sink and unstable node or unstable focus falls under the category of source.
- The situation $\alpha = 0$ is not encountered frequently in cosmology. It represents non hyperbolic critical point. In this case, the critical point is referred to as a center.

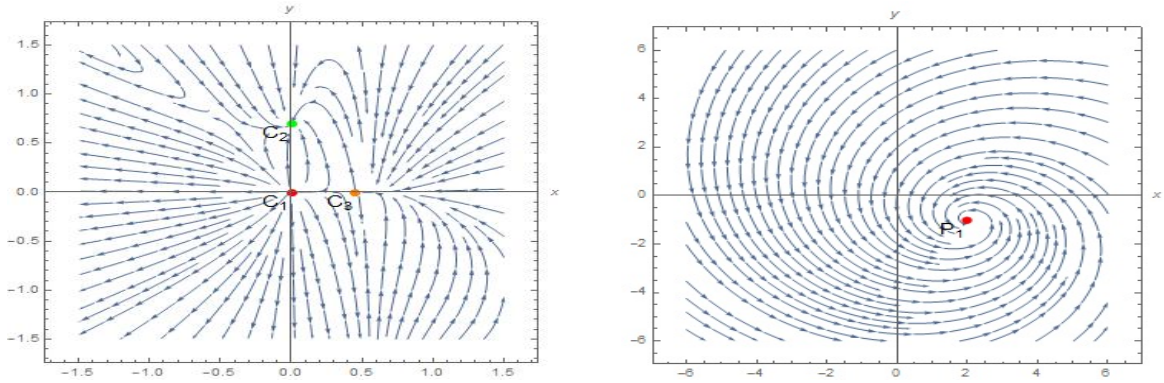


FIGURE 2.1: Figure in the left shows that C_1 is an unstable node, C_2 is a stable node and C_3 is a saddle while the figure in the right shows that P_1 is a stable focus/spiral.

2.2.4 Stable, unstable and center manifold

For the linear system of ordinary differential equations (2.8), the phase space $X \subset \mathbb{R}^n$ is spanned by the eigenvectors obtained from the linearized Jacobian matrix $A = Df(x_0)$ evaluated at the critical point x_0 . The eigenvectors divide the phase space into three distinct subspaces, namely,

- The stable subspace: $E^s = \text{span}\{s_1, s_2, \dots, s_{n_s}\}$.
- The unstable subspace: $E^u = \text{span}\{u_1, u_2, \dots, u_{n_u}\}$.
- The center subspace: $E^c = \text{span}\{c_1, c_2, \dots, c_{n_c}\}$.

where $\{s_1, s_2, \dots, s_{n_s}\}$ are the generalized eigenvectors whose associated eigenvalues have negative real parts, $\{u_1, u_2, \dots, u_{n_u}\}$ are those whose eigenvalues have positive real parts and $\{c_1, c_2, \dots, c_{n_c}\}$ are those whose associated eigenvalues have zero real parts such that $E^s \oplus E^u \oplus E^c = \text{dimension}(X)$. Flows in the stable subspace asymptotically converge to the critical point in future and in unstable subspace, flows asymptote in the past to the critical point.

In the original non linear system of differential equations (2.1), the topologically equivalent flows exhibit in similar kind of fashion. The equivalence only applies in directions where the eigenvalues have non zero real parts, i.e., corresponding to the hyperbolic critical points. In these directions, as the flows remain topologically equivalent to that of the linear system, there exist flows of the non linear system

which are tangent to the eigenvectors. One can generalize the idea of stable, unstable and center manifold from the linear system to the actual non linear system.

- The stable manifold W^s of a critical point x_0 is a differentiable manifold which is tangent to the stable subspace E^s of the linearized system at x_0 such that all orbits in W^s asymptotically converge to x_0 as $t \rightarrow \infty$.
- In a similar manner, the unstable manifold W^u of a critical point x_0 is a differentiable manifold which is tangent to the unstable subspace E^u of the linearized system at x_0 so that all the orbits of W^u are asymptotic to x_0 as $t \rightarrow -\infty$.
- Finally, a center manifold W^c of a critical point x_0 is a differentiable manifold which is tangent to the center subspace E^c at x_0 .

A center manifold has orbits whose asymptotic behaviour can not be characterized through the linearization technique. Other tools like center manifold theory comes into play in this sort of scenario which have been later discussed briefly.

The stable, unstable, and center manifolds associated with a critical point have dimensions equal to those of the respective stable, unstable, and center subspaces of the system's linearization at that point. W^s and W^u are determined uniquely while there can be infinite number of center manifolds.

The local behaviour of a critical point can be influenced by one or more arbitrary parameters. When a small change in these parameters lead to abrupt changes in the qualitative nature of the dynamics, the critical point is said to experience a bifurcation. Such bifurcations can often be identified by examining the linearized system, particularly when the eigenvalues depend on the parameters. A bifurcation typically occurs at the parameter values, when the corresponding real part of at least one eigenvalue becomes zero.

2.2.5 Lyapunov's stability method

Although we have not used Lyapunov's stability theory in this thesis, it remains a crucial method for studying dynamical system, beyond the major applicability of

linear stability theory. Without considering linear stability theory, owing to construction of Lyapunov function [306], this method can be applied directly to any dynamical system problem, making it a very powerful tool for stability analysis. This method can be useful to analyze the stability around a non hyperbolic critical point. But there is a major drawback of this method as it depends on constructing a suitable Lyapunov function pertaining to each dynamical system problem. There is no proper way to identify such function in a systematic manner and hence one needs to guess a suitable choice. Besides these, if a Lyapunov function can not be constructed for a particular system, it can not be concluded that the system's stability does not exist according to Lyapunov's sense.

Definition 2.13. Lyapunov function: Let $\dot{x} = f(x)$ with $x \in X \subset \mathbb{R}^n$ be a smooth dynamical system with critical point x_0 . Let $V : U \rightarrow \mathbb{R}$ be a C^1 function defined on some neighbourhood U of x_0 . Then V is called a Lyapunov function for the critical point x_0 if

1. $V(x_0) = 0$ and $V(x) > 0$ if $x \neq x_0$.
2. $\dot{V}(x) \leq 0 \forall x \in U - \{x_0\}$

Theorem 2.14. Lyapunov stability: Let x_0 be a critical point of the system $\dot{x} = f(x)$ and let U be an open subset of \mathbb{R}^n containing x_0 . If \exists a Lyapunov function $V(x)$ for which

1. $\dot{V}(x) \leq 0 \forall x \in U - \{x_0\}$, then x_0 is stable.
2. $\dot{V}(x) < 0 \forall x \in U - \{x_0\}$, then x_0 is asymptotically stable.

2.2.6 Center manifold theory

According to Hartman-Grobman theorem, in a neighbourhood of a hyperbolic critical point $x_0 \in \mathbb{R}^n$, the non linear system $\dot{x} = f(x)$ is topologically equivalent to the linear system $\dot{x} = Ax$ where A is the linearized Jacobian matrix $Df(x_0)$. Therefore, Hartman-Grobman theorem is conclusive in studying the stability and qualitative behaviour of the system in the neighbourhood of a hyperbolic critical point. But to study the behaviour of the system for a critical point with zero real part(non

hyperbolic critical point), linear stability theory remains inconclusive and here the center manifold theory [302, 303, 307] comes into scenario. This theory reduces the dimensionality of the dynamical system and investigates the stability of the reduced system and this leads to the study of the stability of critical points of the whole system.

Let us consider a dynamical system which is denoted by the following equations

$$\begin{aligned}\dot{x} &= Ax + f(x, y) \\ \dot{y} &= By + g(x, y)\end{aligned}\tag{2.9}$$

where $(x, y) \in \mathbb{R}^c \times \mathbb{R}^s$, $f(0, 0) = 0$, $Df(0, 0) = 0$, $g(0, 0) = 0$, $Dg(0, 0) = 0$, A is a $c \times c$ matrix having eigenvalues with zero real part, B is a $s \times s$ matrix having eigenvalues with negative real parts and f, g are C^r ($r \geq 2$) functions.

Definition 2.15. Center manifold: An invariant manifold is said to be a center manifold pertaining to (2.9) if locally, it can be denoted as

$$W^c(0) = \{(x, y) \in \mathbb{R}^c \times \mathbb{R}^s \mid y = h(x), |x| < \delta, h(0) = 0, Dh(0) = 0\}\tag{2.10}$$

for sufficiently small δ . Conditions $h(0) = 0$ and $Dh(0) = 0$ imply that $W^c(0)$ is a tangent to the center manifold E^c at $(x, y) = (0, 0)$.

Theorem 2.16. Existence theorem: *There exists a C^r center manifold for (2.9). The dynamics of (2.9) restricted to the center manifold for sufficiently small u is defined by the c -dimensional vector field*

$$\dot{u} = Au + f(u, h(u)), \quad u \in \mathbb{R}^c\tag{2.11}$$

Theorem 2.17. Stability theorem: *Let the zero solution of (2.11) is stable or asymptotically stable or unstable. Then the zero solution of (2.9) is also stable, asymptotically stable or unstable respectively. Moreover, let zero solution of (2.11) is stable. Then if $(x(t), y(t))$ is a solution of (2.9) with $(x(0), y(0))$, \exists a solution $u(t)$ of (2.11) such that as $t \rightarrow \infty$*

$$\begin{aligned}x(t) &= u(t) + \mathcal{O}(e^{-\gamma t}) \\ y(t) &= h(u(t)) + \mathcal{O}(e^{-\gamma t})\end{aligned}\tag{2.12}$$

where $\gamma > 0$ is a constant.

To apply the stability theorem, an equation that $h(x)$ must satisfy in order for its graph to be a center manifold for (2.9), must be derived. (x, y) coordinate of any point on (2.10) must satisfy

$$y = h(x) \quad (2.13)$$

Differentiating it with respect to time, one can obtain

$$\dot{y} = Dh(x)\dot{x} \quad (2.14)$$

which must be satisfied by any (\dot{x}, \dot{y}) pertaining to any point (x, y) on (2.10) as (x, y) on (2.10) satisfies (2.13). Dynamics generated by (2.9) must be satisfied by $W^c(0)$. Hence (2.9) transforms into

$$\begin{aligned} \dot{x} &= Ax + f(x, h(x)) \\ \dot{y} &= Bh(x) + g(x, h(x)) \end{aligned} \quad (2.15)$$

(2.14) gets converted to

$$Bh(x) + g(x, h(x)) = Dh(x)[Ax + f(x, h(x))] \quad (2.16)$$

which can be rearranged as

$$\mathcal{N}(h(x)) \equiv Dh(x)[Ax + f(x, h(x))] - Bh(x) + g(x, h(x)) = 0 \quad (2.17)$$

(2.17) is a quasilinear partial differential equation which $h(x)$ must satisfy to make its graph as an invariant center manifold. One has to solve (2.17) in order to find a center manifold. But it is very difficult to solve (2.17) than our original problem. Following theorem provides an insight to find an approximate solution of (2.17).

Theorem 2.18. Approximation theorem: Let $\psi : \mathbb{R}^c \rightarrow \mathbb{R}^s$ be a C^1 mapping with $\psi(0) = D\psi(0)$ such that $\mathcal{N}(\psi(x)) = \mathcal{O}(|x|^q)$ as $x \rightarrow 0$ for some $q > 1$. Then $|h(x) - \psi(x)| = \mathcal{O}(|x|^q)$ as $x \rightarrow 0$.

This theorem allows us to compute the center manifold to any desired degree of accuracy same as solving (2.17)

2.2.7 Asymptotic behaviour in plane

In the theory of dynamical system, it is the main target to identify future ($t \rightarrow \infty$) and past ($t \rightarrow -\infty$) asymptotic behaviour of the non linear system which may be interpreted by any singular or periodic structure. In the case of a planar system i.e., in two dimensional phase space, the possible asymptotic states can be explicitly determined which is noted in the Poincare-Bendixon theorem [308, 309]. In cosmology, one might be interested to know the asymptotic behaviour near the initial singularity i.e., in the past and behaviour at late times i.e., the future asymptotic behaviour by introducing a dimensionless time variable which tends to $-\infty$ and ∞ respectively. The most important concept is ω -limit set [310] to study this behaviour.

Definition 2.19. ω and α limit sets: Let ϕ_t be a flow in \mathbb{R}^n and let $x_0 \in \mathbb{R}^n$. A point $x \in \mathbb{R}^n$ is called a ω -limit point of x_0 if \exists a sequence $\{t_n\}$ such that $t_n \rightarrow \infty$ implies $\lim_{n \rightarrow \infty} \phi_{t_n}(x_0) = x$. The set of all ω -limit points of x_0 is termed as the ω -limit set of x_0 and is denoted by $\omega(x_0)$. The α -limit set $\alpha(x_0)$ corresponding to x_0 is defined similarly by using the sequence $\{t_n\}$ such that $t_n \rightarrow -\infty$.

The ω -limit set $\omega(x_0)$ of a point x_0 exhibits the future asymptotic behaviour of the dynamical system when it starts at the initial state x_0 and similarly $\alpha(x_0)$ describes the past asymptotic state. Any ω -limit set is a closed invariant set but the reverse is not true.

Definition 2.20. Future and past attractor: Let ϕ_t be a flow in \mathbb{R}^n and let $x_0 \in \mathbb{R}^n$. Then the future attractor A^+ is the smallest closed invariant set such that $\omega(x_0) \subset A^+ \forall x_0 \in \mathbb{R}^n$. The past attractor A^- can be defined similarly by replacing $\omega(x_0)$ by $\alpha(x_0)$.

Theorem 2.21. Poincare-Bendixon theorem: *Let us consider an autonomous differential equation $\dot{x} = f(x)$, $x \in \mathbb{R}^2$ with $f \in C^2$ and let there be at most a finite number of critical points i.e., there are only isolated critical points. Then any compact limit set is one of the following*

1. a critical point
2. a periodic orbit
3. the union of critical points and homoclinic and heteroclinic orbits.

An important consequence of this theorem is that, if the presence of a closed orbit such as a periodic, heteroclinic, or homoclinic orbits can be excluded, then all asymptotic behaviour must be confined to a critical point. There are various approaches to rule out closed orbits, among which one of the most common theorem which can be derived from Green's Theorem, is described as below.

Theorem 2.22. Dulac's Criterion: *If $D \subseteq \mathbb{R}^2$ is a simply connected open set and $\nabla(Bf) = \frac{\partial}{\partial x_1}(Bf_1) + \frac{\partial}{\partial x_2}(Bf_2) > 0$ or $(< 0) \forall x \in D$ where B is C^1 function, the autonomous differential equation $\dot{x} = f(x)$, $x \in \mathbb{R}^2$ with $f \in C^1$ has no periodic or (closed) orbit which is contained in D .*

2.2.8 Asymptotic behaviour in higher dimension

A key condition for the applicability of the Poincaré–Bendixson theorem is that the phase space must be two-dimensional. In a system with higher-dimensional phase spaces, the restriction that orbits cannot intersect no longer leads to similarly conclusive results. The dynamics in such spaces can be exceedingly complex, often involving behaviours like recurrence and strange attractors [303, 311]. Consequently, the study of nonlinear systems in three or higher-dimensional spaces is typically limited to the local analysis of critical points. However, some advancement in understanding such systems can be achieved through the identification of monotonic functions. Many of the autonomous differential equations which arise in cosmology acknowledge a variety of monotonic functions which significantly makes the dynamics simple and helps to study the system analytically.

Theorem 2.23. LaSalle Invariance Principle: *Let us consider an autonomous differential equation $\dot{x} = f(x)$, $x \in \mathbb{R}^n$ with flow ϕ_t . Let S be a closed, bounded and positively invariant set of ϕ_t and let Z be a C^1 monotone function. Then $\forall x_0 \in S$ $\omega(x_0) \subseteq \{x \in S \mid \dot{Z} = 0\}$. where $\omega(x_0)$ is a ω -limit set.*

The next theorem is the generalization of the LaSalle Invariance Principle [312].

Theorem 2.24. Monotonicity Principle: *Let ϕ_t be a flow in \mathbb{R}^n with an invariant set S . Let $Z : S \rightarrow \mathbb{R}$ be a C^1 function whose range is the interval (a, b) , where $a \in \mathbb{R} \cup \{-\infty\}$, $b \in \mathbb{R} \cup \{\infty\}$ and $a < b$. If Z is decreasing on orbits in S , then $\forall x \in S$*

$$\begin{aligned}\omega(x) &\subseteq \{s \in \bar{S} \setminus S \mid \lim_{y \rightarrow s} Z(y) \neq b\}, \\ \alpha(x) &\subseteq \{s \in \bar{S} \setminus S \mid \lim_{y \rightarrow s} Z(y) \neq a\}.\end{aligned}$$

2.3 Formulation of an Autonomous Dynamical System: An Example

In this section, we will discuss how to construct a system of autonomous differential equations corresponding to a cosmological model so that we can incorporate the requisite dynamical system tools to study the qualitative behaviour and evolution of the respective cosmological model. Einstein field equations is the governing equation for evolution of cosmological model. So, by introducing suitable dimensionless variables, we need to convert the Einstein field equations pertaining to a cosmological model into a system of autonomous differential equations.

Let us consider a holographic dark energy(HDE) model without interaction. Einstein field equations for such model can be written as

$$3H^2 = \rho_m + \rho_d \quad (2.18)$$

$$2\dot{H} = -\rho_m - (1 + \omega_d)\rho_d \quad (2.19)$$

where H is Hubble's parameter, ρ_m is dark matter density, ρ_d is the holographic dark energy density and ω_d is the equation of state parameter corresponding to holographic dark energy, defined as $\frac{p_d}{\rho_d}$, p_d being the pressure, connected to holographic dark energy. “.” denotes derivative with respect to time. The corresponding continuity equations are as follows:

$$\dot{\rho}_m + 3H\rho_m = 0 \quad (2.20)$$

$$\dot{\rho}_d + 3H(1 + \omega_d)\rho_d = 0 \quad (2.21)$$

Here we introduce two dimensionless variables

$$x = \frac{\rho_m}{3H^2}, \quad y = \frac{\rho_d}{3H^2} \quad (2.22)$$

(2.18) and (2.22) indicate towards the following relation between dark matter density parameter Ω_m and HDE density parameter Ω_d as

$$\begin{aligned}
 \Omega_m &= x \\
 \Omega_d &= y \\
 \Omega_m + \Omega_d &= 1 \\
 \implies x + y &= 1
 \end{aligned} \tag{2.23}$$

Using (2.18) and (2.19) we try to frame the system of autonomous differential equation in terms of variable x and y with respect to the independent variable $N = \ln a$ where $a(t)$ is the scale factor. Hence $\frac{d}{dN} = \frac{1}{H} \frac{d}{dt}$.

$$\begin{aligned}
 \frac{dx}{dN} &= \frac{1}{H} \frac{dx}{dt} \\
 \implies \frac{dx}{dN} &= \frac{1}{H} \frac{d}{dt} \left(\frac{\rho_m}{3H^2} \right) \\
 \implies \frac{dx}{dN} &= \frac{\dot{\rho}_m}{3H^3} - \frac{2\rho_m \dot{H}}{3H^4} \\
 \implies \frac{1}{x} \frac{dx}{dN} &= \frac{\dot{\rho}_m}{H\rho_m} - \frac{2\dot{H}}{H^2} \\
 \implies \frac{1}{x} \frac{dx}{dN} &= -3 - \frac{2\dot{H}}{H^2}
 \end{aligned} \tag{2.24}$$

In the above derivation, we substitute $\frac{\dot{\rho}_m}{\rho_m} = -3H$ from (2.20).

Similarly,

$$\begin{aligned}
 \frac{dy}{dN} &= \frac{1}{H} \frac{dy}{dt} \\
 \implies \frac{dy}{dN} &= \frac{1}{H} \frac{d}{dt} \left(\frac{\rho_d}{3H^2} \right) \\
 \implies \frac{dy}{dN} &= \frac{\dot{\rho}_d}{3H^3} - \frac{2\rho_d \dot{H}}{3H^4} \\
 \implies \frac{1}{y} \frac{dy}{dN} &= \frac{\dot{\rho}_d}{H\rho_m} - \frac{2\dot{H}}{H^2} \\
 \implies \frac{1}{y} \frac{dy}{dN} &= -3(1 + \omega_d) - \frac{2\dot{H}}{H^2}
 \end{aligned} \tag{2.25}$$

Here, we substitute $\frac{\dot{\rho}_d}{\rho_d} = -3H(1 + \omega_d)$ from (2.21).

From (2.19), by dividing the equation by $2H^2$ and using (2.18), (2.22), we obtain

$$\begin{aligned}
& \frac{\dot{H}}{H^2} = -\frac{\rho_m}{2H^2} - (1 + \omega_d)\frac{\rho_d}{2H^2} \\
\implies & \frac{\dot{H}}{H^2} = -\frac{3\rho_m}{6H^2} - (1 + \omega_d)\frac{3\rho_d}{6H^2} \\
\implies & \frac{\dot{H}}{H^2} = -\frac{3x}{2} - (1 + \omega_d)\frac{3y}{2} \\
\implies & \frac{\dot{H}}{H^2} = -\frac{3(x + y)}{2} - \omega_d\frac{3y}{2} \\
\implies & \frac{\dot{H}}{H^2} = -\frac{3}{2} - \omega_d\frac{3y}{2}
\end{aligned} \tag{2.26}$$

Finally, upon substituting (2.26) in (2.24) and (2.25), we formulate the following system of autonomous differential equation

$$\begin{aligned}
& \frac{dx}{dN} = 3xy\omega_d \\
& \frac{dy}{dN} = -3y(1 - y)\omega_d
\end{aligned} \tag{2.27}$$

ω_d , the equation of state parameter can be evaluated for different HDE models and hence respective system of autonomous differential equations can be formulated.

One can follow chapter-5 for detailed discussion. After identifying the critical points and studying the qualitative behaviour of the cosmological model around these critical points, evolution of universe can be looked into along with the precise characterization of different cosmological parameters.

Chapter 3

Dynamical system analysis on conformally coupled massless scalar field in semiclassical gravity

3.1 Introduction

Current observational data [16, 131, 313, 314] strongly suggests an accelerated expansion [77, 315] of the universe. Initially this was explained using the cosmological constant Λ [3, 316, 317] where the pressure p and energy density ρ are connected through the equation $p = -\rho$ which is also consistent with the current observational value [318] of the equation of state parameter ω . However, the cosmological constant fails to address two significant problems namely the “fine tuning problem” and the “coincidence problem” [78, 319].

To resolve these issues, scientists introduced the concept of “dark energy” [69, 320, 321, 322] within the frame work of Einstein’s General Relativity. Dark energy is characterized by having a positive energy density and negative pressure, with vacuum energy which is often considered as the source of dark energy [323, 324]. To address the problems associated with the cosmological constant, it is typically assumed that the vacuum energy is balanced by an unknown cancellation mechanism and there is a dark energy component associated with a variable equation of state parameter. Different values of this parameter [325, 326] lead to different possible

fates for the future of the universe. For instance, if $-1 < \omega < -\frac{1}{3}$, dark energy represents quintessence fluid. For $\omega = -1$, dark energy corresponds to the cosmological constant and the universe follows an asymptotically de-sitter nature. If $\omega < -1$, General Relativity suggests the existence of “phantom energy”. As the universe expands ($\omega < -\frac{1}{3}$), the “phantom energy” increases and within a finite amount of proper time, the phantom energy density [48] becomes infinite causing the universe to expand infinitely. This would lead to the eventual disintegration of all bounded objects, from clusters of galaxies to atomic nuclei, as the universe approaches a future singularity [48], known as the “Big Rip”. To resolve different kinds of singularity and different issues faced in very early cosmological models like Big Bang theory, inflation theory, cosmological constant; different theoretical models of dark energy have been developed like scalar field models including unified dark energy and matter, k-essence, quintessence, coupled dark energy and matter etc [87, 108, 327, 328, 329, 330].

Several physicists have thought of combining the quantum theory of gravity to eradicate future singularity [278, 331, 332]. Since, they felt that the quantum theory and General Relativity are quite incompatible, they proposed a semiclassical theory where an amalgamation between classical theories of gravity and quantum field theory [44, 333, 334] was made.

In classical gravity, the Einstein field equation governs the dynamics of spacetime

$$G^{\mu\nu} = \frac{8\pi G}{c^4} T^{\mu\nu} \quad (3.1)$$

where the left side of the equation (3.1) represents the gravity part which influences the spacetime geometry and right hand side represents the energy-momentum tensor which is analogous to the matter part of the universe.

In semiclassical gravity theory [39, 41, 42, 335, 336, 337, 338, 339], gravity is represented classically but the matter part is represented quantum mechanically which leads to semi classical Einstein field equation

$$G^{\mu\nu} = \frac{8\pi G}{c^4} \langle \hat{T}^{\mu\nu} \rangle \quad (3.2)$$

where the energy-momentum tensor $T^{\mu\nu}$ is replaced by a quantum operator $\hat{T}^{\mu\nu}$ whose expected value represents mass and energy.

Energy momentum tensor plays a crucial role for becoming the origin of curvature in

General Relativity. Energy momentum tensor is divergenceless, signifying the conservation of energy and momentum. This symmetry is preserved when transitioning from classical to quantum theory. In massless theories, there is an interesting symmetry known as conformal symmetry, which, in the classical case is reflected through the tracelessness of the energy-momentum tensor. However, in the quantum case, this is not always true and can be identified through trace anomalies [340, 341, 342]. In this chapter, we focus on the conformally coupled [343, 344, 345, 346, 347, 348] massless scalar field characterized by an improvised stress-energy tensor, capable of classically violating the null energy condition [343].

3.2 Semiclassical dynamical equations in conformally coupled massless scalar field

In this section, we explore modified field equations in a conformally coupled massless scalar field. We are considering here a homogeneous and isotropic FRW metric

$$ds^2 = -dt^2 + a^2(t) \left[\frac{dr^2}{1 - kr^2} + r^2(d\theta^2 + \sin^2\theta d\phi^2) \right] \quad (3.3)$$

It is known that in semiclassical gravity in conformally coupled mass less scalar field, the energy momentum tensor is not traceless [346, 347]. Vacuum trace anomaly of energy momentum tensor can be denoted as

$$T_{vac} = \frac{1}{2880\pi^2} (\square R + G) \quad (3.4)$$

where R is the enrgy-momentum curvature and $G = -2R_{\mu\nu}R^{\mu\nu} - \frac{1}{3}R^2$ is the Gauss-Bonnet curvature invariant [348]. Here we consider that the Weyl tensor diminishes in FRW geometry to obtain the expression of G . By substituting Hubble parameter H in (3.4) one can obtain [337, 349]

$$T_{vac} = \frac{1}{480\pi^2} (\ddot{H} + 12H^2\dot{H} + 7H\ddot{H} + 4\dot{H}^2) + \frac{1}{240\pi^2} (H^4 + H^2\dot{H}) \quad (3.5)$$

Here, we use the trace anomaly

$$T_{vac} = \rho_{vac} - 3p_{vac} \quad (3.6)$$

After inserting (3.5) in the conservation equation

$$\rho_{vac} + 3H(\rho_{vac} + p_{vac}) = 0 \quad (3.7)$$

and using (3.6), vacuum energy density becomes

$$\rho_{vac} = \frac{1}{480\pi^2}(3H^2H + H\ddot{H} - \frac{1}{2}\dot{H}^2) + \frac{1}{960\pi^2}H^4 \quad (3.8)$$

The semiclassical Friedmann equation can be defined here as

$$3H^2 = 8\pi(\rho + \rho_{vac}) \quad (3.9)$$

3.3 Dynamical system analysis in semiclassical gravity for a conformally coupled massless scalar field

To use the dynamical system tools in this current cosmological model, we need to frame a system of autonomous equations using semiclassical Friedmann equations and conservation equation (3.5), (3.6), (3.7), (3.8), (3.9). To construct such self-autonomous system, we consider the following dimensionless variables.

$$\bar{t} = H_+ t, \quad \bar{H} = \frac{H}{H_+}, \quad \bar{Y} = \frac{\dot{H}}{H_+^2}, \quad \bar{\rho} = \frac{8\pi\rho}{3H_+^2} \quad (3.10)$$

where $H_+ = \sqrt{360\pi}$.

Using (3.10) in (3.7), (3.8), (3.9), we obtain the following system of autonomous

differential equations in terms of dimensionless variables,

$$\begin{aligned} \bar{H}' &= \bar{Y} \\ \bar{Y}' &= \frac{1}{2\bar{H}}(\bar{H}^2 - \bar{\rho} - 6\bar{H}^2\bar{Y} + \bar{Y}^2 - \bar{H}^4) \\ \bar{\rho}' &= -3\bar{H}(1 + \omega)\bar{\rho} \end{aligned} \tag{3.11}$$

where ' denotes the derivative with respect to the time \bar{t} . To solve the above autonomous system we frame a linearized Jacobian matrix from (3.11)

$$J = \begin{pmatrix} 0 & 1 & 0 \\ 1 - 6\bar{Y} - 2\bar{H}^2 - \frac{1}{2\bar{H}^2}(\bar{H}^2 - \bar{\rho} - 6\bar{H}^2\bar{Y} + \bar{Y}^2 - \bar{H}^4) & -3\bar{H} + \frac{\bar{Y}}{\bar{H}} & -\frac{1}{2\bar{H}} \\ -3(1 + \omega)\bar{\rho} & 0 & -3\bar{H}(1 + \omega) \end{pmatrix} \tag{3.12}$$

Corresponding to all critical points obtained from (3.11), eigenvalues are fetched from the linearized Jacobian matrix (3.12) which are given in table 3.1.

TABLE 3.1: Critical points and their corresponding eigenvalues for the autonomous system (3.11).

Critical points $(\bar{H}, \bar{Y}, \bar{\rho})$	Eigenvalues
$A(1, 0, 0)$	$-(3 + 3\omega), \frac{-3-\sqrt{5}}{2}, \frac{-3+\sqrt{5}}{2}$
$B(-1, 0, 0)$	$(3 + 3\omega), \frac{-3-\sqrt{5}}{2}, \frac{-3+\sqrt{5}}{2}$

Here, from table 3.1, we can deduce the stability of the 3D autonomous system (3.11) through the signature of eigenvalues using the linearized technique.

- **Case-I:** When $\omega > -1$, critical point A is stable while B is saddle.
- **Case-II:** When $\omega < -1$, A is saddle and B is stable.
- **Case-III:** For $\omega = -1$, linearized technique remains inconclusive for analyzing the stability of A and B as both the critical points become non hyperbolic for the aforesaid value of ω .

Now let us consider a 2D autonomous system in \bar{H} , \bar{Y} variables from (3.11) for $\bar{\rho} = 0$. Then the autonomous system (3.11) gets converted into

$$\begin{aligned} \bar{H}' &= \bar{Y} \\ \bar{Y}' &= \frac{1}{2\bar{H}}(\bar{H}^2 - 6\bar{H}^2\bar{Y} + \bar{Y}^2 - \bar{H}^4) \end{aligned} \quad (3.13)$$

A linearized Jacobian matrix

$$J = \begin{pmatrix} 0 & 1 \\ 1 - 6\bar{Y} - 2\bar{H}^2 - \frac{1}{2\bar{H}^2}(\bar{H}^2 - 6\bar{H}^2\bar{Y} + \bar{Y}^2 - \bar{H}^4) & -3\bar{H} + \frac{\bar{Y}}{\bar{H}} \end{pmatrix} \quad (3.14)$$

is constructed from (3.13). Eigenvalues corresponding to the critical points, obtained from the autonomous system (3.13) are evaluated from (3.14). Critical points and the respective eigenvalues are enlisted in the table 3.2.

TABLE 3.2: Critical points and their corresponding eigenvalues for the autonomous system (3.13).

Critical points (\bar{H}, \bar{Y})	Eigenvalues
$A_1(1, 0)$	$-0.3820, -2.6180$
$B_1(-1, 0)$	$0.3820, 2.6180$

According to the eigenvalues corresponding to the critical points A_1 and B_1 as shown in the table 3.2, A_1 is always stable while B_1 is unstable which is similar to the behaviour of A and B as discussed earlier for $\omega > -1$.

To identify the qualitative nature of the system around the critical points, we consider the 2D phase plot diagram in (\bar{H}, \bar{Y}) plane which depicts in figure 3.1 that A_1 is stable and B_1 is unstable.

We also consider a 2D phase plot projection in $(\bar{H}, \bar{\rho})$ plane to identify the qualitative behaviour around the critical points A and B for different choices of equation of state parameter ω . Figure 3.2 shows that A is becoming stable and B is becoming saddle while ω is chosen as -0.85 which is greater than -1 while figure 3.3 shows that A is becoming saddle and B is becoming stable while ω is chosen as -1.25 which is less than -1 .

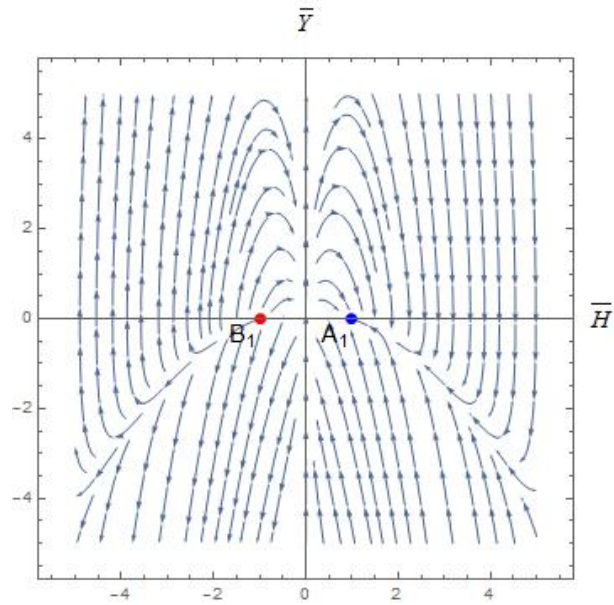


FIGURE 3.1: Phase plot corresponding to the critical point $A_1(1, 0)$ and $B_1(-1, 0)$ in (\bar{H}, \bar{Y}) plane

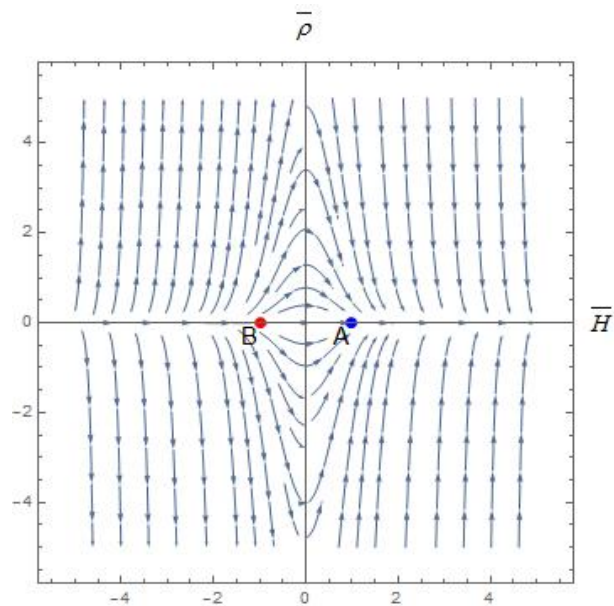


FIGURE 3.2: Phase plot corresponding to the critical point A and B with $\omega = -0.85$ in $(\bar{H}, \bar{\rho})$ plane

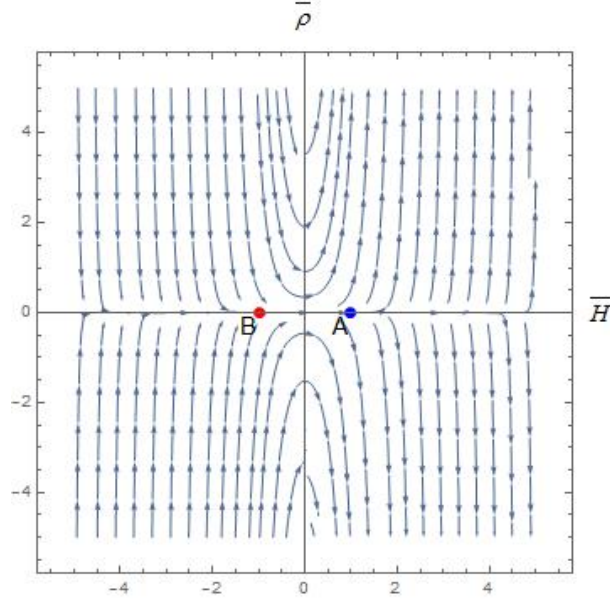


FIGURE 3.3: Phase plot corresponding to the critical point A and B with $\omega = -1.25$ in $(\bar{H}, \bar{\rho})$ plane

3.4 Summary and discussion

In this chapter, we have not considered any particular fluid description like baryon, radiation and dust, rather we have assumed general description of fluid. Here, in the context of semi classical gravity with massless conformally coupled scalar field, energy density is completely characterized by the trace anomaly.

The hyperbolic critical point A behaves very interestingly. If the equation of state parameter lies within $(-1, -\frac{1}{3})$, i.e., $-1 < \omega < -\frac{1}{3}$, it becomes stable and indicates that the energy density considered here represents quintessence description of fluid with an accelerated phase. As A is becoming stable for $\omega = 0$ and $\omega = \frac{1}{3}$, it can characterize early stages of dust and radiation dominated epochs respectively.

But while we are taking the value of the equation of state parameter $\omega = -1$, both the nodes A and B represent a non hyperbolic critical point which we are unable to analyze here as we are only considering the linearized method. So, we can't conclude anything regarding the model's resemblance with Λ CDM model.

As, $\omega < -1$, B is becoming stable and therefore we can claim here that B stands for a phantom description of fluid. While we are considering vacuum energy density, from the 2D autonomous system in (\bar{H}, \bar{Y}) , we find that the corresponding critical

points A_1 and B_1 are behaving similar to A and B with $\omega > -1$. But as the equation of state parameter remains undetermined, we can't conclude anything regarding the acceleration.

So, from here, we can state that A represents a quintessence era while B exhibits a phantom era with accelerated expansion. As a result, we can claim that semiclassical gravity with conformally coupled scalar field can represent quintessence and phantom like fluid description with an accelerated nature which fits well with the current observational scenario as well as it can explain the early stages of matter and radiation dominated scenarios.

Chapter 4

Dynamical system analysis on non-minimally coupled $f(Q)$ gravity

4.1 Introduction

Recent observational findings [62, 313] on late time acceleration of current universe [77] have posed some theoretical challenges to gravity theories. Although the General theory of Relativity is the most successful theory of last century for the description of gravitational interaction, it has also been struggling with several limitations like flatness, initial singularity etc. A satisfactory answer requires more generalized theory of gravity involving more general geometric structures. Thus, extended theories of gravity [350, 351, 352] have been developed.

Extended theories of gravity [198] have been made through several modifications in Einstein's theory [199, 353] and in general these modified theories will have General Relativity as a particular case. These theories are developed by modifying Einstein Hilbert action which yields Einstein field equations and these modifications created interest amongst scientific community as scientists thought that it would be relevant at scales close to Plank scale which is considered at the very early universe near black hole singularity. But eventually, it provided a significant breakthrough in studying universe at low energies i.e., at large scale in late universe. Alternative gravitational

theories are nothing but the attempts in introducing semiclassical schemes in which most of the useful features of General Relativity can be identified.

Recent observational data depict that the approximate proportions of ordinary baryonic matter, dark matter and dark energy are respectively 4%, 20% and 76% [18, 62, 354]. Dark matter has the clustering property like ordinary matter but dark energy is not describable in that way. Both of them can be distinguished through energy conditions [355].

In between two accelerated epoch, there are decelerated expansion, radiation and matter dominated eras. The proportions of matter and energy in the Universe, as supported by observational data, are truly astonishing. Cosmological observations suggest that Λ CDM model is the best fitted model till date with some anomalies. To alleviate those anomalies in Λ CDM model, other different cosmological models like quintessence, k-essence, coupled dark energy, unified dark energy, $f(R)$, $f(R,T)$ etc. have been studied extensively i.e., to resolve these issues, models have been developed in two approaches. One approach is to modify Einstein gravity in terms of geometrical effects resulting various models of modified theories of gravity such as $f(R)$, $f(R,T)$, $f(T)$, etc [200, 201, 202, 356, 357, 358]. Another approach is to modify the right hand side of Einstein Field equation i.e., modifying the matter part, thereby yielding different dark energy models [58, 67, 68, 69, 70, 71, 89, 359, 360, 361, 362, 363, 364].

Thus modifications in gravity [203, 365, 366] is a different approach and interesting way to explain universe's late time accelerated expansion whose limiting conditions can be obtained as General Relativity(GR).

We know that gravitational phenomena is represented by curved spacetime. Along with the curvature, torsion and non metricity are associated with the connections of a metric space. In standard General Relativity, both non metricity and torsion vanish. In this framework, Ricci curvature R is one of the fundamental quantities that describes the curvature of spacetime. Another approach is to describe the gravity by torsion T only. A third alternative representation is developed on a flat spacetime without curvature and torsion, where non metricity Q represents the gravitational interaction, known as the symmetric teleparallel gravity. It is to be remembered that non metricity is the property of connection, not of the manifold. Jimenez et al. [265] have developed the symmetric teleparallel gravity into $f(Q)$ gravity.

We have considered a cosmological model where gravitational interactions are represented by non-metricity Q which has been taken into account for gravitational modifications. So, we are considering newly proposed symmetric teleparallel $f(Q)$ gravity [236, 237, 238, 239, 240, 241, 266, 267, 270, 367, 368, 369, 370, 371, 372, 373] where Q is non-metricity [268, 269, 374].

Our motivation for this work is to incorporate late time cosmic acceleration with the help of some functional forms of $f(Q)$ which we have considered as a combination of $f_1(Q)$ and $f_2(Q)$. We have used dynamical system tools [297, 300, 302, 303] to analyze the stability of such model. We all are aware that the equation of state parameter plays an important role in predicting different fluid description of universe. Similarly, some other cosmological parameters play major role in describing the evolution of universe. So, here we shall be considering current observational data [18, 131, 375, 376, 377, 378] of different cosmological parameters for analyzing the model.

4.2 Basic tools of $f(Q)$ gravity

General theory of gravity is based on metric theory and in this case, connection is symmetric and metric dependent. However, different approaches can be considered to characterize the space-time. One such type of approach is to consider symmetric teleparallel ($\int d^4x \sqrt{-g} Q$) action instead of normal Einstein-Hilbert action. Here, the modified gravity theory is dependent on the nonlinear extension of non-metric scalar Q and the corresponding gravity theory is noted as $f(Q)$ gravity theory.

Here, we consider the action for matter coupling [379] in $f(Q)$ gravity with the help of two functions, which is defined by

$$S = \int d^4x \sqrt{-g} \left[\frac{1}{2} f_1(Q) + f_2(Q) \mathcal{L}_m \right] \quad (4.1)$$

where g is the determinant of the metric, $f_1(Q)$ and $f_2(Q)$ are two arbitrary functions of the non metricity Q , \mathcal{L}_m is the Lagrangian function for the matter field.

Here, the non-metricity tensor and the traces are

$$Q_{\alpha\beta\gamma} = \nabla_{\alpha} g_{\beta\gamma} \quad (4.2)$$

$$Q_\alpha = Q_\alpha^\beta{}_\beta, \tilde{Q}_\alpha = Q_{\alpha\beta}^\alpha \quad (4.3)$$

Superpotential can be introduced as a function of non metric tensor with the following equation

$$4P_{\beta\gamma}^\alpha = -Q_{\beta\gamma}^\alpha + 2Q_{(\beta\alpha\gamma)} - Q^\alpha g_{\beta\gamma} - \tilde{Q}^\alpha g_{\beta\gamma} - \delta_{(\beta}^\alpha{}_{\gamma)} \quad (4.4)$$

where the trace of the nonmetricity tensor takes the form

$$Q = -Q_{\alpha\beta\gamma} P^{\alpha\beta\gamma} \quad (4.5)$$

For simplicity, let us consider the following equations

$$f = f_1(Q) + 2f_2(Q)\mathcal{L}_m \quad (4.6)$$

$$F = f_1'(Q) + 2f_2'(Q)\mathcal{L}_m \quad (4.7)$$

where (') signifies the derivatives of the functions $f_1(Q)$ and $f_2(Q)$ with respect to Q .

To identify the fluid description of the spacetime, energy-momentum tensor can be introduced as

$$T_{\beta\gamma} = -\frac{2}{\sqrt{-g}} \frac{\delta(\sqrt{-g}L_M)}{\delta g^{\beta\gamma}} \quad (4.8)$$

By varying the action, considered in equation (4.1) with respect to the metric tensor, following gravitational field equation can be obtained

$$\begin{aligned} & \frac{2}{\sqrt{-g}} \nabla_\alpha (\sqrt{-g} F P_{\beta\gamma}^\alpha) + \frac{1}{2} g_{\beta\gamma} f_1 \\ & + F (P_{\beta\mu\nu} Q_\gamma{}^{\mu\nu} - 2Q_{\mu\nu\beta} P_{\gamma}^{\mu\nu}) = -f_2 T_{\beta\gamma} \end{aligned} \quad (4.9)$$

Now, equation (4.9) can be used for different cosmological applications in $f(Q)$ gravity.

4.3 Implementation of $f(Q)$ gravity in FLRW space-time

For exploring several cosmological phenomena, we consider the isotropic, homogeneous, spatially flat line element as

$$ds^2 = -N^2(t)dt^2 + a^2(t)\delta_{ij}dx^i dx^j \quad (4.10)$$

Here, $N(t)$ denotes the lapse function and in the present case due to usual time reparametrization freedom, we may impose $N = 1$ in any time. δ_{ij} denotes Kronecker delta and i, j run over the spatial components.

Now, it is customary to define the expansion and dilation parameters as

$$H = \frac{\dot{a}}{a} \quad \text{and} \quad T = \frac{\dot{N}}{N} \quad (4.11)$$

In this current line element, the nonmetricity Q is considered as

$$Q = 6H^2 \quad (4.12)$$

Here, we consider matter as the standard perfect fluid whose energy-momentum tensor, given by (4.8) is diagonal. So, the field equation (4.9) provides us two generalized Friedman equations as

$$f_2\rho = \frac{f_1}{2} - 6F\frac{H^2}{N^2} \quad (4.13)$$

$$-f_2p = \frac{f_1}{2} - \frac{2}{N^2}[(\dot{F} - FT)H + F(\dot{H} + 3H^2)] \quad (4.14)$$

Here, ρ is the energy density and p is the pressure of the fluid content in the space-time. It is very trivial to verify that by putting $f_1 = -Q$ and $f_2 = 1 = -F$, the aforesaid Friedman equations (4.13) and (4.14) reduce to the standard Friedman equations.

The continuity equation of motion for matter field can be derived from (4.13) and (4.14) as

$$\dot{\rho} + 3H(\rho + p) = -\frac{6f_2'H}{f_2N^2}(\dot{H} - HT)(\mathcal{L}_m + \rho) \quad (4.15)$$

From (4.15), the standard continuity equation can be derived by substituting $\mathcal{L}_m = -\rho$ as

$$\dot{\rho} + 3H(\rho + p) = 0 \quad (4.16)$$

This is now compatible with the homogeneous and isotropic nature of the universe. Here, we shall proceed with $N = 1$. As, we are working in the framework of standard Friedman-Robertson-Walker (FRW) geometry, dilation parameter T and the non-metricity Q are transformed to

$$T = 0 \text{ and } Q = 6H^2 \quad (4.17)$$

respectively. Hence the equations (4.13) and (4.14) can be reframed as

$$3H^2 = \frac{f_2}{2F}(-\rho + \frac{f_1}{2f_2}) \quad (4.18)$$

$$\dot{H} + 3H^2 + \frac{\dot{F}}{F}H = \frac{f_2}{2F}(p + \frac{f_1}{2f_2}) \quad (4.19)$$

4.4 Formation of autonomous system and stability analysis by dynamical system approach

In this section, we confine ourselves to the dynamical system approach to analyze the stability of the system using linearized Jacobian matrix. We consider two arbitrary functions of the non metricity Q as

$$f_1(Q) = \alpha Q^n, \quad n \neq 1 \text{ and } f_2(Q) = Q \quad (4.20)$$

Here, α and n are arbitrary constants.

Let us introduce following dimensionless variables

$$x = -\frac{-\rho f_2}{QF} \text{ and } y = \frac{f_1}{2QF} \quad (4.21)$$

4.4.1 Autonomous system with equation of state parameter

Let us consider the equation of state parameter $p = \rho \omega$ where ρ is the energy density and p is the pressure of fluid content in spacetime. Using equations (4.17) and (4.21) in the Friedmann equations (4.18) and (4.19), we can formulate following system of autonomous equations

$$x' = -\frac{11}{3}\epsilon x - 3x\omega - 3xy + 3\omega x^2 \quad (4.22)$$

$$y' = -y\epsilon(2n - 1) - 3y^2 + 3xy\omega + 3y \quad (4.23)$$

Here (\prime) denotes the derivative with respect to $\eta = \ln a$ and

$$\epsilon = -\frac{\dot{H}}{H^2} = q + 1 \quad (4.24)$$

where q is the deceleration parameter.

At the very beginning, by implementing dimensionless variables, defined in in equation (4.21) and using (4.17), (4.18), (4.19), (4.20), we have obtained autonomous system of equations (4.22) and (4.23). From the aforesaid system, we have obtained three set of critical points (in table 4.1) solving

$$x' = 0, \quad y' = 0 \quad (4.25)$$

Apart from the first point $(0, 0)$, other two points are denoted in terms of deceleration parameter q (in equation (4.24)), n and equation of state parameter, ω . By varying the values of these parameters, we have considered different cases corresponding to the aforesaid critical points and analyzed the stability of the universe in the current late time acceleration epoch. We have formed the linearized matrix and obtained the corresponding eigenvalues with respect to the critical points. Then considering different values of the parameters supported by current observational data, we have performed stability analysis around the critical points.

From the autonomous system (4.22) and (4.23), we frame the required linearized Jacobian matrix

$$J = \begin{pmatrix} \frac{-11}{3}\epsilon - 3\omega - 3y + 6\omega x & -3x \\ 3y\omega & -\epsilon(2n - 1) - 6y + 3x\omega + 3 \end{pmatrix}$$

for three hyperbolic critical points and eigenvalues corresponding to those critical points are found which have been represented in table 4.1.

TABLE 4.1: Set of critical points and corresponding eigenvalues.

Critical points(x, y)	Eigenvalues
$(0, 0)$	$3 - \epsilon(2n - 1), -\frac{11}{3}\epsilon - 3\omega$
$(\frac{1.22\epsilon + \omega}{\omega}, 0)$	$\frac{11}{3}\epsilon + 3\omega, \frac{11}{3}\epsilon + 3\omega - \epsilon(2n - 1) + 3$
$(0, 0.33\epsilon - 0.67\epsilon n + 1)$	$2.01\epsilon n - 3\omega - 4.66\epsilon - 3, 4\epsilon n - 2\epsilon - \epsilon(2n - 1) - 3$

Here critical points and the corresponding eigenvalues depend on the predefined parameters $\epsilon = q + 1$, ω and n . Now, we shall be explicitly doing stability analysis around those critical points. Critical points will vary with the value of above parameters. We have taken q in the range of -0.48 to -0.55 as prescribed in [131, 368, 380]. By varying n , we can find a form of $f(Q)$ for stable universe.

Critical point $(0, 0)$ and the eigenvalues corresponding to different values of q and n are given in table 4.2. Here, the eigenvalues depend on the value of equation of state parameter, ω .

TABLE 4.2: For $q = -0.53$, $q = -0.48$ and for $n=2, 3, 4, 5, 6$, this table shows eigenvalues corresponding to the critical point $(0, 0)$.

No	q	ϵ	n	point	Eigenvalues
P_1	-0.53	0.47	2	$(0,0)$	1.59, -1.72-3 ω
P_2	-0.53	0.47	3	$(0,0)$	0.65, -1.72-3 ω
P_3	-0.53	0.47	4	$(0,0)$	-0.29, -1.72-3 ω
P_4	-0.53	0.47	5	$(0,0)$	-1.23, -1.72-3 ω
P_5	-0.53	0.47	6	$(0,0)$	-2.17, -1.72-3 ω
P_6	-0.48	0.52	2	$(0,0)$	1.44, -1.90-3 ω
P_7	-0.48	0.52	3	$(0,0)$	0.4, -1.90-3 ω
P_8	-0.48	0.52	4	$(0,0)$	-0.64, -1.90-3 ω
P_9	-0.48	0.52	5	$(0,0)$	-1.68, -1.90-3 ω
P_{10}	-0.48	0.52	6	$(0,0)$	-2.72, -1.90-3 ω

According to table 4.2, we can clearly observe that as $q = -0.53$:

- For $n = 2$ and 3 (P_1, P_2 from table 4.2, the point $(0, 0)$ is saddle when $\omega > -0.57$ and unstable whenever $\omega < -0.57$.
- For $n \geq 4$ (P_3, P_4, P_5 table 4.2), $(0, 0)$ will be stable node when $\omega > -0.57$ and saddle node when $\omega < -0.57$.

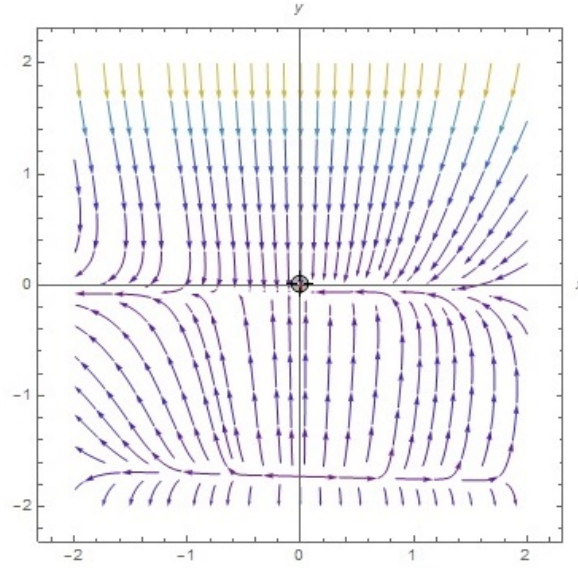


FIGURE 4.1: Phase plot corresponding to the point $(0, 0)$ for $q = -0.53$, $n = 20$, $\omega = -0.4$ which shows that for the choices of aforesaid values of q , ω and n , $(0, 0)$ is locally stable node

Similarly, while we consider, $q = -0.48$:

- For $n = 2$ and 3 (P_6, P_7 from table 4.2), the point $(0, 0)$ is saddle when $\omega > -0.63$ and unstable whenever $\omega < -0.63$.
- For $n \geq 4$ (P_8, P_9, P_{10} from table 4.2), $(0, 0)$ will be stable node when $\omega > -0.63$ and saddle node when $\omega < -0.63$.

Critical point $(\frac{1.22\epsilon+\omega}{\omega}, 0)$ and the corresponding eigenvalues for various values of q and n are given in table 4.3. Here, like the previous case, respective eigenvalues depend on the value of equation of state parameter, ω .

According to table 4.3, we can clearly observe that while we take, $q = -0.53$:

- For $n = 2$ (P_{11} in table 4.3), the point $(\frac{1.22\epsilon+\omega}{\omega}, 0)$ is stable when $\omega < -1.10$, saddle node when $-1.10 < \omega < -0.57$ and unstable when $\omega > -0.57$.
- If $n = 3$ (P_{12} in table 4.3), the point $(\frac{1.22\epsilon+\omega}{\omega}, 0)$ becomes stable when $\omega < -0.79$, saddle node when $-0.79 < \omega < -0.57$ and unstable when $\omega > -0.57$.

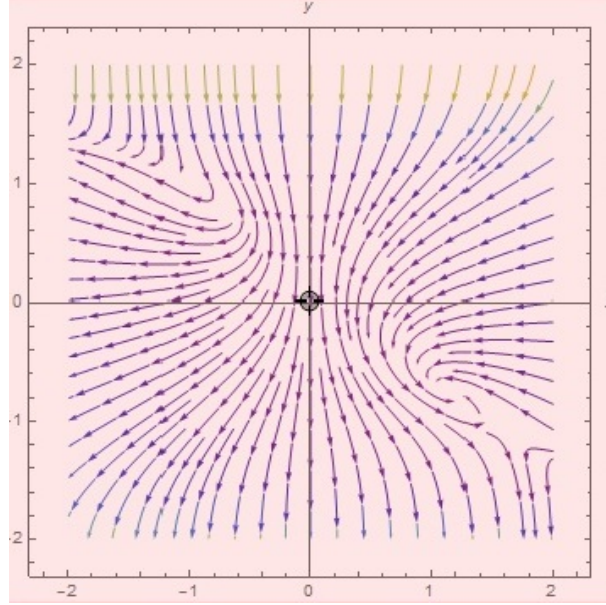


FIGURE 4.2: Phase plot corresponding to the point $(0, 0)$ for $q = -0.48$, $n = 3$, $\omega = -0.87$ (P_6 in table 4.2) which shows that for the choices of aforesaid values of q , ω and n , $(0, 0)$ is locally unstable node.

TABLE 4.3: For $q = -0.53$, $q = -0.48$ and for $n=2, 3, 4, 5, 6$, this table shows the eigenvalues corresponding to the critical point $(\frac{1.22\epsilon+\omega}{\omega}, 0)$.

No	q	ϵ	n	point	Eigenvalues
P_{11}	-0.53	0.47	2	$(\frac{0.9044+\omega}{\omega}, 0)$	$1.72+3\omega, 3.3133+3\omega$
P_{12}	-0.53	0.47	3	$(\frac{0.9044+\omega}{\omega}, 0)$	$1.72+3\omega, 2.3733+3\omega$
P_{13}	-0.53	0.47	4	$(\frac{0.9044+\omega}{\omega}, 0)$	$1.72+3\omega, 1.4333+3\omega$
P_{14}	-0.53	0.47	5	$(\frac{0.9044+\omega}{\omega}, 0)$	$1.72+3\omega, 0.4933+3\omega$
P_{15}	-0.53	0.47	6	$(\frac{0.9044+\omega}{\omega}, 0)$	$1.72+3\omega, -0.4467+3\omega$
P_{16}	-0.48	0.52	2	$(\frac{0.6355+\omega}{\omega}, 0)$	$1.91+3\omega, 3.3467+3\omega$
P_{17}	-0.48	0.52	3	$(\frac{0.6355+\omega}{\omega}, 0)$	$1.91+3\omega, 2.3067+3\omega$
P_{18}	-0.48	0.52	4	$(\frac{0.6355+\omega}{\omega}, 0)$	$1.91+3\omega, 1.2667+3\omega$
P_{19}	-0.48	0.52	5	$(\frac{0.6355+\omega}{\omega}, 0)$	$1.91+3\omega, 0.2267+3\omega$
P_{20}	-0.48	0.52	6	$(\frac{0.6355+\omega}{\omega}, 0)$	$1.91+3\omega, -0.8133+3\omega$

- For $n \geq 4$ (P_{13}, P_{14}, P_{15} in table 4.3), $(\frac{1.22\epsilon+\omega}{\omega}, 0)$ will be a stable node when $\omega < -0.57$.
- For $n = 4$ (P_{13} in table 4.3), $(\frac{1.22\epsilon+\omega}{\omega}, 0)$ becomes an unstable node when $\omega > -0.48$ and saddle node when $-0.57 < \omega < -0.48$.
- For $n = 5$ (P_{14} in table 4.3), $(\frac{1.22\epsilon+\omega}{\omega}, 0)$ will be an unstable node when $\omega > -0.16$ and saddle node when $-0.57 < \omega < -0.16$.
- For $n = 6$ (P_{15} in table 4.3), $(\frac{1.22\epsilon+\omega}{\omega}, 0)$ turns to be an unstable node when $\omega > 0.14$ and saddle node when $-0.57 < \omega < 0.14$.

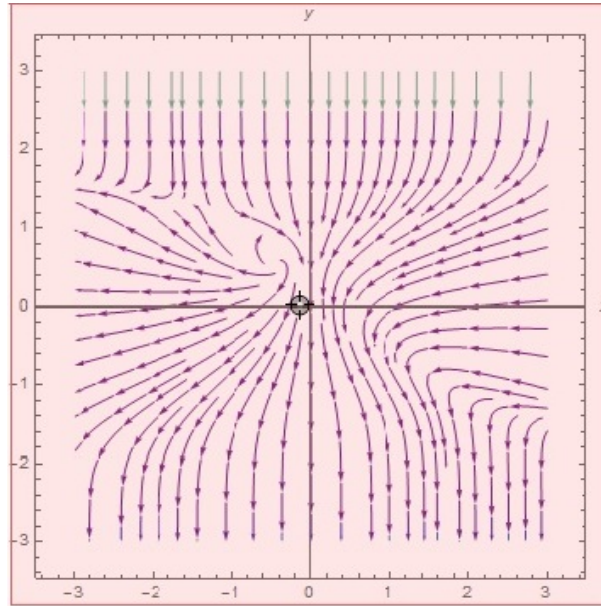


FIGURE 4.3: Phase plot corresponding to the point $(-0.1305, 0)$ (P_{11} in table 4.3) for $q = -0.53$, $n = 2$, $\omega = -0.8$ which shows that for the choices of aforesaid values of q , ω and n , $(-0.1305, 0)$ is a saddle node.

Similarly, as we consider, $q = -0.48$:

- For $n = 2$ (P_{16} table 4.3), the point $(\frac{1.22\epsilon+\omega}{\omega}, 0)$ is stable when $\omega < -1.11$, saddle node when $-1.11 < \omega < -0.64$ and unstable when $\omega > -0.64$.
- For $n = 3$ (P_{17} in table 4.3), the point $(\frac{1.22\epsilon+\omega}{\omega}, 0)$ becomes stable when $\omega < -0.77$, saddle node when $-0.77 < \omega < -0.64$ and unstable when $\omega > -0.64$.
- For $n \geq 4$ (P_{18}, P_{19}, P_{20} in table 4.3), $(\frac{1.22\epsilon+\omega}{\omega}, 0)$ will be a stable node when $\omega < -0.63$.

- For $n = 4$ (P_{18} in table 4.3), $(\frac{1.22\epsilon+\omega}{\omega}, 0)$ becomes an unstable node when $\omega > -0.42$ and saddle node when $-0.63 < \omega < -0.42$.
- For $n = 5$ (P_{19} in table 4.3), $(\frac{1.22\epsilon+\omega}{\omega}, 0)$ will be an unstable node when $\omega > -0.07$ and saddle node when $-0.63 < \omega < -0.07$.
- For $n = 6$ (P_{20} in table 4.3), $(\frac{1.22\epsilon+\omega}{\omega}, 0)$ turns into an unstable node when $\omega > 0.27$ and saddle node when $-0.63 < \omega < 0.27$.

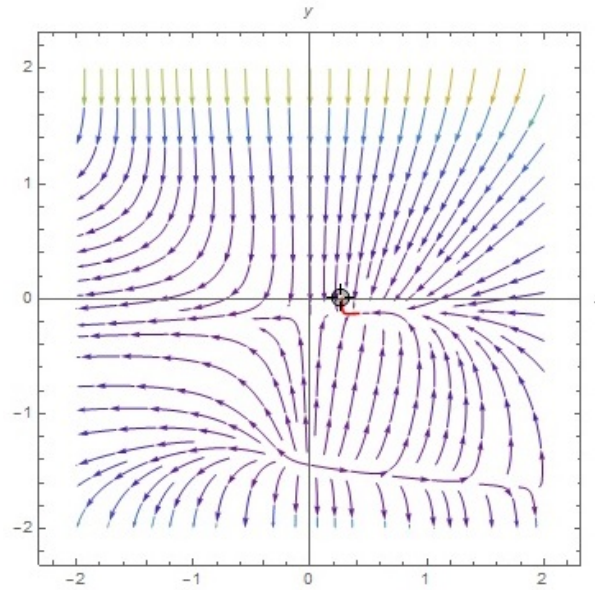


FIGURE 4.4: Phase plot corresponding to the point $(0.2695, 0)$ for $q = -0.48$, $n = 10$, $\omega = -0.87$ which shows that for the choices of aforesaid values of q , ω and n , $(0.2056, 0)$ is locally stable node.

Critical point $(0, 0.33\epsilon - 0.67\epsilon n + 1)$ and the eigenvalues corresponding to various choices of q and n are given in table 4.4. Here, the eigenvalues are dependent on the value of equation of state parameter, ω .

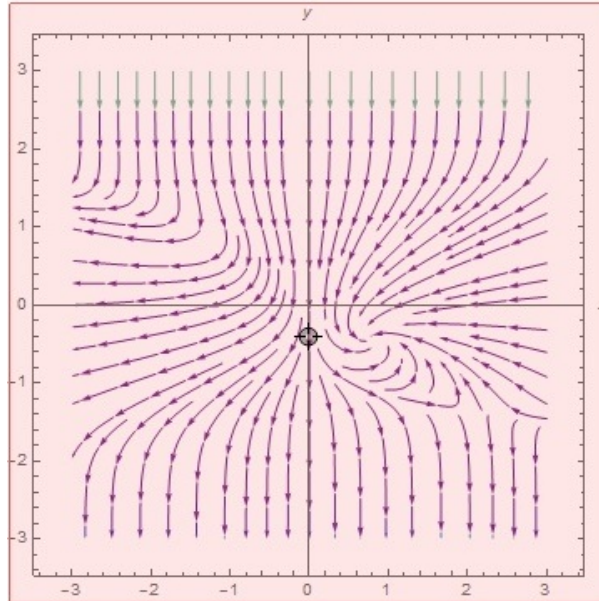
According to table 4.4, we can clearly observe that while we assume, $q = -0.53$:

- For $n = 2$ (P_{21} in table 4.4), the point $(0, 0.33\epsilon - 0.67\epsilon n + 1)$ is stable when $\omega > -1.1$ and saddle node when $\omega < -1.1$.
- For $n = 3$ (P_{22} in table 4.4), the point $(0, 0.33\epsilon - 0.67\epsilon n + 1)$ will be stable when $\omega > -0.78$ and saddle node when $\omega < -0.78$.

TABLE 4.4: For $q = -0.53$, $q = -0.48$ and for $n=2, 3, 4, 5, 6$, this table shows the eigenvalues corresponding to the critical point $(0, 0.33\epsilon - 0.67\epsilon n + 1)$.

No	q	ϵ	n	point	Eigenvalues
P_{21}	-0.53	0.47	2	(0,0.5253)	-3.3008- 3ω , -1.59
P_{22}	-0.53	0.47	3	(0,0.2104)	-2.3561- 3ω , -0.65
P_{23}	-0.53	0.47	4	(0,-0.1045)	-1.4114- 3ω , 0.29
P_{24}	-0.53	0.47	5	(0,-0.4194)	-0.4667- 3ω , 1.23
P_{25}	-0.48	0.52	2	(0,0.4748)	-3.3328- 3ω , -1.44
P_{26}	-0.48	0.52	3	(0,0.1264)	-2.2876- 3ω , -0.4
P_{27}	-0.48	0.52	4	(0,-0.2220)	-1.2424- 3ω , 0.64
P_{28}	-0.48	0.52	5	(0,-0.5704)	-0.1972- 3ω , 1.68

- For $n = 4$ (P_{23} in table 4.4), $(0, 0.33\epsilon - 0.67\epsilon n + 1)$ becomes a saddle node for $\omega > -0.47$ and an unstable node when $\omega < -0.47$.
- For $n = 5$ (P_{24} in table 4.4), $(0, 0.33\epsilon - 0.67\epsilon n + 1)$ will be a saddle node when $\omega > -0.15$ and an unstable node when $\omega < -0.15$.


 FIGURE 4.5: Phase plot corresponding to the point $(0, -0.4194)$ (P_{24} in table 4.4) for $q = -0.53$, $n = 5$, $\omega = -0.7$ which shows that for the choices of aforesaid values of q , ω and n , $(0, -0.4194)$ is an unstable node.

Similarly, as we take, $q = -0.48$:

- For $n = 2$ (P_{25} in table 4.4), the point $(0, 0.33\epsilon - 0.67\epsilon n + 1)$ is stable when $\omega > -1.11$ and saddle node when $\omega < -1.11$.

- For $n = 3$ (P_{26} in table 4.4), the point $(0, 0.33\epsilon - 0.67\epsilon n + 1)$ becomes stable when $\omega > -0.76$ and saddle node when $\omega < -0.76$.
- For $n = 4$ (P_{27} in table 4.4), $(0, 0.33\epsilon - 0.67\epsilon n + 1)$ turns to be a saddle node for $\omega > -0.41$ and an unstable node when $\omega < -0.41$.
- For $n = 5$ (P_{28} in table 4.4), $(0, 0.33\epsilon - 0.67\epsilon n + 1)$ will be a saddle node when $\omega > -0.06$ and an unstable node when $\omega < -0.06$.

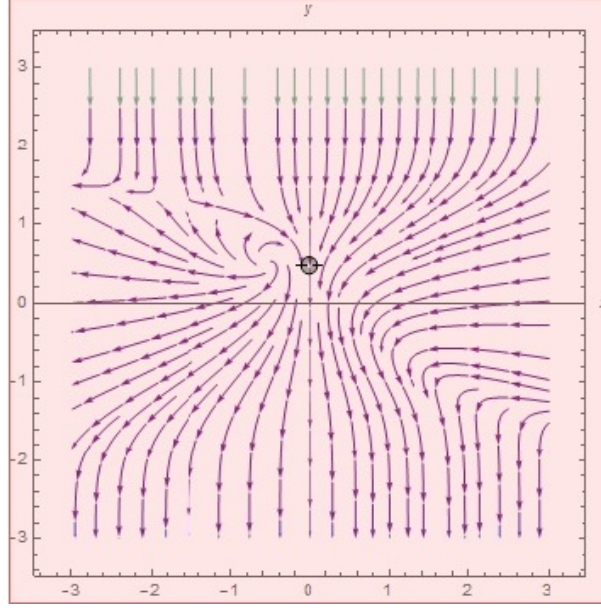


FIGURE 4.6: Phase plot corresponding to the point $(0, 0.4748)$ (P_{25} in table 4.4) for $q = -0.48$, $n = 2$, $\omega = -0.75$ which shows that for the choices of aforesaid values of q , ω and n , $(0, 0.4748)$ is locally stable node.

4.4.2 Autonomous system with equation of state parameter in terms of dimensionless variables

Here, equation of state parameter is denoted as

$$\omega = \frac{p}{\rho} = \frac{-2\dot{H} - 3H^2}{3H^2} \quad (4.26)$$

Using (4.18) and (4.19) in (4.26), we obtain

$$\omega \left(1 + \frac{f_2 \rho}{3H^2 F} \right) = -\frac{f_2 \rho}{3H^2 F} + \frac{2\dot{F}}{3FH} - 1 \quad (4.27)$$

With the help of the choices of $f_1(Q)$ and $f_2(Q)$ in (4.20) and dimensionless variables given in (4.21), (4.26) yields the expression for equation of state parameter ω as

$$\omega = \frac{-2x - \frac{8}{3}(n-1)^2\epsilon y + 1}{2x-1} \quad (4.28)$$

where ϵ is defined in (4.24). Substituting ω from (4.28) in (4.22) and (4.23), autonomous equations for this current model transform into

$$x' = -\frac{11}{3}\epsilon x - 3xy + \frac{9x^2}{2x-1} + \frac{8(n-1)^2\epsilon yx}{2x-1} - \frac{3x}{2x-1} - \frac{6x^3}{2x-1} - \frac{8(n-1)^2\epsilon yx^2}{2x-1} \quad (4.29)$$

$$y' = -y\epsilon(2n-1) - 3y^2 + 3y - \frac{6x^2y}{2x-1} + \frac{8(n-1)^2\epsilon xy^2}{2x-1} - \frac{3xy}{2x-1} \quad (4.30)$$

Here(') denotes the derivative with respect to $\eta = \ln a$. To study this model, we consider the value of deceleration parameter $q_0 = -0.55$ [131, 368, 380]. From the above autonomous system of differential equations, we find the critical points, given in table 4.5.

TABLE 4.5: Critical points corresponding to autonomous system (4.29), (4.30).

No	Point	(x, y)
1	A	$(0, 0)$
2	B	$(0, \frac{1}{3}(3.45 - 0.9n))$
3	C	$(0.45, 0)$

At those aforesaid critical points, we construct the linearized Jacobian matrix and corresponding to the Jacobian matrix, we obtain the eigenvalues and respective values of equation of state parameter ω , given in table 4.6.

TABLE 4.6: Eigenvalues corresponding to critical points A, B and C and the respective value of ω at those points.

Point	Eigenvalues	ω
A	$(1.35, 3.45 - 0.9n)$	-1
B	$(-3.45 + 0.9n, -6.24 + 10.26n - 6.3n^2 + 1.08n^3)$	$-1 + 0.4(3.45 - 0.9n)(n - 1)^2$
C	$(-1.35, 2.1 - 0.9n)$	-1

From table 4.6, we get that A is a unstable node while B becomes stable when $n < 3.68$ and C represents a stable node if $n > 2.33$.

Since corresponding to the critical point B , ω depends on the value of n and the point becomes stable for $n < 3.68$, choosing $n = 3.6$ yields equation of state parameter, $\omega = -0.43$.

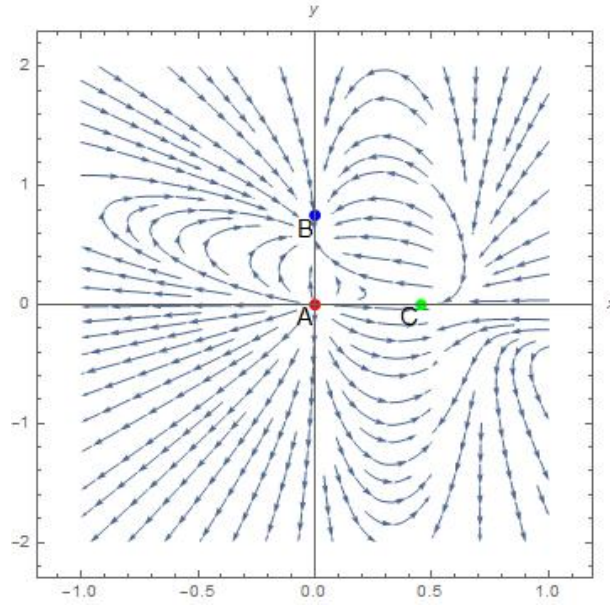


FIGURE 4.7: Phase plot presenting the behaviour of the trajectories for the model when $n = 2$ and $q_0 = -0.55$ which shows that A is unstable, B is stable and C is a saddle node for the aforesaid values of the parameter.

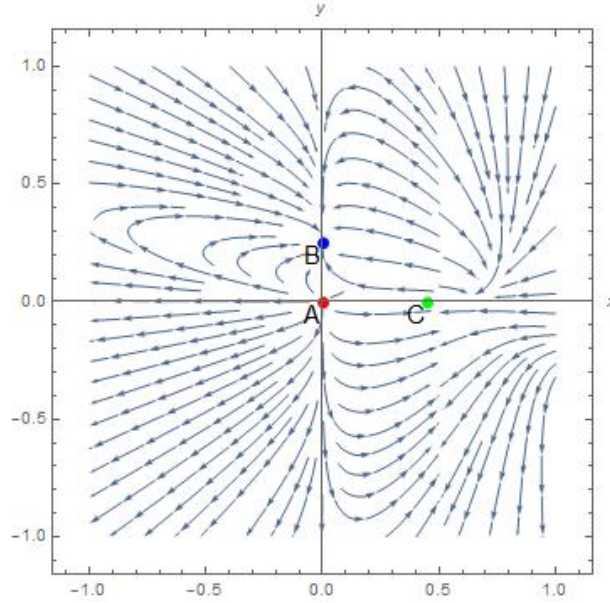


FIGURE 4.8: Phase plot presenting the behaviour of the trajectories for the model as $n = 3$ and $q_0 = -0.55$ which shows that A is unstable, B is stable and C is stable node for the aforesaid values of the parameter.

4.5 Summary and discussion

In this chapter, we have considered a cosmological model with modified gravity where non-metricity Q has been incorporated as gravitational interaction. We have employed symmetric teleparallel $f(Q)$ gravity and instead of considering action for normal $f(Q)$ gravity, we have taken the functional form of $f(Q)$ as a combination of two functions of non-metricity Q , namely $f_1(Q) = \alpha Q^n$ and $f_2(Q) = Q$ where $f_2(Q) = Q$ is coupled with the Lagrangian matter.

In subsection 4.4.1, we have considered two values of deceleration parameter q which is close to -0.5 corresponding to three critical points with various choices of n . We observe that the stability of critical points is not affected by the values of α . So, we ignore α in our analysis. Although we have used two different values of q , we see that if we change the value of q nearly around -0.5 , our analysis does not vary significantly.

From table 4.2, we see that critical point $(0, 0)$ is a stable node (Phase plot in figure 4.1) for any value of $n \geq 4$ ($P_3, P_4, P_5, P_8, P_9, P_{10}$ in table 4.2) corresponding to equation of state parameter $-0.63 < \omega$. So ω lies in the admissible range $-1 < \omega < -\frac{1}{3}$, representing quintessence behaviour.

Critical point $(\frac{1.22\epsilon+\omega}{\omega}, 0)$ is stable and represents observed accelerated expansion and the value of ω implies phantom behaviour for $n = 2$ (P_{11}, P_{16} in table 4.3). This node represents an accelerated universe for all other values of n ($P_{12}, P_{13}, P_{14}, P_{15}, P_{17}, P_{18}, P_{19}, P_{20}$ in table 4.3) and it indicates quintessence behaviour for these n . So, this critical point is very interesting and can represent a viable solution with late time acceleration.

Critical point $(0, 0.33\epsilon - 0.67\epsilon n + 1)$ is stable only for $n = 2$ (Phase plot in figure 4.6) and $n = 3$ ($P_{21}, P_{22}, P_{25}, P_{26}$ in table 4.4) as well as it may represent accelerated expansion depending on ω .

In subsection 4.4.2, we express the equation of state parameter in terms of dimensionless variables x, y but here, ω is also dependent on n and ϵ , so on q . Here also, we get three critical points for some particular choice of q which are dependent on n , given in table 4.5.

Though A is unstable, but ω being -1 , represents late time acceleration. Again critical point B and C both are stable with late time acceleration. Point C may represent Λ CDM model with $\omega = -1$. Here, for this chapter, we have not considered any particular fluid like radiation, baryon, dark energy or dust, rather we focused on general description of fluid.

Depending on ω , the dynamics of universe changes and we can say that this chapter incorporates late time acceleration very well. So, we can see that $f(Q)$ gravity models can be thought as an alternative to Λ CDM model.

Chapter 5

Dynamical system analysis on Rényi holographic dark energy

5.1 Introduction

Several dynamical dark energy models have been suggested to explain the current scenario of the universe. Among which, holographic dark energy models [151, 152, 153, 154, 155, 156, 157, 381, 382, 383, 384] play an important role in explaining the riddle of dark energy. Holographic dark energy models which are based on holographic principle, have received considerable attentions from researchers in context of quantum gravity.

In a cosmological context, the holographic principle imposes a fundamental upper limit on the total entropy. According to holographic principle, the total entropy enclosed within a region of size L must not surpass that of a black hole of the same scale. This implies that the vacuum energy within such a region must be constrained to avoid gravitational collapse, thereby maintaining consistency with the holographic bound. Guided by the Bekenstein bound, it is natural to impose that, for an effective quantum field theory confined to a region of size L with an ultraviolet (UV) cutoff Λ , the total entropy should respect the holographic limit-meaning it must not exceed the entropy of a black hole occupying the same volume. The total entropy

should satisfy the relation

$$L^3 \Lambda^3 \leq S_{BH} = \pi L^2 M_p^2 \quad (5.1)$$

where M_p is the reduced Plank mass and S_{BH} is the entropy of a black hole with radius L which is assumed as a long distance IR cut off. Miao Li [151] had suggested a more rigorous bound which tells that total energy of a region of size L must not surpass the mass of a black hole with same size.

As a result, this UV-IR relation provides an upper bound on the energy density

$$\rho_\Lambda \leq L^{-2} M_p^2 \quad (5.2)$$

Thus the holographic dark energy density is obtained as

$$\rho_\Lambda = \frac{3c^2 M_p^2}{L^2} \quad (5.3)$$

where c is a free dimensionless parameter.

It seems there is deep connection between dark energy, horizon entropy and laws of thermodynamics. Thus horizon entropy and dark energy candidates may influence one another from a thermodynamic perspective. Recently, generalized entropy formalisms have been widely used to study various cosmological and gravitational scenarios because of the unknown nature of spacetime, the long-range nature of gravity and the fact that the Bekenstein–Hawking entropy is a non-extensive entropy measure.

Amongst them the Rényi [184], Tsallis [181], Sharma–Mittal [191, 192], Kanidakis [163] entropies acquired considerable interest. Recently, using the Rényi entropy [184], Moradpour et. al. [177] has suggested a new type of DE model, called the Rényi holographic dark energy (RHDE) model, to understand the gravitational and cosmological incidences. Moradpour et al. has shown that if there is no interaction between the dark matter and energy then the RHDE model is more stable. Also, there are various other works on the RHDE [385, 386, 387, 388, 389].

The effectiveness of these attempts to describe the current accelerating universe encourages us to study cosmic evolution considering generalized entropies as the horizon entropy instead of the Bekenstein entropy. We will use this formalism to consider a HDE model in flat FRW spacetime with Rényi generalized entropy by

taking the Hubble radius as its IR cutoff.

5.2 Introduction of Rényi entropy in holographic dark energy

Rényi holographic dark energy model [177, 182] is connected to Rényi entropy [183, 184]. For a system with w discrete states, it is defined by

$$S_R = k \frac{\ln \sum_{i=1}^w p_i^q}{1 - q} \quad (5.4)$$

where q is a non extensive parameter, k is a positive constant and p_i is the probability for i th state. Rényi entropy reduces to standard Boltzmann-Gibbs entropy for $\lim q \rightarrow 1$. Using Tsallis entropy defined as

$$S_T = k \frac{1 - \sum_{i=1}^w p_i^q}{q - 1} \quad (5.5)$$

relation between Tsallis entropy and Rényi entropy can be written as

$$S_R = \frac{1}{\delta} \ln(1 + \delta S_T) \quad (5.6)$$

where $\delta = 1 - q$ is a parameter which measures whether the system is non-additive or not. To calculate the Rényi entropy related to black hole [187, 188, 189, 190], Tsallis entropy is considered as formal Bekenstein-Hawking entropy. As a result (5.6) is redefined as

$$S_R = \frac{1}{\delta} \ln(1 + \delta S_{BH}) \quad (5.7)$$

where S_{BH} is Bekenstein-Hawking entropy which is denoted as

$$S_{BH} = \frac{k_B c^3 A}{4 \hbar G} \quad (5.8)$$

where k_B , c , A , \hbar , G are respectively Boltzmann constant, speed of light, area of the black hole horizon, reduced Plank constant and Newton's gravitational constant.

Considering in natural units where $k_B = \hbar = c = G = 1$, it simplifies to:

$$S_{BH} = \frac{A}{4} \tag{5.9}$$

Assuming $A = 4\pi L^2$, where L is the IR cut off and using (5.9) , (5.7) transforms into

$$S_R = \frac{1}{\delta} \ln(1 + \pi\delta L^2) \tag{5.10}$$

Now, using the thermodynamic relation

$$TdS_R \propto \rho_d dV \tag{5.11}$$

Rényi holographic dark energy density is defined as

$$\rho_d = \frac{3d^2}{8\pi L^2} (1 + \pi\delta L^2)^{-1} \tag{5.12}$$

where d is a constant, δ is the non-extensive Rényi parameter and L is the IR cutoff. In this chapter, we will consider Rényi holographic dark energy with Hubble's cut off.

So, we will assume

$$L = \frac{1}{H} \tag{5.13}$$

where H is the Hubble's parameter. Considering equation (5.13), equation (5.12) changes to

$$\rho_d = \frac{3d^2}{8\pi} \frac{H^4}{H^2 + \pi\delta} \tag{5.14}$$

5.3 Basic equations

We assume the universe is homogeneous and isotropic on large scales and is described by the spatially flat Friedmann–Lemaître–Robertson–Walker (FLRW) metric with the line element:

$$ds^2 = dt^2 - a^2(t)(dr^2 + r^2 d\Omega^2) \tag{5.15}$$

where $a(t)$ is the scale factor and $d\Omega^2 = d\theta^2 + \sin^2\theta d\phi^2$ which denotes a two dimensional sphere.

In FLRW cosmology, matter density will follow the energy-momentum tensor pertaining to the perfect fluid, which is denoted by

$$T_{\mu\nu} = (p + \rho)u_\mu u_\nu - pg_{\mu\nu} \quad (5.16)$$

In this framework, u_μ is the four-velocity of the fluid, satisfying the normalization condition $u^\mu u_\mu = 1$ while the cosmic objects are characterized by their energy density ρ and pressure p . Here, we assume that the universe is filled with dark matter in the form of dust and dark energy in the form of Rényi holographic dark energy with variable equation of state parameter.

The Einstein field equations pertaining to the current cosmological model can be written as

$$3H^2 = \rho = \rho_m + \rho_d \quad (5.17)$$

$$2\dot{H} + 3H^2 = -p = -p_m - p_d \quad (5.18)$$

Equation (5.18) can be rewritten as

$$2\dot{H} = -\rho_m - (1 + \omega_d)\rho_d \quad (5.19)$$

Here ρ_m, ρ_d are the energy density of dark matter and holographic dark energy density while p_m, p_d denote the pressure of dark matter and holographic dark energy respectively. ω_d is the variable equation of state parameter pertaining to the holographic dark energy which is defined as $\omega_d = \frac{p_d}{\rho_d}$.

Using (5.17) and (5.19), acceleration of the universe is denoted by

$$\ddot{a} = -\frac{a}{6}[\rho_m + p_d(1 + 3\omega_d)] \quad (5.20)$$

which shows that for cosmic acceleration, $\omega_d < -\frac{1}{3}$. Dark matter and dark energy components satisfy the continuity equation individually as

$$\dot{\rho}_m + 3H\rho_m = 0 \quad (5.21)$$

and

$$\dot{\rho}_d + 3H(1 + \omega_d)\rho_d = 0 \quad (5.22)$$

Considering the interaction term between two dark components, the continuity equations transform into

$$\dot{\rho}_m + 3H\rho_m = Q \quad (5.23)$$

$$\dot{\rho}_d + 3H(1 + \omega_d)\rho_d = -Q \quad (5.24)$$

The interaction term Q is not uniquely determined; however, we adopt the choice $Q > 0$, implying an energy flow from dark energy to dark matter i.e., dark energy decays into dark matter. This positive sign of Q supports the second law of thermodynamics by ensuring non-decreasing entropy and also contributes toward addressing the coincidence problem. It is worth mentioning that baryonic matter is excluded from the interaction, as such couplings are tightly constrained by local gravitational observations [390, 391, 392].

In our current work, we have considered four different types of interaction terms which include both linear and non-linear interaction terms, namely:

- $Q = 3H(\rho_m + \rho_d)$.
- $Q = 3H\rho_d$.
- $Q = 3H\rho_m$.
- $Q = 3H\frac{\rho_d}{\rho_m + \rho_d}$.

5.4 Rényi holographic dark energy model with Hubble horizon as IR cut off (without interaction)

In the present study, we explore a dynamical dark energy model comprising both dark energy and dark matter, under the assumption that there is no interaction between them. The dark energy component is described by the Rényi holographic dark energy which is the exclusive source of dark energy where the Hubble horizon is employed as the infrared (IR) cutoff.

We would like to study aforesaid model by using dynamical system tools, as the field

equations derived here will be very complex and non-linear in nature. Let us introduce the dimensionless variables :

$$x = \frac{\rho_m}{3H^2}, \quad y = \frac{\rho_d}{3H^2} \tag{5.25}$$

Here, matter and energy density parameters are defined as

$$\Omega_m = \frac{\rho_m}{3H^2} = x, \quad \Omega_d = \frac{\rho_d}{3H^2} = y \tag{5.26}$$

Using equation (5.17) and (5.26), we can deduce that

$$\Omega_m + \Omega_d = x + y = 1 \tag{5.27}$$

By employing equations (5.17), (5.21), (5.22), (5.25) and (5.27), we derive the corresponding autonomous system of differential equations as follows:

$$\begin{aligned} \frac{dx}{dN} &= 3xy\omega_d \\ \frac{dy}{dN} &= -3y(1-y)\omega_d \end{aligned} \tag{5.28}$$

Now, Using (5.14), from (5.22), we can obtain the equation of state parameter, ω_d for Rényi HDE as

$$\omega_d = -1 - \frac{4}{3} \frac{\dot{H}}{H^2} + \frac{2}{3} \frac{\dot{H}}{H^2 + \pi\delta} \tag{5.29}$$

From (5.19), we deduce the value of $\frac{\dot{H}}{H^2}$ as

$$\frac{\dot{H}}{H^2} = -\frac{3}{2}(1 + y\omega_d) \tag{5.30}$$

Using (5.30) in (5.29), equation of state parameter pertaining to Rényi HDE can be simplified as

$$\omega_d = \frac{1 + \frac{2}{3} \frac{\dot{H}}{H^2 + \pi\delta}}{1 - 2y} \tag{5.31}$$

For analyzing the cosmological model, we have to transform the nonlinear autonomous system presented in equation (5.28) into a simplified form by substituting

ω_d from equation (5.31). For such purpose, we are introducing a function of dimensionless variables x and y as

$$\lambda(x, y) = \frac{\dot{H}}{H^2 + \pi\delta} \quad (5.32)$$

In this section, where we study the Rényi HDE model without interaction, we consider two different choices of $\lambda(x, y)$ as:

- $\lambda(x, y) = \alpha x + \beta y$.
- $\lambda(x, y) = e^{\alpha x + \beta y}$.

Here α and β are two arbitrary constants.

5.4.1 Analysis of non-interacting Rényi HDE with $\lambda(x, y) = \alpha x + \beta y$

Substituting ω_d from (5.31) and considering $\lambda(x, y) = \alpha x + \beta y$, (5.28) reduces to

$$\begin{aligned} \frac{dx}{dN} &= \frac{3xy + 2xy(\alpha x + \beta y)}{1 - 2y} \\ \frac{dy}{dN} &= \frac{-3y(1 - y) - 2y(1 - y)(\alpha x + \beta y)}{1 - 2y} \end{aligned} \quad (5.33)$$

and

$$\omega_d = \frac{1 + \frac{2}{3}(\alpha x + \beta y)}{1 - 2y} \quad (5.34)$$

To perform dynamical system analysis, we need to identify the critical points corresponding to the autonomous system (5.33). To find out the critical points of the system, we need to solve the system of algebraic equations :

$$\begin{aligned} \frac{dx}{dN} &= 0 \\ \frac{dy}{dN} &= 0 \end{aligned} \quad (5.35)$$

The critical points of the said autonomous system (5.33) have been listed in table 5.1.

TABLE 5.1: Set of critical points and their coordinates.

Critical Points	Coordinates (x, y)
A	$(0, 1)$
A_1	$(1, 0)$
A_2	$\left(\frac{3\beta}{2\alpha^2}, 0\right)$
A_3	$\left(0, -\frac{3}{2\beta}\right)$
A_4	$\left(\frac{\beta+\frac{3}{2}}{\beta-\alpha}, \frac{-\alpha-\frac{3}{2}}{\beta-\alpha}\right)$

The eigenvalues corresponding to each critical point is obtained from the linearized Jacobian matrix and are summarized in table 5.2.

TABLE 5.2: Critical points and their corresponding eigenvalues, obtained from the linearized Jacobian matrix.

Critical Points	Eigenvalues
A	$(-3 - 2\beta, -3 - 2\beta)$
A_1	$(-3 - 2\alpha, 0)$
A_2	$\left(0, \frac{-3\alpha - 3\beta}{\alpha}\right)$
A_3	$\left(0, \frac{9+2\beta}{6+2\beta}\right)$
A_4	$\left(0, \frac{6\alpha+6\beta+4\alpha\beta}{2\beta+2\alpha+6}\right)$

Let us now study the characteristics of the critical points along with their stability criteria. We will also study the behaviour of physical parameters corresponding to the critical points.

- Critical point A becomes a stable node when $\beta > -\frac{3}{2}$ and unstable otherwise. Equation of the state parameter, $\omega_d < 0$ when A is stable. For $\beta = 0$, we get $\omega_d = -1$, i.e., the stable node is representing Λ CDM. The fluid description is like phantom pertaining to Rényi HDE when $\beta > 0$ and the fluid description is like quintessence when $-\frac{3}{2} < \beta < 0$. The universe experiences an accelerated expansion when $\beta > -1$. So, the stable node always represents either phantom or quintessence like fluid description of universe pertaining to Rényi HDE without interaction.

Around the critical point, universe is completely dark energy dominated as the matter density, $\Omega_m = 0$ and the dark energy density pertaining to HDE, $\Omega_d = 1$.

Figure 5.1 shows that for $\beta = -0.1$ which lies in between $(-\frac{3}{2}, 0)$, A is a stable node with equation of state parameter, $\omega_d = -0.93$ which depicts the quintessence like fluid with accelerated expansion. The parameter d which is

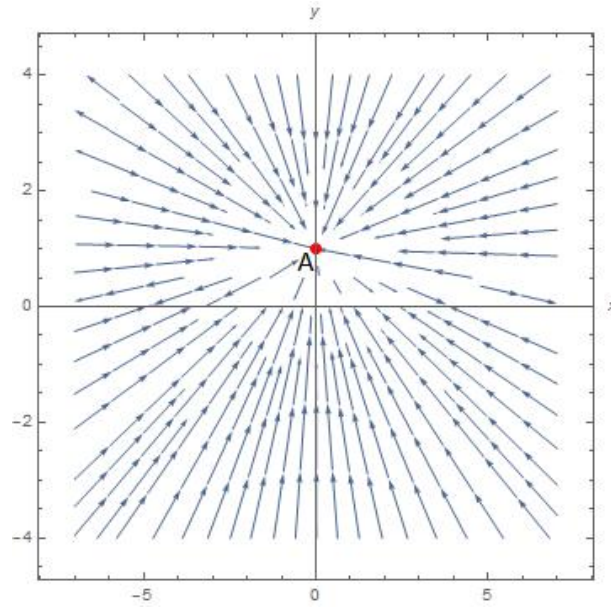


FIGURE 5.1: Phase plot corresponding to the point $(0, 1)$ for $\alpha = 0.2$, $\beta = -0.1$

there in the Rényi holographic dark energy density corresponding to (5.14) does not impact much in our model. But $\frac{\pi\delta}{H^2}$ can be evaluated by using (5.31) and (5.32) as -0.3 at the critical point A for $\beta = -0.1$ and $w_d = -0.93$.

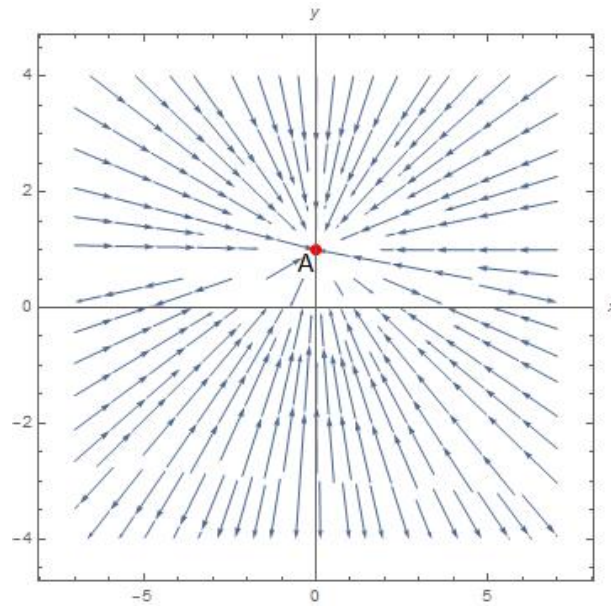


FIGURE 5.2: Phase plot corresponding to the point $(0, 1)$ for $\alpha = 0.02$, $\beta = 0.5$

Figure 5.2 shows that for $\beta = 0.5 > 0$, A represents a stable node with equation of state parameter, $\omega_d = -1.33$ which depicts the phantom like fluid with

accelerated expansion. Here, $\frac{\pi\delta}{H^2}$ can also be evaluated by using (5.31) and (5.32) as -0.34 at the critical point A for $\beta = 0.5$ and $w_d = -1.33$. So, we can conclude here that the value of δ is negative. Figure 5.3 shows that for

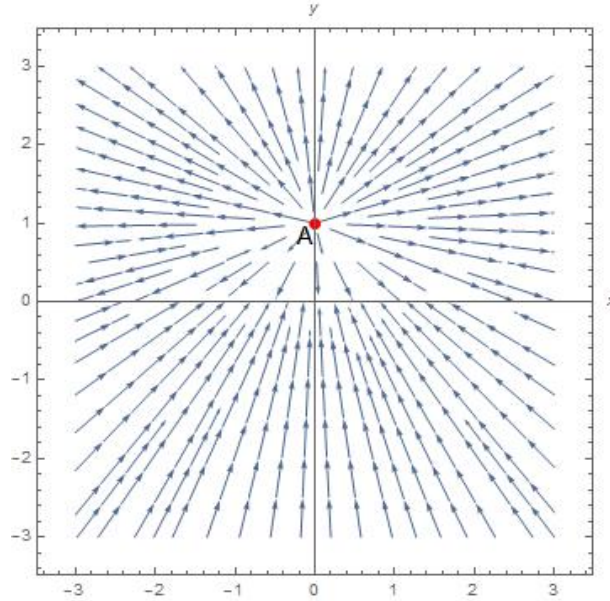


FIGURE 5.3: Phase plot corresponding to the point $(0, 1)$ for $\alpha = -0.2$, $\beta = -2.5$

$\beta = -2.5 < -\frac{3}{2}$, A represents an unstable node with equation of state parameter $\omega_d = 0.66$. Figure 5.4 shows that for $\beta = -0.75$ which lies in between $(-\frac{3}{2}, 0)$, A represents a stable node with equation of state parameter $\omega_d = -0.5$ which depicts the quintessence like fluid with accelerated expansion.

So, more we are shifting the value of β from 0 towards -1 , the value of equation of state parameter increases from -1 towards -0.33 and represents the quintessence like fluid description with accelerating nature of the universe. Figure 5.5 shows that there is a transition from phantom to quintessence era and it also shows the existence of dark energy dominated era and the source of dark energy is influenced here by Rényi HDE.

- Critical points A_1, A_2, A_3, A_4 are non hyperbolic in nature as they are having one of the eigenvalues with zero real part. So, we can not analyze them because the current linearization tools which we are using here fail to provide any conclusive information regarding non-hyperbolic points.

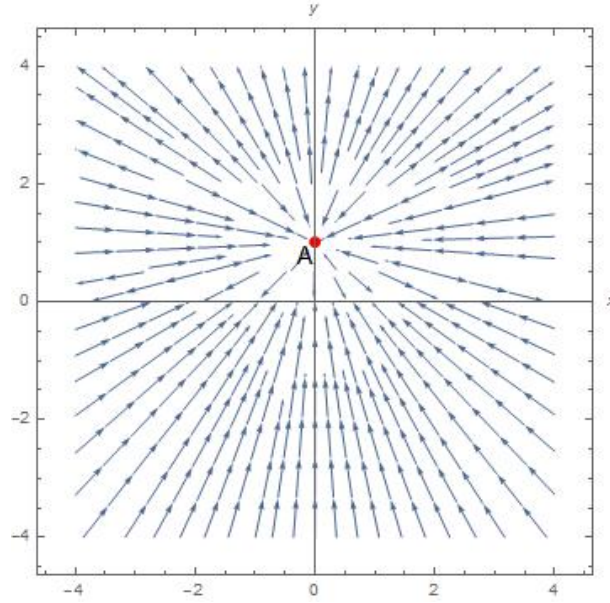


FIGURE 5.4: Phase plot corresponding to the point $(0, 1)$ for $\alpha = -0.02$, $\beta = -0.75$

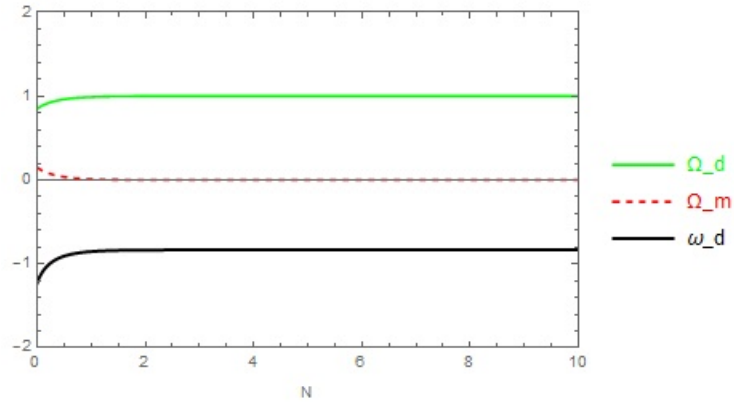


FIGURE 5.5: Evolution of cosmological parameters corresponding to the point $(0, 1)$ for $\alpha = 0.2$, $\beta = -0.25$

5.4.2 Analysis of non-interacting Rényi HDE with $\lambda(x, y) = e^{\alpha x + \beta y}$

Substituting ω_d from (5.31) and considering $\lambda(x, y) = e^{\alpha x + \beta y}$, (5.28) reduces to

$$\begin{aligned} \frac{dx}{dN} &= \frac{3xy + 2xye^{\alpha x + \beta y}}{1 - 2y} \\ \frac{dy}{dN} &= \frac{-3y(1 - y) - 2y(1 - y)e^{\alpha x + \beta y}}{1 - 2y} \end{aligned} \quad (5.36)$$

and

$$\omega_d = \frac{1 + \frac{2}{3}e^{\alpha x + \beta y}}{1 - 2y} \tag{5.37}$$

To perform dynamical system analysis, we need to identify the critical points corresponding to the autonomous system (5.36). The critical points of the said autonomous system (5.36) have been listed in table 5.3. The eigenvalues correspond-

TABLE 5.3: Set of critical points and their coordinates.

Critical Points	Coordinates (x, y)
B	$(0, 1)$
B_1	$(1, 0)$

ing to each critical point are obtained from the linearized Jacobian matrix and are summarized in table 5.4.

TABLE 5.4: Critical points and their corresponding eigenvalues, obtained from the linearized Jacobian matrix.

Critical Points	Eigenvalues
B	$(-3 - e^{2\beta}, -3 - e^{2\beta})$
B_1	$(0, -3 - e^{2\alpha})$

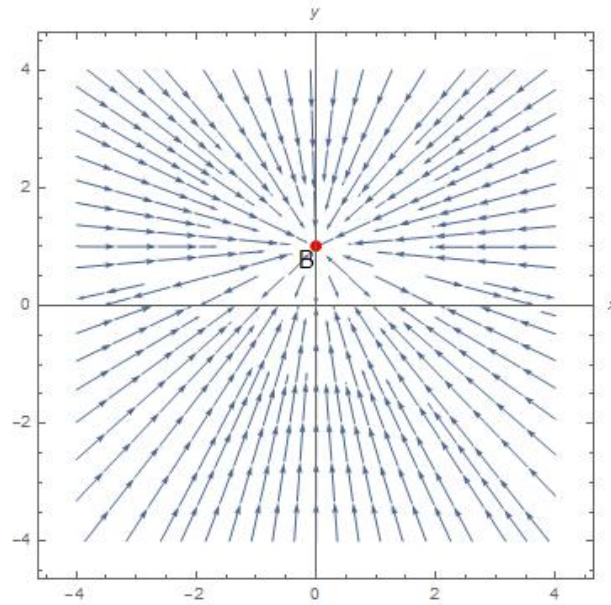
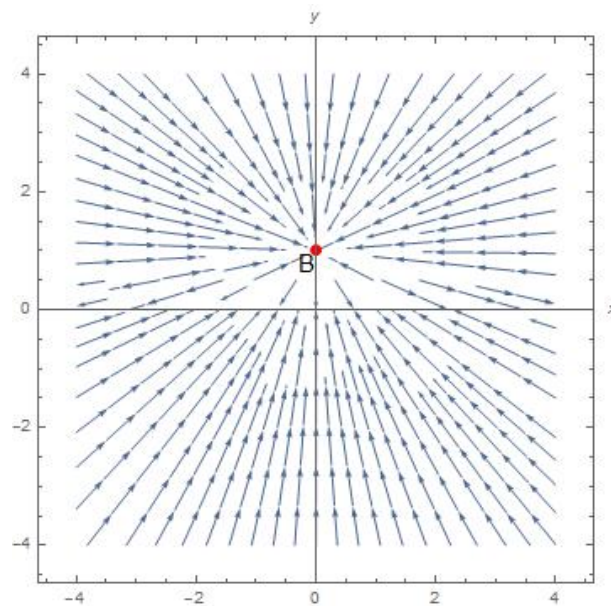
Now, we investigate the characteristics of the critical points along with their stability criteria. We will also study the behaviour of physical parameters corresponding to the critical points.

- Critical point B becomes a stable node for any $\beta \in \mathbb{R}$. Equation of the state parameter is always less than -1, i.e., $\omega_d < -1$. So, the fluid description is always like phantom pertaining to Rényi HDE. System around this critical point always indicates towards the accelerated expansion of the universe.

Around the critical point, universe is completely dark energy dominated as the matter density, $\Omega_m = 0$ and the dark energy density pertaining to HDE, $\Omega_d = 1$.

Figure 5.6 shows that B is a stable node with equation of state parameter $\omega_d = -2.81$ which depicts the phantom like fluid with accelerated expansion. Figure 5.7 shows that B represents a stable node with equation of state parameter $\omega_d = -1.31$ which depicts the phantom like fluid with accelerated expansion.

More over, we find that as the value of the parameter β decreases from 1, equation of state parameter, ω_d approaches asymptotically towards -1. Figure 5.8

FIGURE 5.6: Phase plot corresponding to the point $(0, 1)$ for $\alpha = 2, \beta = 1$ FIGURE 5.7: Phase plot corresponding to the point $(0, 1)$ for $\alpha = 0.25, \beta = -0.75$

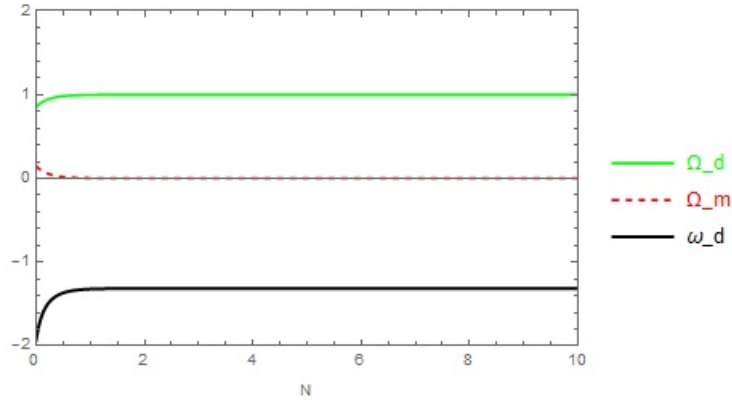


FIGURE 5.8: Evolution of cosmological parameters corresponding to the point $(0, 1)$ for $\alpha = 0.25$, $\beta = -0.75$

shows that equation of state parameter increases towards -1 and it also shows the existence of dark energy dominated era and the source of dark energy is influenced here by Rényi HDE.

- Critical point B_1 is non hyperbolic in nature as one of its eigenvalues possesses a vanishing real part. So we are not studying it's nature in details in our present work.

5.5 Rényi holographic dark energy model with Hubble horizon as IR cut off (with interaction)

In this section, we would like to consider interaction between matter and energy and we want to study the behaviour of our cosmological model. Here, we are considering both linear and nonlinear interactions without coupling constant.

5.5.1 Analysis of interacting Rényi HDE with linear interaction $Q = 3H(\rho_m + \rho_d)$

Here, we study our said model with Rényi HDE considering a linear interaction Q in the form of

$$Q = 3H(\rho_m + \rho_d) \quad (5.38)$$

By using (5.38), equations (5.23) and (5.24) transform into

$$\dot{\rho}_m = 3H\rho_d \quad (5.39)$$

and

$$\dot{\rho}_d = -6H\rho_d - 3H\rho_d\omega_d - 3H\rho_m \quad (5.40)$$

By incorporating the dimensionless variables defined in (5.25) and using the equations (5.30), (5.39) and (5.40), we obtain the following system of autonomous equations.

$$\begin{aligned} \frac{dx}{dN} &= 3 + 3xy\omega_d \\ \frac{dy}{dN} &= -3 - 3y(1-y)\omega_d \end{aligned} \quad (5.41)$$

Now, using (5.14) and (5.30), from (5.40), we obtain the equation of state parameter, ω_d for Rényi HDE as

$$\omega_d = \frac{\frac{2}{3}\frac{\dot{H}}{H^2+\pi\delta} - \frac{x}{y}}{1-2y} \quad (5.42)$$

Here, we assume as earlier $\lambda(x, y) = \frac{\dot{H}}{H^2+\pi\delta}$. Here, we are assuming only one choice of $\lambda(x, y)$, given by

$$\lambda(x, y) = \alpha x + \beta y \quad (5.43)$$

as the choice of an exponential function like previous case is not giving us any viable critical points. By using (5.42) and (5.43), our system of autonomous equations (5.41) transforms into

$$\begin{aligned} \frac{dx}{dN} &= 3 + \frac{2xy(\alpha x + \beta y) - 3x^2}{1-2y} \\ \frac{dy}{dN} &= -3 + \frac{-2y(1-y)(\alpha x + \beta y) + 3x(1-y)}{1-2y} \end{aligned} \quad (5.44)$$

The critical points of this autonomous system are enlisted in table 5.5.

TABLE 5.5: Set of critical points and their coordinates.

Critical Points	Coordinates (x, y)
C	$(1, 0)$
D_1	$(1 - \frac{3+4\alpha-2\beta+\sqrt{9+24\alpha-12\beta+4\beta^2}}{4(\alpha-\beta)}, \frac{3+4\alpha-2\beta+\sqrt{9+24\alpha-12\beta+4\beta^2}}{4(\alpha-\beta)})$
D_2	$(1 - \frac{3+4\alpha-2\beta-\sqrt{9+24\alpha-12\beta+4\beta^2}}{4(\alpha-\beta)}, \frac{3+4\alpha-2\beta-\sqrt{9+24\alpha-12\beta+4\beta^2}}{4(\alpha-\beta)})$

Now, we study the characteristics of the system around the critical points and we will also study the evolution of the cosmological parameters.

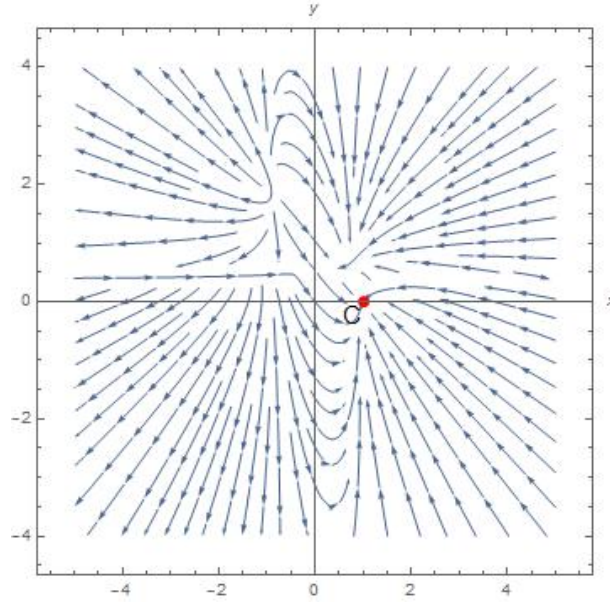
- For critical point C , we evaluate the eigenvalues from the linearized Jacobian matrix which is formed from the autonomous system (5.44). Both the eigenvalues corresponding to C are $(-3, -2\alpha)$ which indicates that C is a stable node for any $\alpha > 0$. Equation of the state parameter is undefined here. So, we can't conclude anything regarding acceleration corresponding to the said critical point.

Around the critical point, universe is completely dark matter dominated as the matter density, $\Omega_m = 1$ and the dark energy density pertaining to HDE, $\Omega_d = 0$. Figure 5.9 shows that C is locally stable for $\alpha = 4 > 0$.

- It is very difficult to calculate the eigenvalues corresponding to D_1 and D_2 . For this we are having different choices of the values of parameters α , β and corresponding to those values, we are representing respective points associated to D_1 and D_2 along with their eigenvalues and different cosmological parametric values in table 5.6 and table 5.7 respectively.

TABLE 5.6: Eigenvalues and the value of other cosmological parameters corresponding to D_1 for different choices of α and β

Choices of (α, β)	D_1	Eigenvalues	Ω_m	Ω_d	ω_d
$(0, -3)$	$(-\frac{1}{2}, \frac{3}{2})$	$(6, \frac{27}{4})$	$-\frac{1}{2}$	$\frac{3}{2}$	1.33
$(-4, -3.5)$	$(-1, 2)$	$(\frac{4}{3}, 3)$	-1	2	0.5
$(\frac{2}{3}, 3)$	$(\frac{3}{2}, -\frac{1}{2})$	$(-2, \frac{5}{4})$	$\frac{3}{2}$	$-\frac{1}{2}$	1.33
$(5, 2)$	$(-\frac{3}{2}, \frac{5}{2})$	$(2, \frac{55}{8})$	$-\frac{3}{2}$	$\frac{5}{2}$	0.26

FIGURE 5.9: Phase plot corresponding to the point $(1, 0)$ for $\alpha = 4$, $\beta = 0.25$ TABLE 5.7: Eigenvalues and the value of other cosmological parameters corresponding to D_2 for different choices of α and β

Choices of (α, β)	D_2	Eigenvalues	Ω_m	Ω_d	ω_d
$(0, -3)$	$(1, 0)$	$(-3, 0)$	1	0	Undetermined
$(-4, -3.5)$	$(-3, 4)$	$(-\frac{8}{7}, 1)$	-3	4	0.08
$(\frac{2}{3}, 3)$	$(\frac{3}{7}, \frac{4}{7})$	$(-\frac{228}{7}, -\frac{65}{7})$	$\frac{3}{7}$	$\frac{4}{7}$	-4.08
$(5, 2)$	$(\frac{1}{3}, \frac{2}{3})$	$(-22, -9)$	$\frac{1}{3}$	$\frac{2}{3}$	-4.5

Figure 5.10 shows that $D_1(\frac{3}{2}, -\frac{1}{2})$ is a saddle node while $D_2(\frac{3}{7}, \frac{4}{7})$ is locally stable for $\alpha = \frac{2}{3}$, $\beta = 3$. Figure 5.11 shows that $D_1(-\frac{3}{2}, \frac{5}{2})$ is an unstable node while $D_2(\frac{1}{3}, \frac{2}{3})$ is locally stable for $\alpha = 5$, $\beta = 2$.

From here we can comment that for positive values of α and β , D_1 is saddle or unstable while D_2 is becoming stable and D_2 represents a phantom like fluid description while it is stable with accelerated nature of the universe.

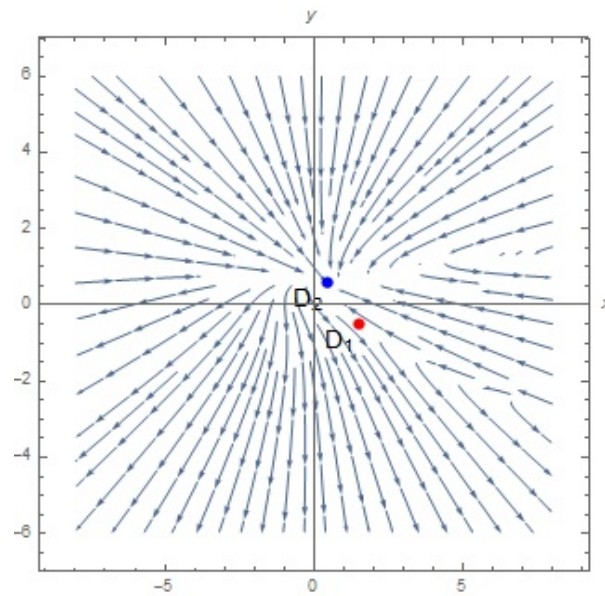


FIGURE 5.10: Phase plot corresponding to the point $D_1(\frac{3}{2}, -\frac{1}{2})$ and $D_2(\frac{3}{7}, \frac{4}{7})$ for $\alpha = \frac{2}{3}, \beta = 3$

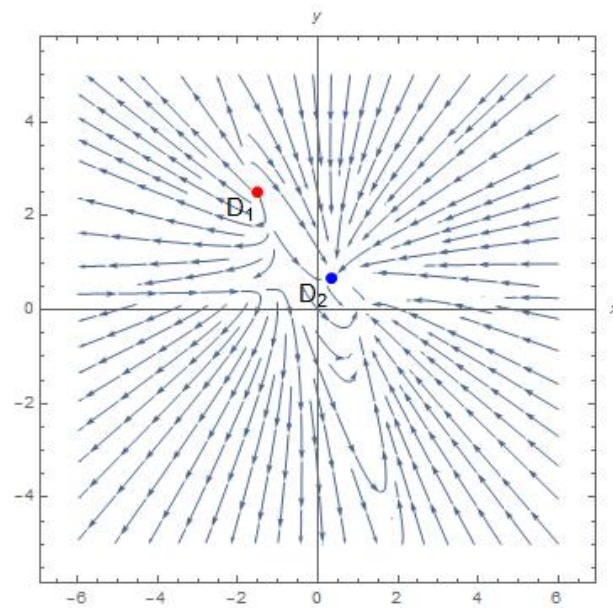


FIGURE 5.11: Phase plot corresponding to the point $D_1(-\frac{3}{2}, \frac{5}{2})$ and $D_2(\frac{1}{3}, \frac{2}{3})$ for $\alpha = 5, \beta = 2$

5.5.2 Analysis of interacting Rényi HDE with linear interaction $Q = 3H\rho_d$

Here, we study our said model with Rényi HDE considering a linear interaction Q in the form of

$$Q = 3H\rho_d \quad (5.45)$$

Using (5.45), equations (5.23) and (5.24) transform into

$$\dot{\rho}_m = -3H\rho_m + 3H\rho_d \quad (5.46)$$

and

$$\dot{\rho}_d = -6H\rho_d - 3H\rho_d\omega_d \quad (5.47)$$

Upon incorporating the dimensionless variables, defined in (5.25) and using the equations (5.30), (5.46) and (5.47), we obtain the following system of autonomous equations.

$$\begin{aligned} \frac{dx}{dN} &= 3y + 3xy\omega_d \\ \frac{dy}{dN} &= -3y - 3y(1-y)\omega_d \end{aligned} \quad (5.48)$$

Now, using (5.14) and (5.30), from (5.47), we obtain the equation of state parameter, ω_d for Rényi HDE as

$$\omega_d = \frac{\frac{2}{3}\frac{\dot{H}}{H^2+\pi\delta}}{1-2y} \quad (5.49)$$

Here, we again assume $\lambda(x, y) = \frac{\dot{H}}{H^2+\pi\delta}$. Here, we are also assuming only one choice of $\lambda(x, y)$, defined by

$$\lambda(x, y) = \alpha x + \beta y \quad (5.50)$$

as the choice of an exponential function like previous case is not giving us any viable critical points. By using (5.49) and (5.50), our system of autonomous equations (5.48) transforms into

$$\begin{aligned} \frac{dx}{dN} &= 3y + \frac{2xy(\alpha x + \beta y)}{1-2y} \\ \frac{dy}{dN} &= -3y + \frac{-2y(1-y)(\alpha x + \beta y)}{1-2y} \end{aligned} \quad (5.51)$$

The critical points of this autonomous system are enlisted in table 5.8.

TABLE 5.8: Set of critical points and their coordinates.

Critical Points	Coordinates (x, y)
E	$(0, 0)$
E'	$(0, 1)$
E_1	$(1 - \frac{3+2\alpha-\beta+\sqrt{9+6\alpha+\beta^2}}{2(\alpha-\beta)}, \frac{3+2\alpha-\beta+\sqrt{9+6\alpha+\beta^2}}{2(\alpha-\beta)})$
E_2	$(1 - \frac{3+2\alpha-\beta-\sqrt{9+6\alpha+\beta^2}}{2(\alpha-\beta)}, \frac{3+2\alpha-\beta-\sqrt{9+6\alpha+\beta^2}}{2(\alpha-\beta)})$

Now, we study the characteristics of the system around the critical points and we will also study the evolution of the cosmological parameters.

- For critical point E and E' , we evaluate the eigenvalues from the linearized Jacobian matrix which is formed from the autonomous system (5.51). Both the eigenvalues corresponding to E are $(-3, 0)$ and eigenvalues corresponding to E' are $(-2\alpha - 3, 0)$.

So, here both these critical points are non-hyperbolic in nature. Hence, we won't study them in this thesis.

- It is very difficult to calculate the eigenvalues corresponding to E_1 and E_2 . For this we are having different choices of the values of parameters α , β and corresponding to those values, we are representing respective points associated to E_1 and E_2 along with their eigenvalues and different cosmological parametric values in table 5.9 and table 5.10 respectively.

TABLE 5.9: Eigenvalues and the values of other cosmological parameters corresponding to E_1 for different choices of α and β

Choices of (α, β)	E_1	Eigenvalues	Ω_m	Ω_d	ω_d
$(15, 1)$	$(-\frac{1}{2}, \frac{3}{2})$	$(9, 15)$	$-\frac{1}{2}$	$\frac{3}{2}$	2
$(6, -2)$	$(-\frac{1}{2}, \frac{3}{2})$	$(\frac{21}{2}, 9)$	$-\frac{1}{2}$	$\frac{3}{2}$	2
$(-3, -5)$	$(-\frac{1}{2}, \frac{3}{2})$	$(6, 9)$	$-\frac{1}{2}$	$\frac{3}{2}$	2
$(4.5, 0)$	$(-1, 2)$	$(6, 8)$	-1	2	1

TABLE 5.10: Eigenvalues and the values of other cosmological parameters corresponding to E_2 for different choices of α and β

Choices of (α, β)	E_2	Eigenvalues	Ω_m	Ω_d	ω_d
(15, 1)	$(\frac{3}{14}, \frac{11}{14})$	$(-\frac{55}{2}, -11)$	$\frac{3}{14}$	$\frac{11}{14}$	-4.66
(6, -2)	$(\frac{3}{8}, \frac{5}{8})$	$(-35, -5)$	$\frac{3}{8}$	$\frac{5}{8}$	-2.66
(-3, -5)	$(\frac{3}{2}, -\frac{1}{2})$	$(-2, 1)$	$\frac{3}{2}$	$-\frac{1}{2}$	-0.66
(4.5, 0)	$(\frac{1}{3}, \frac{2}{3})$	$(-24, -6)$	$\frac{1}{3}$	$\frac{2}{3}$	-3

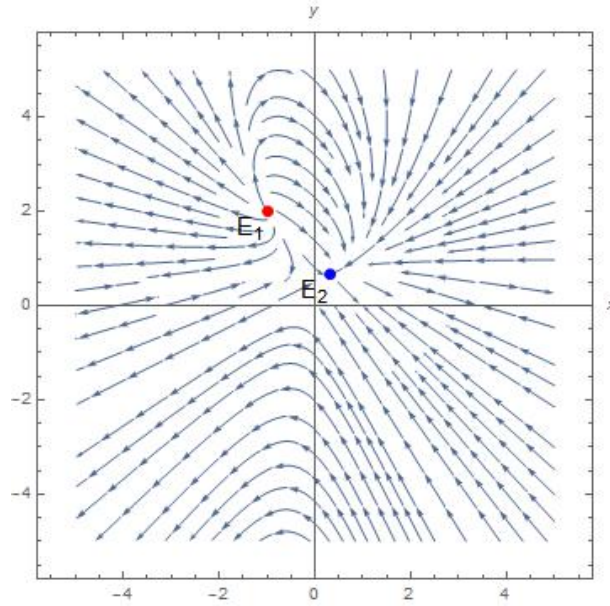

 FIGURE 5.12: Phase plot corresponding to the point $E_1(-1, 2)$ and $E_2(\frac{1}{3}, \frac{2}{3})$ for $\alpha = 4.5, \beta = 0$

Figure 5.12 shows that $E_1(-1, 2)$ is a saddle node while $E_2(\frac{1}{3}, \frac{2}{3})$ is locally stable for $\alpha = 4.5, \beta = 0$.

Figure 5.13 shows that $E_1(-\frac{1}{2}, \frac{3}{2})$ is an unstable node while $E_2(\frac{3}{8}, \frac{5}{8})$ is locally stable for $\alpha = 6, \beta = -2$.

From here we can comment that E_1 is unstable or saddle and E_2 is stable for any β when $\alpha > 0$.

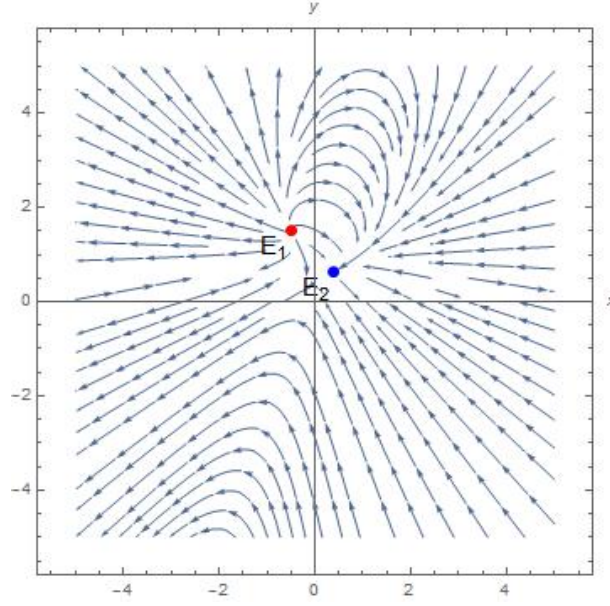


FIGURE 5.13: Phase plot corresponding to the point $E_1(-\frac{1}{2}, \frac{3}{2})$ and $E_2(\frac{3}{8}, \frac{5}{8})$ for $\alpha = 6$, $\beta = -2$

5.5.3 Analysis of interacting Rényi HDE with linear interaction $Q = 3H\rho_m$

Here, we consider a linear interaction Q in the form of

$$Q = 3H\rho_m \quad (5.52)$$

By using (5.52), equations (5.23) and (5.24) change into

$$\begin{aligned} \dot{\rho}_m &= -3H\rho_m + 3H\rho_m \\ \implies \dot{\rho}_m &= 0 \end{aligned} \quad (5.53)$$

and

$$\dot{\rho}_d = -3H\rho_d - 3H\rho_d\omega_d - 3H\rho_m \quad (5.54)$$

Using the dimensionless variables defined in (5.25) and the equations (5.30), (5.53) and (5.54), we obtain the following system of autonomous equations.

$$\begin{aligned}\frac{dx}{dN} &= 3x + 3xy\omega_d \\ \frac{dy}{dN} &= -3x - 3y(1-y)\omega_d\end{aligned}\tag{5.55}$$

Now, using (5.14) and (5.30), from (5.54), we obtain the equation of state parameter, ω_d for Rényi HDE as

$$\omega_d = \frac{1 + \frac{2}{3} \frac{\dot{H}}{H^2 + \pi\delta} - \frac{x}{y}}{1 - 2y}\tag{5.56}$$

Similar to the previous occasions, we assume $\lambda(x, y) = \frac{\dot{H}}{H^2 + \pi\delta}$. Here, we again assume only one choice of $\lambda(x, y)$, expressed by,

$$\lambda(x, y) = \alpha x + \beta y\tag{5.57}$$

since like previous interacting cases, choice of an exponential function is not giving us any viable critical points. By using (5.56) and (5.57), our system of autonomous equations (5.55) changes to

$$\begin{aligned}\frac{dx}{dN} &= 3x + \frac{2xy(\alpha x + \beta y) + 3xy - 3x^2}{1 - 2y} \\ \frac{dy}{dN} &= -3x + \frac{-2y(1-y)(\alpha x + \beta y) - 3y(1-y) + 3x(1-y)}{1 - 2y}\end{aligned}\tag{5.58}$$

The critical points of this autonomous system are given in table 5.11.

TABLE 5.11: Set of critical points and their coordinates.

Critical Points	Coordinates (x, y)
F_1	(0, 0)
F_2	(0, 1)
F_3	(0, $-\frac{3}{2\beta}$)

Eigenvalues corresponding to all critical points are given in the table 5.12.

- F_1 always represents a saddle. In this case, we are unable to draw any conclusion regarding the acceleration of the universe as the equation of state parameter remains undetermined here.

TABLE 5.12: Eigenvalues pertaining to all critical points of autonomous system (5.58).

Critical Points	Eigen values
F_1	$(-3, 3)$
F_2	$(-2\beta - 3, -2\beta)$
F_3	$(3, \frac{9+6\beta}{6+2\beta})$

- F_2 becomes stable when $\beta > 0$, represents a saddle when $-\frac{3}{2} < \beta < 0$ and becomes unstable when $\beta < -\frac{3}{2}$. Stable F_2 always indicates a phantom like fluid description as the equation of state parameter, $\omega_d < -1$. In this case, the universe is completely dark energy dominated as the dark energy density corresponding to the Rényi HDE with the chosen interaction is 1, i.e., $\Omega_d = 1$.
- F_3 is unstable when $\beta > -\frac{3}{2}$ and saddle when $\beta < -\frac{3}{2}$.

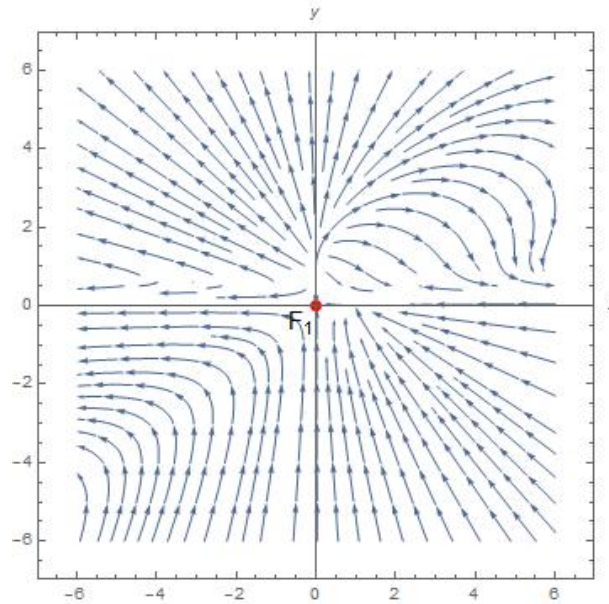
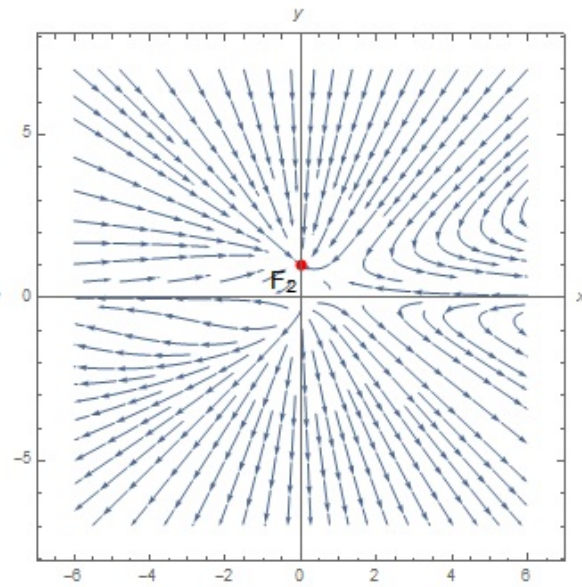
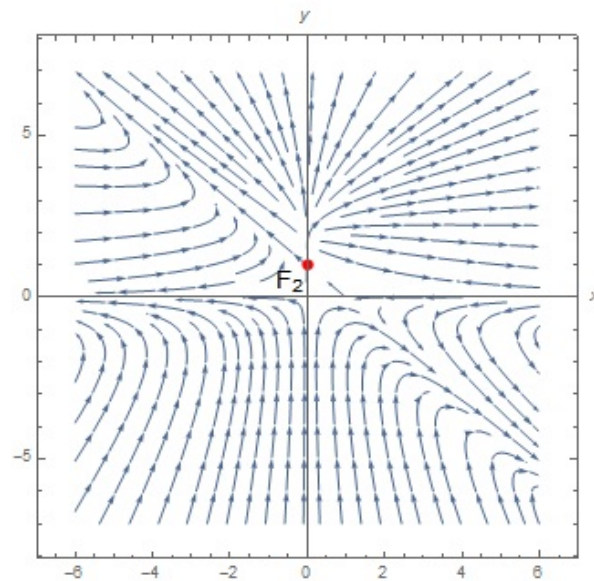

 FIGURE 5.14: Phase plot corresponding to the point $F_1(0,0)$ for $\alpha = 2$, $\beta = -3$

Figure 5.14 shows that $F_1(0,0)$ represents a saddle.

Figure 5.15 shows that $F_2(0,1)$ is stable when β is positive while figure 5.16 shows that $F_2(0,1)$ is saddle when β lies in between $(-\frac{3}{2}, 0)$. Figure 5.17 shows that F_2 is indicating towards a dark energy dominated era and the equation of state parameter evolving towards -1 but completely denoting the phantom description of cosmic fluid.

FIGURE 5.15: Phase plot corresponding to the point $F_2(0, 1)$ for $\alpha = -1$, $\beta = 4$ FIGURE 5.16: Phase plot corresponding to the point $F_2(0, 1)$ for $\alpha = -1$, $\beta = -1$

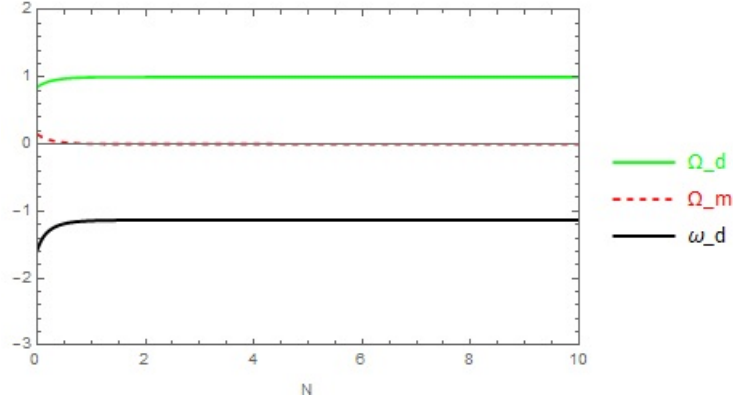


FIGURE 5.17: Evolution of cosmological parameters near $F_2(0, 1)$ for $\alpha = -1$, $\beta = 0.2$

5.5.4 Analysis of interacting Rényi HDE with non-linear interaction $Q = 3H \frac{\rho_d}{\rho_m + \rho_d}$

Here, we study our said model with Rényi HDE considering a non-linear interaction Q in the form of

$$Q = 3H \frac{\rho_d}{\rho_m + \rho_d} \quad (5.59)$$

By using (5.59), equations (5.23) and (5.24) are transformed into

$$\dot{\rho}_m = -3H\rho_m + 3H \frac{\rho_d}{\rho_m + \rho_d} \quad (5.60)$$

and

$$\dot{\rho}_d = -3H\rho_d - 3H\rho_d\omega_d - 3H \frac{\rho_d}{\rho_m + \rho_d} \quad (5.61)$$

To frame an autonomous system of differential equations, we introduce new variables.

$$x = \rho_m, \quad y = \rho_d \quad (5.62)$$

Hence, the energy density parameters will be in the following form.

$$\Omega_m = \frac{x}{x+y}, \quad \Omega_d = \frac{y}{x+y}, \quad 3H^2 = x+y \quad (5.63)$$

Using (5.60), (5.61) and (5.62), we construct the following system of autonomous equations.

$$\begin{aligned}\frac{dx}{dN} &= -3x + \frac{3y}{x+y} \\ \frac{dy}{dN} &= -3y - \frac{3y}{x+y} - 3y\omega_d\end{aligned}\quad (5.64)$$

Using Rényi HDE with Hubble's cut off i.e., equation (5.14), from (5.61), we derive the expression for the equation of state parameter, ω_d as

$$\omega_d = -\frac{4}{3} \frac{\dot{H}}{H^2} + \frac{2}{3} \frac{\dot{H}}{H^2 + \pi\delta} - 1 - \frac{1}{\rho_m + \rho_d}\quad (5.65)$$

From (5.19), we find the expression for

$$\frac{\dot{H}}{H^2} = -\frac{3}{2} - \frac{3}{2} \cdot \frac{y}{x+y} \omega_d\quad (5.66)$$

Using (5.65) and (5.66), the system of autonomous equations in (5.64) further transforms into

$$\begin{aligned}\frac{dx}{dN} &= -3x + \frac{3y}{x+y} \\ \frac{dy}{dN} &= -3y - \frac{3y}{x+y} - \frac{3y(x+y-1)}{x-y} - \frac{2\frac{\dot{H}}{H^2+\pi\delta}(x+y)y}{x-y}\end{aligned}\quad (5.67)$$

Using (5.66), equation of the state parameter takes the following form.

$$\omega_d = \frac{x+y-1}{x-y} + \frac{\frac{2}{3}(x+y)\frac{\dot{H}}{H^2+\pi\delta}}{x-y}\quad (5.68)$$

Here, we put $\lambda(x, y) = \frac{\dot{H}}{H^2+\pi\delta}$ and assume only one choice of $\lambda(x, y)$, given by

$$\lambda(x, y) = \alpha x + \beta y\quad (5.69)$$

as choice of an exponential function is not giving us any viable critical points. By using (5.68) and (5.69), our system of autonomous equations (5.67) changes into

$$\begin{aligned} \frac{dx}{dN} &= -3x + \frac{3y}{x+y} \\ \frac{dy}{dN} &= -3y - \frac{3y}{x+y} - \frac{3y(x+y-1)}{x-y} - \frac{2(\alpha x + \beta y)(x+y)y}{x-y} \end{aligned} \tag{5.70}$$

The critical point corresponding to this autonomous system can be found as given in table 5.13.

TABLE 5.13: Set of critical points and their coordinates.

Critical Points	Coordinates (x, y)
G	$\left(\frac{\alpha}{\alpha-\beta}, -\frac{\alpha^2}{(\alpha-\beta)\beta}\right)$

While we are trying to find the eigenvalues from the linearized matrix pertaining to the critical point G , evaluated from the system of autonomous equations in (5.70), it becomes very complicated.

For that we are representing a tabular form of eigenvalues in table 5.14 corresponding to the critical point G for different choices of α and β .

TABLE 5.14: Eigenvalues corresponding to G for different choices of α and β

Choices of (α, β)	G	Eigenvalues	Ω_m	Ω_d	ω_d
$(1, 2)$	$(-1, \frac{1}{2})$	$(\frac{-4-\sqrt{83}i}{3}, \frac{-4+\sqrt{83}i}{3})$	2	-1	1
$(-2, -1)$	$(2, -4)$	$(\frac{5-\sqrt{313}}{6}, \frac{5+\sqrt{313}}{6})$	-1	2	-0.5
$(4, 1)$	$(\frac{4}{3}, -\frac{16}{3})$	$(\frac{-35-\sqrt{67}\sqrt{5}i}{10}, \frac{-35+\sqrt{67}\sqrt{5}i}{10})$	$-\frac{1}{3}$	$\frac{4}{3}$	-0.75
$(-1, -2)$	$(-1, \frac{1}{2})$	$(\frac{-2-\sqrt{59}i}{3}, \frac{-2+\sqrt{59}i}{3})$	2	-1	1
$(-6, -2)$	$(\frac{3}{2}, -\frac{9}{2})$	$(\frac{33-3\sqrt{329}}{8}, \frac{33+3\sqrt{329}}{8})$	$-\frac{1}{2}$	$\frac{3}{2}$	-0.66

Figure 5.18 shows that $G(\frac{4}{3}, -\frac{16}{3})$ is a stable node while figure 5.19 shows that $G(\frac{3}{2}, -\frac{9}{2})$ is an unstable node.

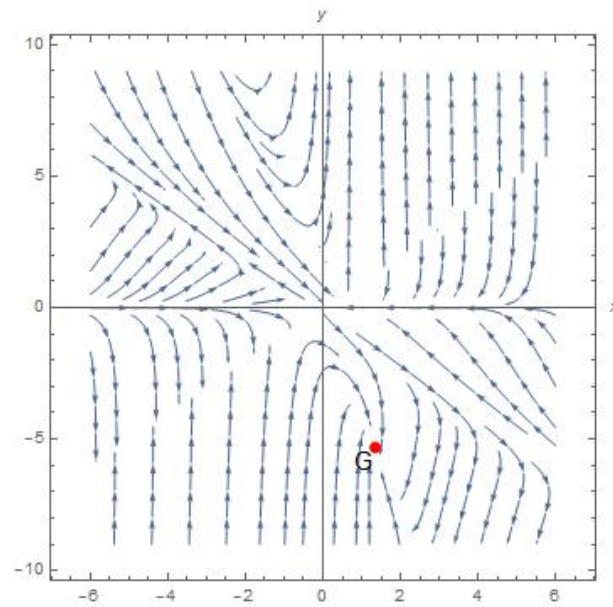


FIGURE 5.18: Phase plot corresponding to the point $G(\frac{4}{3}, -\frac{16}{3})$ for $\alpha = 4$, $\beta = 1$

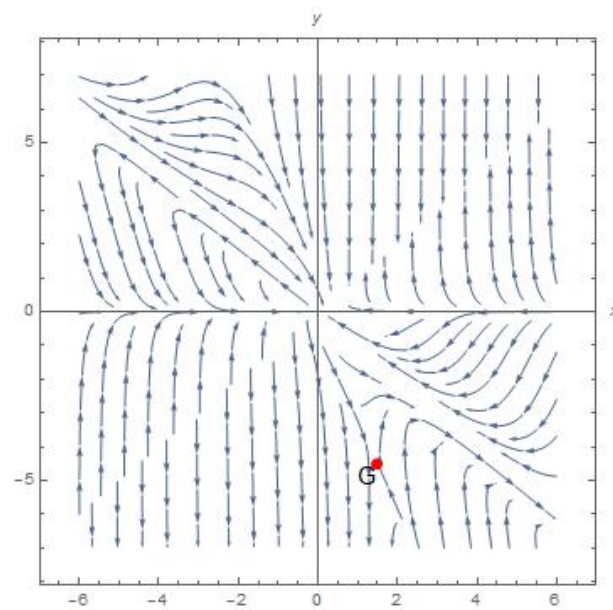


FIGURE 5.19: Phase plot corresponding to the point $G(\frac{3}{2}, -\frac{9}{2})$ for $\alpha = -6$, $\beta = -2$

5.6 Summary and discussion

In this chapter, we consider a cosmological model of the universe filled with a perfect fluid within the framework of a spatially flat Friedmann–Lemaître–Robertson–Walker (FLRW) metric. The universe is assumed to contain only dark matter and dark energy components, with the Rényi holographic dark energy serving as the sole source of dark energy. Both non-interacting and interacting scenarios between dark matter and dark energy have been examined.

To analyze the model’s dynamical behaviour, we employ the tools of dynamical system theory. Accordingly, we construct an autonomous system to study the evolution and stability of the cosmological model around its critical points. In this formulation, we introduce a functional expression involving the Hubble parameter, given by $\frac{\dot{H}}{H^2 + \pi\delta}$, as a key component of the system.

In the non-interacting case, we explore two functional forms—linear and exponential of the dynamical variables, parametrized by two arbitrary constants α and β . These choices lead to rich and interesting dynamical behaviour, offering insights into the evolution of the universe under the Rényi holographic dark energy framework.

We find that, corresponding to the stable hyperbolic node A (as shown in figures 5.1, 5.2, and 5.4), where a linear function of the dynamical variables is considered, the cosmological model exhibits interesting behaviour depending on the choice of the parameter β . Specifically, for different values of β , the model is capable of describing both quintessence-like and phantom-like dark energy regimes, each associated with accelerated cosmic expansion.

Pertaining to the stable hyperbolic node B (as shown in figures 5.6 and 5.7) where an exponential function of the dynamical variables is considered, the cosmological model is becoming stable for any choice of β but the fluid description is always indicating towards phantom era with accelerated expansion.

For both these linear and exponential functions, our non-interacting Rényi HDE model indicates a dark energy dominated era (as shown in figures 5.5 and 5.8) as well as we can conclude that the parameter d which is considered in the Rényi HDE energy density does not impact much in our model but the value of δ is negative for some choices of parameters. The evolution of equation of state parameter (as shown in Figure 5.5) for the choice of linear function shows a shifting from phantom era to

quintessence era.

For, interacting Rényi HDE, we have assumed four interactions as

- $Q = 3H(\rho_m + \rho_d)$.
- $Q = 3H\rho_d$.
- $Q = 3H\rho_m$.
- $Q = 3H\frac{\rho_d}{\rho_m + \rho_d}$.

For the 1st interaction, we are having a stable node C (as shown in figure 5.9) which is stable for $\alpha > 0$ but nothing can be told regarding the fluid description or the acceleration here. This node indicates a matter dominated universe. The node D_1 is unstable in most cases (as shown in figures 5.10 and 5.11) for different choices of parameters α and β whereas D_2 (as shown in figures 5.10 and 5.11) is stable for positive α and β as well as it indicates a phantom era with accelerated expansion. Corresponding to 2nd interaction, similarly hyperbolic node E_1 is unstable in most cases and E_2 is stable for any β when $\alpha > 0$ (as shown in figures 5.12 and 5.13). Stable E_2 indicates a phantom era with accelerated expansion.

In the 3rd linear interaction, we have considered that interaction is proportional to ρ_m . Here critical point F_2 seems interesting as it is becoming stable for positive values of the parameter β (as shown in figure 5.15) and it is indicating a phantom era with dark energy domination (as shown in figure 5.17).

Pertaining to 4th interaction which is non-linear in nature, node G is stable for some choices of parameters α and β and some stable node indicates towards an accelerated expansion with quintessence era.

In summary, the non-interacting Rényi holographic dark energy model exhibits the capability to describe both quintessence and phantom eras, with a clear indication of dark energy domination in the late-time evolution of the universe. When interactions are introduced, the nature of the interaction function plays a significant role: our chosen linear interactions tend to favor a phantom-like behaviour while non-linear interaction typically leads to a quintessence-like regime.

Importantly, in nearly all scenarios explored—whether interacting or non-interacting—the Rényi HDE model demonstrates a stable dynamical behaviour characterized by a late-time accelerated expansion. This robustness highlights the potential of Rényi

entropy-based dark energy as a viable candidate for explaining the current accelerated phase of the universe.

Chapter 6

Discussion and future direction

Einstein field equations govern the evolution of universe in General Relativity. To obtain the solution of the field equations, symmetric FLRW spacetime metric is considered though it's not always possible to find the analytical solutions pertaining to the aforesaid equations as the equations constitute a system of nonlinear differential equations which are very complex in nature. Dynamical system analysis leads us towards the qualitative study of such complex system of nonlinear differential equations. In this thesis, we have used linearized method to study field equations by using dynamical system tools upon converting the differential equations into an autonomous system of differential equations.

The theory of General Relativity fails to explain some cosmological phenomena. Different modifications in basic Einstein field equations have been deployed and as a result, different theoretical cosmological models have been developed. We have studied few of such cosmological models and the qualitative behaviour of the models has been extensively analyzed with the help of dynamical system techniques.

In chapter-1, we have discussed different cosmological observations that have laid the foundation for developing various theoretical approaches for explaining the observational evidences. Different cosmological epochs from the inception of the universe to the current era have been addressed as well as various future singularities. Fundamental cosmological equations along with key cosmological parameters have been discussed. We have also briefly reviewed different theoretical cosmological models starting from the basic Λ CDM model to different models which have been developed by modifying the matter part and the gravity part of Einstein field equations such

as various dark energy models and modified gravity models.

In chapter-2, basic framework of dynamical system has been elaborately reviewed along with some key definitions. Qualitative behaviour of a dynamical system is studied around the critical points of the system which can be either hyperbolic or non hyperbolic in nature. In this thesis, we have extensively studied the qualitative nature around the hyperbolic critical points and for that purpose, our chosen method of stability analysis is linear stability method. We have addressed the key tools related to the linear stability method. We have also discussed other methods for analyzing the stability around non-hyperbolic critical points, namely method of deploying Lyapunov function and center manifold theory. We have also discussed how to construct an autonomous system of differential equations from the governing equations of a cosmological model through an example.

In chapter-3, we have chosen a conformally coupled massless scalar field in semiclassical gravity. We have shown that this model can explain the late time acceleration of the universe. In this model, the stable attractor can explain the early dust and radiation dominated era. This model can also exhibit quintessence description of fluid as well as phantom era for some different parametric choices. Here we are unable to explore this model's resemblance with Λ CDM model as we have not studied the non hyperbolic critical points of the system.

In chapter-4, we have considered a non-minimally coupled $f(Q)$ gravity where we have shown that the stable attractors can describe the quintessence as well as phantom era depending on the choices of the equation of state parameter and other parameters associated to the model and as a result the dynamics of the universe changes. This model is also capable of explaining late-time acceleration of the universe. Some stable attractors here also indicate towards Λ CDM model. So, we can consider $f(Q)$ gravity model as an alternative of the Λ CDM model.

In chapter 5, we have investigated a Rényi holographic dark energy model. For non-interacting RHDE model, we have considered two functional forms of the dimensionless variables. The linear form of such functional is showing a transition of the equation of state parameter from phantom era to quintessence era at late time while, in the case of exponential functional, the equation of state parameter is staying completely in the phantom era. But in both these cases, it is clearly indicating towards a dark energy dominated era. For interacting case, the choices of linear interactions are showing a phantom era while some stable attractor, obtained from

the chosen nonlinear interaction is showing a quintessence era.

In this thesis, we have not studied qualitative analysis around the non hyperbolic critical points. In future, we are keen to study the behaviour of the cosmological models for non hyperbolic critical points by deploying center manifold theory and other dynamical system techniques and would like to verify whether the models remain consistent or not with our current findings. We are also interested to study a modified gravity model where the source of the matter part will be the holographic dark energy. Also, we want to analyze other HDE models, obtained through the change of entropy term. We would also like to engage in studying non minimally coupled $f(Q)$ gravity by deploying other connections.

Bibliography

- [1] R. Bartlett, “*A New Earth and a New Universe*”. PublishAmerica, 2009.
- [2] E. W. Kolb and M. S. Turner, “*The Early Universe*”. Westview Press, 1990.
- [3] A. Einstein, “Cosmological considerations in the General Theory of Relativity,” *Sitzungsber. Preuss. Akad. Wiss. Phys. math. Classe VI*, p. 142, 1917.
- [4] A. R. Liddle, “*An Introduction to Modern Cosmology*”. Wiley, 2003.
- [5] S. Dodelson, “*Modern Cosmology*”. Academic Press, 2003.
- [6] G. F. R. Ellis, “A history of cosmology 1917-1955,” in *Einstein and the History of General Relativity* (D. Howard and J. Stachel, eds.), vol. 1 of *Einstein Study series*, Birkhäuser, 1989.
- [7] E. Hubble, “A relation between distance and radial velocity among extragalactic nebulae,” *Proceedings of the National Academy of Sciences*, vol. 15, p. 168, 1929.
- [8] A. A. Penzias and R. W. Wilson, “A measurement of excess antenna temperature at 4080 mc/s.,” *Astrophys. J.*, vol. 142, p. 419, 1965.
- [9] G. Gamow, “Expanding universe and the origin of elements.,” *Phys. Rev.*, vol. 70, p. 572, 1946.
- [10] B. Greene, “*The New York Times Book of Science: More Than 150 Years of Groundbreaking Scientific Coverage*”. Union Square & Co., 2015.
- [11] E. R. Harrison, “The redshift-distance and velocity-distance laws.,” *Astrophys. J.*, vol. 403, p. 28, 1993.

- [12] A. Friedmann, "On the curvature of space.," *Zeitschrift für Physik*, vol. 10, p. 377, 1922.
- [13] G. Lemaitre, "Expansion of the universe, a homogeneous universe of constant mass and increasing radius accounting for the radial velocity of extra-galactic nebulae.," *Mon. Not. R. Astron. Soc.*, vol. 91, p. 483, 1931.
- [14] A. G. Riess, A. V. Filippenko, P. Challis, A. Clocchiatti, A. Diercks, P. M. Garnavich, R. L. Gilliland, C. J. Hogan, S. Jha, R. P. Kirshner, *et al.*, "Observational evidence from supernovae for an accelerating universe and a cosmological constant," *The astronomical journal*, vol. 116, no. 3, p. 1009, 1998.
- [15] A. G. Riess, L.-G. Strolger, S. Casertano, H. C. Ferguson, B. Mobasher, B. Gold, P. J. Challis, A. V. Filippenko, S. Jha, W. Li, *et al.*, "New hubble space telescope discoveries of type Ia supernovae at $z \geq 1$: narrowing constraints on the early behavior of dark energy," *The Astrophysical Journal*, vol. 659, no. 1, p. 98, 2007.
- [16] S. Perlmutter, G. Aldering, G. Goldhaber, R. A. Knop, P. Nugent, P. G. Castro, S. Deustua, S. Fabbro, A. Goobar, D. E. Groom, *et al.*, "Measurements of Ω and Λ from 42 high-redshift supernovae," *The Astrophysical Journal*, vol. 517, no. 2, p. 565, 1999.
- [17] C. Bennett *et al.*, "First year Wilkinson microwave anisotropy probe (WMAP) observations: Preliminary maps and basic results," *Astrophys. J. Suppl.*, vol. 148, no. 1, 2003.
- [18] D. J. Eisenstein, I. Zehavi, D. W. Hogg, R. Scoccimarro, M. R. Blanton, R. C. Nichol, R. Scranton, H.-J. Seo, M. Tegmark, Z. Zheng, *et al.*, "Detection of the baryon acoustic peak in the large-scale correlation function of SDSS luminous red galaxies," *The Astrophysical Journal*, vol. 633, no. 2, p. 560, 2005.
- [19] M. Tegmark *et al.*, "The 3D power spectrum of galaxies from the SDSS, 2004," *Astrophys. J.*, vol. 606, p. 702, 2004.
- [20] T. M. Davis, E. Mörtzell, J. Sollerman, A. C. Becker, S. Blondin, P. Challis, A. Clocchiatti, A. Filippenko, R. Foley, P. M. Garnavich, *et al.*, "Scrutinizing exotic cosmological models using ESSENCE supernova data combined with

- other cosmological probes,” *The Astrophysical Journal*, vol. 666, no. 2, p. 716, 2007.
- [21] E. Komatsu, J. Dunkley, M. Nolta, C. Bennett, B. Gold, G. Hinshaw, N. Jarosik, D. Larson, M. Limon, L. Page, *et al.*, “Five year Wilkinson microwave anisotropy probe observations: cosmological interpretation,” *The Astrophysical Journal Supplement Series*, vol. 180, no. 2, p. 330, 2009.
- [22] L. Page, G. Hinshaw, E. Komatsu, M. Nolta, D. Spergel, C. Bennett, C. Barnes, R. Bean, O. Doré, J. Dunkley, *et al.*, “Three year Wilkinson microwave anisotropy probe (WMAP) observations: polarization analysis,” *The Astrophysical Journal Supplement Series*, vol. 170, no. 2, p. 335, 2007.
- [23] M. Hicken, W. M. Wood-Vasey, S. Blondin, P. Challis, S. Jha, P. L. Kelly, A. Rest, and R. P. Kirshner, “Improved dark energy constraints from ~ 100 new CfA supernova type Ia light curves,” *The Astrophysical Journal*, vol. 700, no. 2, p. 1097, 2009.
- [24] D. Larson, J. Dunkley, G. Hinshaw, E. Komatsu, M. Nolta, C. Bennett, B. Gold, M. Halpern, R. Hill, N. Jarosik, *et al.*, “Seven year wilkinson microwave anisotropy probe (WMAP) observations: power spectra and WMAP-derived parameters,” *The Astrophysical Journal Supplement Series*, vol. 192, no. 2, p. 16, 2011.
- [25] W. J. Percival, S. Cole, D. J. Eisenstein, R. C. Nichol, J. A. Peacock, A. C. Pope, and A. S. Szalay, “Measuring the baryon acoustic oscillation scale using the sloan digital sky survey and 2dF galaxy redshift survey,” *Monthly Notices of the Royal Astronomical Society*, vol. 381, no. 3, p. 1053, 2007.
- [26] A. G. Sánchez, C. G. Scóccola, A. Ross, W. Percival, M. Manera, F. Montesano, X. Mazzalay, A. Cuesta, D. Eisenstein, E. Kazin, *et al.*, “The clustering of galaxies in the SDSS-III Baryon Oscillation Spectroscopic Survey: cosmological implications of the large-scale two-point correlation function,” *Monthly Notices of the Royal Astronomical Society*, vol. 425, no. 1, p. 415, 2012.

-
- [27] P. M. Garnavich, R. P. Kirshner, P. Challis, J. Tonry, R. L. Gilliland, R. C. Smith, A. Clocchiatti, A. Diercks, A. V. Filippenko, M. Hamuy, *et al.*, “Constraints on cosmological models from hubble space telescope observations of high- z supernovae,” *The Astrophysical Journal*, vol. 493, p. L53, 1998.
- [28] D. N. Spergel and et al., “First year Wilkinson Microwave Anisotropy Probe (WMAP) Observations: Determination of Cosmological Parameters,” *The Astrophysical Journal Supplement Series*, vol. 148, p. 175, 2003.
- [29] P. J. E. Peebles, D. N. Schramm, E. L. Turner, and R. G. Kron, “The case for the relativistic hot big bang cosmology,” *Nature*, vol. 352, p. 769, 1991.
- [30] H. P. Robertson, “Kinematics and world-structure,” *Astrophys. J.*, vol. 82, p. 284, 1935.
- [31] A. G. Walker, “On milne’s theory of world-structure,” *Proc. London. Math. Soc. s2-42*, p. 90, 1937.
- [32] B. Ryden, “*Introduction to cosmology*”. Cambridge University Press, 2017.
- [33] P. J. E. Peebles, “*Principles of Physical Cosmology*”. Princeton University Press, 1993.
- [34] A. Belenkiy, “Alexander friedmann and the origins of modern cosmology,” *Physics Today*, vol. 65, no. 10, p. 38, 2012.
- [35] R. J. Nemiroff and B. Patla, “Adventures in Friedmann cosmology: A detailed expansion of the cosmological Friedmann equations,” *American Journal of Physics*, vol. 76, no. 3, p. 265, 2008.
- [36] NASA/WMAP Science Team and others, “Cosmology: The study of the universe,” *Universe 101: Big Bang Theory*, 2011.
- [37] D. N. Page and C. D. Geilker, “Indirect evidence for quantum gravity,” *Physical Review Letters*, vol. 47, p. 979, 1981.
- [38] M. Albers, C. Kiefer, and M. Reginatto, “Measurement analysis and quantum gravity,” *Physical Review D*, vol. 78, p. 064051, 2008.

-
- [39] C. Kiefer, “*Quantum Gravity*”, vol. 124 of *International Series of Monographs on Physics*. Oxford University Press, 2004.
- [40] P. Meda, N. Pinamonti, and D. Siemssen, “Existence and uniqueness of solutions of the semiclassical Einstein equation in cosmological models,” *Annales Henri Poincaré*, vol. 22, p. 3965, 2021.
- [41] L. H. Ford, “Spacetime in semiclassical gravity,” in *100 Years of Relativity: Space-Time Structure: Einstein and Beyond* (A. Ashtekar, ed.), World Scientific, 2005.
- [42] B. A. Juárez-Aubry and S. K. Modak, “Semiclassical gravity with a conformally covariant field in globally hyperbolic spacetimes,” *Journal of Mathematical Physics*, vol. 63, p. 092303, 2022.
- [43] W. Struyve, “Towards a novel approach to semi-classical gravity,” *Proceedings of Science (PoS), Conference on Quantum Gravity in the Physical Universe (QG-Ph)*, vol. 033, 2007.
- [44] R. M. Wald, “*Quantum Field Theory in Curved Spacetime and Black Hole Thermodynamics*”. University of Chicago Press, 1994.
- [45] N. D. Birrell and P. C. W. Davies, “*Quantum Fields in Curved Space*”. Cambridge University Press, 1982.
- [46] M. J. Duff, “Quantum corrections to the schwarzschild solution,” *Physical Review D*, vol. 9, p. 1837, 1974.
- [47] B. S. DeWitt, “Quantum field theory in curved spacetime,” *Physics Reports*, vol. 19, p. 295, 1975.
- [48] J. D. Bates and P. R. Anderson, “Effects of quantized scalar fields in cosmological spacetimes with big rip singularities,” *Physical Review D*, vol. 82, p. 024018, 2010.
- [49] P. R. Anderson, “Effects of quantum fields on singularities and particle horizons in the early universe. ii,” *Physical Review D*, vol. 29, p. 615, 1984.
- [50] S. W. Hawking, “Particle creation by black holes,” *Communications in Mathematical Physics*, vol. 43, p. 199, 1975.

-
- [51] L. Parker, "Particle creation in expanding universes," *Physical Review Letters*, vol. 21, p. 562, 1968.
- [52] K. Eppley and E. Hannah, "The necessity of quantizing the gravitational field," *Foundations of Physics*, vol. 7, p. 51, 1977.
- [53] C.-I. Kuo and L. H. Ford, "Semiclassical gravity theory and quantum fluctuations," *Physical Review D*, vol. 47, p. 4510, 1993.
- [54] S. Burles, K. M. Nollett, and M. S. Turner, "Sharpening the predictions of big-bang nucleosynthesis," *Physical Review Letters*, vol. 82, p. 4176, 1999.
- [55] D. N. Schramm and M. S. Turner, "Big-bang nucleosynthesis enters the precision era," *Reviews of Modern Physics*, vol. 70, p. 303, 1998.
- [56] G. Gamow, "The origin of elements and the separation of galaxies," *Physical Review*, vol. 74, p. 505, 1948.
- [57] K. Garrett and G. Dūda, "Dark matter: A primer," *Advances in Astronomy*, vol. 2011, p. 968283, 2011.
- [58] G. Jungman, M. Kamionkowski, and K. Griest, "Supersymmetric dark matter," *Physics Reports*, vol. 267, p. 195, 1996.
- [59] W. J. Percival *et al.*, "The 2dF Galaxy Redshift Survey: The power spectrum and the matter content of the universe," *Monthly Notices of the Royal Astronomical Society*, vol. 327, p. 1297, 2001.
- [60] M. Tegmark, M. A. Strauss, M. R. Blanton, K. Abazajian, S. Dodelson, H. Sandvik, X. Wang, D. H. Weinberg, I. Zehavi, N. A. Bahcall, *et al.*, "Cosmological parameters from SDSS and WMAP," *Physical review D*, vol. 69, no. 10, p. 103501, 2004.
- [61] W. J. Percival *et al.*, "Measuring the baryon acoustic oscillation scale using the SDSS and 2dFGRS," *Monthly Notices of the Royal Astronomical Society*, vol. 381, p. 1053, 2007.
- [62] D. N. Spergel, R. Bean, O. Doré, M. R.olta, C. L. Bennett, *et al.*, "Three year Wilkinson Microwave Anisotropy Probe (WMAP) Observations: Implications

- for Cosmology,” *Astrophysical Journal Supplement Series*, vol. 170, p. 377, 2007.
- [63] J. H. Goldstein *et al.*, “Estimates of cosmological parameters using the CMB angular power spectrum of ACBAR,” *Astrophysical Journal*, vol. 599, p. 773, 2003.
- [64] S. L. Tonry *et al.*, “Cosmological results from high- z supernovae,” *Astrophysical Journal*, vol. 594, p. 1, 2003.
- [65] S. Jha, A. G. Riess, and R. P. Kirshner, “Improved distances to type Ia Supernovae with Multicolor Light Curve Shapes: MLCS2k2,” *Astrophysical Journal*, vol. 659, pp. 122–148, 2007.
- [66] P. J. E. Peebles and B. Ratra, “The cosmological constant and dark energy,” *Reviews of modern physics*, vol. 75, no. 2, p. 559, 2003.
- [67] T. Padmanabhan, “Dark energy: The cosmological challenge of the millennium,” *Current Science*, vol. 88, p. 1057, 2005.
- [68] E. J. Copeland, M. Sami, and S. Tsujikawa, “Dynamics of dark energy,” *International Journal of Modern Physics D*, vol. 15, p. 1753, 2006.
- [69] L. Amendola and S. Tsujikawa, “*Dark Energy: Theory and Observations*”. Cambridge University Press, 2010.
- [70] V. Sahni, “Dark matter and dark energy,” in *The Physics of the Early Universe* (E. Papantonopoulos, ed.), vol. 653 of *Lecture Notes in Physics*, p. 141, Springer, 2004.
- [71] V. Sahni, T. D. Saini, A. A. Starobinsky, and U. Alam, “Statefinder a new geometrical diagnostic of dark energy,” *JETP Letters*, vol. 77, p. 201, 2003.
- [72] T. Padmanabhan, “Cosmological constant the weight of the vacuum,” *Physics Reports*, vol. 380, p. 235, 2003.
- [73] R. R. Caldwell, R. Dave, and P. J. Steinhardt, “Cosmological imprint of an energy component with general equation of state,” *Phys. Rev. Lett.*, vol. 80, p. 1582, 1998.

-
- [74] J. Yoo and Y. Watanabe, “Theoretical models of dark energy,” *International Journal of Modern Physics D*, vol. 21, p. 1230002, 2012.
- [75] V. Sahni and A. Starobinsky, “Reconstructing dark energy,” *International Journal of Modern Physics D*, vol. 15, p. 2105, 2006.
- [76] S. M. Carroll, W. H. Press, and E. L. Turner, “The cosmological constant,” *Annual Review of Astronomy and Astrophysics*, vol. 30, p. 499, 1992.
- [77] V. Sahni and A. A. Starobinsky, “The case for a positive cosmological lambda term,” *International Journal of Modern Physics D*, vol. 9, p. 373, 2000.
- [78] S. Weinberg, “The cosmological constant problem,” *Reviews of modern physics*, vol. 61, p. 1, 1989.
- [79] S. M. Carroll, “The cosmological constant,” *Living Reviews in Relativity*, vol. 4, 2001.
- [80] P. J. Steinhardt, “Cosmological challenges for the 21st century,” *Critical problems in physics*, vol. 50, 1997.
- [81] R.-J. Yang and S. N. Zhang, “The age problem in Λ CDM model,” *Monthly Notices of the Royal Astronomical Society*, vol. 407, p. 1835, 2010.
- [82] C. Wetterich, “Cosmology and the fate of dilatation symmetry,” *Nuclear Physics B*, vol. 302, p. 668, 1988.
- [83] P. J. Steinhardt, “A quintessential introduction to dark energy,” *Philosophical Transactions of the Royal Society of London. Series A: Mathematical, Physical and Engineering Sciences*, vol. 361, no. 1812, pp. 2497–2513, 2003.
- [84] B. Ratra and P. J. E. Peebles, “Cosmological Consequences of a Rolling Homogeneous Scalar Field,” *Phys. Rev. D*, vol. 37, p. 3406, 1988.
- [85] S. M. Carroll, “Quintessence and the rest of the world: suppressing long-range interactions,” *Physical Review Letters*, vol. 81, p. 3067, 1998.
- [86] M. Gasperini, F. Piazza, and G. Veneziano, “Quintessence as a runaway dilaton,” *Physical Review D*, vol. 65, p. 023508, 2001.

-
- [87] S. Tsujikawa, “Quintessence: A review,” *Classical and Quantum Gravity*, vol. 30, p. 214003, 2013.
- [88] W.-Z. Liu, J. Ouyang, and H.-X. Yang, “Quintessence field as a perfect cosmic fluid of constant pressure,” *Communications in Theoretical Physics*, vol. 63, p. 391, 2015.
- [89] I. Zlatev, L. Wang, and P. J. Steinhardt, “Quintessence, cosmic coincidence, and the cosmological constant,” *Physical Review Letters*, vol. 82, p. 896, 1999.
- [90] C. Armendariz-Picon, V. Mukhanov, and P. J. Steinhardt, “Essentials of k-essence,” *Physical Review D*, vol. 63, p. 103510, 2001.
- [91] T. Chiba, T. Okabe, and M. Yamaguchi, “Kinetically driven quintessence,” *Physical Review D*, vol. 62, p. 023511, 2000.
- [92] C. Armendariz-Picon, V. Mukhanov, and P. J. Steinhardt, “Dynamical solution to the problem of a small cosmological constant and late-time cosmic acceleration,” *Physical Review Letters*, vol. 85, pp. 4438–4441, 2000.
- [93] C. Armendariz-Picon, T. Damour, and V. Mukhanov, “k-inflation,” *Physics Letters B*, vol. 458, pp. 209–218, 1999.
- [94] M. Malquarti, E. J. Copeland, A. R. Liddle, and M. Trodden, “A New view of k-essence,” *Phys. Rev. D*, vol. 67, p. 123503, 2003.
- [95] P. Y. Tsyba, I. I. Kulnazarov, K. K. Yerzhanov, and R. Myrzakulov, “Pure kinetic k-essence as the cosmic speed-up,” *Int. J. Theor. Phys.*, vol. 50, p. 1876, 2011.
- [96] R. R. Caldwell, “A phantom menace? cosmological consequences of a dark energy component with super-negative equation of state,” *Physics Letters B*, vol. 545, p. 23, 2002.
- [97] R. R. Caldwell, M. Kamionkowski, and N. N. Weinberg, “Phantom energy and cosmic doomsday,” *Physical review letters*, vol. 91, p. 071301, 2003.
- [98] A. Paliathanasis and G. Leon, “Dynamics of a two scalar field cosmological model with phantom terms,” *Classical and Quantum Gravity*, vol. 38, p. 075013, 2021.

-
- [99] E. Elizalde, S. Nojiri, and S. D. Odintsov, “Late-time cosmology in a (phantom) scalar-tensor theory: dark energy and the cosmic speed-up,” *Physical Review D*, vol. 70, p. 043539, 2004.
- [100] K. J. Ludwick, “The viability of phantom dark energy: A review,” *Modern Physics Letters A*, vol. 32, p. 1730025, 2017.
- [101] N. Mahata and S. Chakraborty, “Dynamical system analysis for a phantom model,” *General Relativity and Gravitation*, vol. 46, p. 1721, 2014.
- [102] F. Piazza and S. Tsujikawa, “Dilatonic ghost condensate as dark energy,” *Journal of Cosmology and Astroparticle Physics*, vol. 2004, p. 004, 2004.
- [103] A. Y. Kamenshchik, U. Moschella, and V. Pasquier, “An alternative to quintessence,” *Physics Letters B*, vol. 511, p. 265, 2001.
- [104] N. Bilic, G. B. Tupper, and R. D. Viollier, “Unification of dark matter and dark energy: The inhomogeneous chaplygin gas,” *Physics Letters B*, vol. 535, p. 17, 2002.
- [105] M. C. Bento, O. Bertolami, and A. A. Sen, “Generalized chaplygin gas, accelerated expansion and dark energy matter unification,” *Physical Review D*, vol. 66, p. 043507, 2002.
- [106] V. Gorini, A. Kamenshchik, U. Moschella, and V. Pasquier, “The chaplygin gas as a model for dark energy,” in *Proceedings of the 9th Marcel Grossmann Meeting on General Relativity* (V. G. Gurzadyan, R. T. Jantzen, and R. Ruffini, eds.), p. 840, World Scientific, 2002.
- [107] E. N. Saridakis and S. V. Sushkov, “Quintessence and phantom cosmology with non-minimal derivative coupling,” *Phys. Rev. D*, vol. 81, p. 083510, 2010.
- [108] C. G. Boehmer, G. Caldera-Cabral, R. Lazkoz, and R. Maartens, “Dynamics of dark energy with a coupling to dark matter,” *Phys. Rev. D*, vol. 78, p. 023505, 2008.
- [109] L. Amendola, “Coupled quintessence,” *Phys. Rev. D*, vol. 62, p. 043511, 2000.
- [110] W. Zimdahl, D. Pavon, and L. P. Chimento, “Interacting quintessence,” *Phys. Lett. B*, vol. 521, p. 133, 2001.

-
- [111] L. Amendola, “Perturbations in a coupled scalar field cosmology,” *Mon. Not. R. Astron. Soc.*, vol. 312, p. 521, 2000.
- [112] A. P. Billyard and A. A. Coley, “Interactions in scalar field cosmology,” *Phys. Rev. D*, vol. 61, p. 083503, 2000.
- [113] L. P. Chimento, A. S. Jakubi, D. Pavon, and W. Zimdahl, “Interacting quintessence solution to the coincidence problem,” *Phys. Rev. D*, vol. 67, p. 083513, 2003.
- [114] M. Hoffman, “Cosmological constraints on a dark matter - dark energy interaction,” 2003.
- [115] Z. K. Guo, R. G. Cai, and Y. Z. Zhang, “Cosmological evolution of interacting phantom energy with dark matter,” *JCAP*, vol. 0505, 2005.
- [116] W. Zimdahl, “Interacting dark energy and cosmological equations of state,” *Int. J. Mod. Phys. D*, vol. 14, p. 2319, 2005.
- [117] J.-H. He and B. Wang, “Effects of the interaction between dark energy and dark matter on cosmological parameters,” *JCAP*, vol. 0806, p. 010, 2008.
- [118] Z. K. Guo, N. Ohta, and S. Tsujikawa, “Probing the coupling between dark components of the universe,” *Phys. Rev. D*, vol. 76, p. 023508, 2007.
- [119] H. Wei, “Revisiting the cosmological constraints on the interacting dark energy models,” *Phys. Lett. B*, vol. 691, p. 173, 2010.
- [120] L. Amendola, G. C. Campos, and R. Rosenfeld, “Consequences of dark matter-dark energy interaction on cosmological parameters derived from snia data,” *Phys. Rev. D*, vol. 75, p. 083506, 2007.
- [121] S. H. Pereira and J. F. Jesus, “Can dark matter decay in dark energy?,” *Phys. Rev. D*, vol. 79, p. 043517, 2009.
- [122] S. Das, P. S. Corasaniti, and J. Khoury, “Super-acceleration as signature of dark sector interaction,” *Phys. Rev. D*, vol. 73, p. 083509, 2006.
- [123] A. D. Linde, “Chaotic inflation,” *Physics Letters B*, vol. 129, p. 177, 1983.

- [124] R. Kallosh, J. Kratochvil, A. D. Linde, E. V. Linder, and M. Shmakova, “Observational bounds on cosmic doomsday,” *Journal of Cosmology and Astroparticle Physics*, vol. 2003, p. 015, 2003.
- [125] J. A. Frieman, C. T. Hill, A. Stebbins, and I. Waga, “Cosmology with ultralight pseudo nambu-goldstone bosons,” *Physical Review Letters*, vol. 75, p. 2077, 1995.
- [126] R. R. Caldwell and E. V. Linder, “The limits of quintessence,” *Physical Review Letters*, vol. 95, p. 141301, 2005.
- [127] P. S. Corasaniti, M. Kunz, D. Parkinson, E. J. Copeland, and B. A. Bassett, “Foundations of observing dark energy dynamics with the wilkinson microwave anisotropy probe,” *Physical Review D*, vol. 70, no. 083006, p. 1, 2004.
- [128] G. Aldering and et al., “Overview of the supernova/acceleration probe (snap),” in *Proceedings of SPIE, Society of Photo-Optical Instrumentation Engineers*, vol. 4835, p. 146, 2002.
- [129] W. M. Wood-Vasey *et al.*, “Observational constraints on the nature of dark energy: First cosmological results from the essence supernova survey,” *Astrophysical Journal*, vol. 666, p. 694, 2007.
- [130] A. Melchiorri, L. Mersini, C. J. Odman, and M. Trodden, “The state of the dark energy equation of state,” *Physical Review Letters*, vol. 90, p. 031301, 2003.
- [131] N. Aghanim *et al.*, “Planck 2018 results. VI. Cosmological parameters,” *Astron. Astrophys.*, vol. 641, p. A6, 2020.
- [132] V. Sahni and Y. Shtanov, “Brane world models of dark energy,” *Journal of Cosmology and Astroparticle Physics*, vol. 2003, p. 014, 2003.
- [133] F. Hoyle, “A new model for the expanding universe,” *Monthly Notices of the Royal Astronomical Society*, vol. 108, p. 372, 1948.
- [134] F. Hoyle and J. V. Narlikar, “A new theory of gravitation,” *Proceedings of the Royal Society of London. Series A. Mathematical and Physical Sciences*, vol. 282, no. 1389, p. 191, 1964.

-
- [135] L. R. Abramo and N. Pinto-Neto, “On the stability of phantom k-essence theories,” *Physical Review D*, vol. 73, p. 063522, 2006.
- [136] S. M. Carroll, M. Hoffman, and M. Trodden, “Can the dark energy equation of state parameter ω be less than -1?,” *Physical Review D*, vol. 68, p. 023509, 2003.
- [137] R. J. Scherrer, “Phantom dark energy, cosmic doomsday, and the coincidence problem,” *Physical Review D*, vol. 71, p. 063519, 2005.
- [138] J. Kujat, R. J. Scherrer, and A. A. Sen, “Phantom dark energy models with negative kinetic term,” *Physical Review D*, vol. 74, p. 083501, 2006.
- [139] J. D. Barrow and C. G. Tsagas, “On the stability of static ghost cosmologies,” *Classical and Quantum Gravity*, vol. 26, p. 195003, 2009.
- [140] M. Gasperini and G. Veneziano, “The pre-big bang scenario in string cosmology,” *Phys. Rept.*, vol. 373, p. 1, 2003.
- [141] G. Mangano, G. Miele, and V. Pettorino, “Coupled quintessence and the coincidence problem,” *Mod. Phys. Lett. A*, vol. 18, p. 831, 2003.
- [142] G. R. Farrar and P. J. E. Peebles, “Interacting dark matter and dark energy,” *Astrophys. J.*, vol. 604, p. 1, 2004.
- [143] G. Olivares, F. Atrio-Barandela, and D. Pavon, “Observational constraints on interacting quintessence models,” *Phys. Rev. D*, vol. 71, p. 063523, 2005.
- [144] G. Olivares, F. Atrio-Barandela, and D. Pavon, “Matter density perturbations in interacting quintessence models,” *Phys. Rev. D*, vol. 74, p. 043521, 2006.
- [145] B. Wang, J. Zang, C.-Y. Lin, E. Abdalla, and S. Micheletti, “Interacting dark energy and dark matter: Observational constraints from cosmological parameters,” *Nuclear Physics B*, vol. 778, p. 69, 2007.
- [146] C. Feng, B. Wang, E. Abdalla, and R.-K. Su, “Observational constraints on the dark energy and dark matter mutual coupling,” *Physics Letters B*, vol. 665, p. 111, 2008.

-
- [147] E. Abdalla, L. R. Abramo, L. S. Jr., and B. Wang, “Signature of the interaction between dark energy and dark matter in galaxy clusters,” *Physics Letters B*, vol. 673, p. 107, 2009.
- [148] J. Väliviita, R. Maartens, and E. Majerotto, “Observational constraints on an interacting dark energy model,” *Monthly Notices of the Royal Astronomical Society*, vol. 402, p. 2355, 2010.
- [149] S. Kumar, R. C. Nunes, and S. K. Yadav, “Dark sector interaction: a remedy of the tensions between cmb and lss data,” *European Physical Journal C*, vol. 79, p. 576, 2019.
- [150] A. G. Cohen, D. B. Kaplan, and A. E. Nelson, “Effective field theory, black holes, and the cosmological constant,” *Physical Review Letters*, vol. 82, p. 4971, 1999.
- [151] M. Li, “A model of holographic dark energy,” *Physics Letters B*, vol. 603, p. 1, 2004.
- [152] R. Horvat, “Holography and variable cosmological constant,” *Physical Review D*, vol. 70, p. 087301, 2004.
- [153] N. Mahata and S. Chakraborty, “A dynamical system analysis of holographic dark energy models with different IR cutoff,” *Modern Physics Letters A*, vol. 30, p. 1550134, 2015.
- [154] S. D. H. Hsu, “Entropy bounds and dark energy,” *Physics Letters B*, vol. 594, p. 13, 2004.
- [155] B. Guberina, R. Horvat, and H. Nikolic, “Nonsaturated holographic dark energy,” *Journal of Cosmology and Astroparticle Physics*, vol. 2007, p. 012, 2007.
- [156] L. Xu, “Holographic dark energy model with hubble horizon as an IR cut-off,” *Journal of Cosmology and Astroparticle Physics*, vol. 2009, p. 016, 2009.
- [157] D. Pavon and W. Zimdahl, “Holographic dark energy and cosmic coincidence,” *Physics Letters B*, vol. 628, p. 206, 2005.
- [158] L. Susskind, “The world as a hologram,” *Journal of Mathematical Physics*, vol. 36, p. 6377, 1995.

- [159] N. Drepanou, A. Lymperis, E. N. Saridakis, and K. Yesmakhanova, “Kaniadakis holographic dark energy and cosmology,” *The European Physical Journal C*, vol. 82, p. 10415, 2022.
- [160] E. M. C. Abreu, J. A. Neto, E. M. Barboza, and R. C. Nunes, “Jeans instability criterion from the viewpoint of Kaniadakis’ statistics,” *EPL (Europhysics Letters)*, vol. 114, no. 5, p. 55001, 2016.
- [161] U. K. Sharma, V. C. Dubey, A. H. Ziaie, and H. Moradpour, “Kaniadakis holographic dark energy in non-flat universe,” *International Journal of Modern Physics D*, vol. 31, p. 2250013, 2022.
- [162] A. Hernández-Almada, G. León, J. Magaña, M. A. García-Aspeitia, V. Motta, E. N. Saridakis, and K. Yesmakhanova, “Kaniadakis-holographic dark energy: observational constraints and global dynamics,” *Monthly Notices of the Royal Astronomical Society*, vol. 511, p. 4147, 2022.
- [163] G. Kaniadakis, “Statistical mechanics in the context of Special Relativity,” *Physical Review E*, vol. 66, no. 5, p. 056125, 2002.
- [164] G. Kaniadakis, “Statistical mechanics in the context of Special Relativity. II,” *Physical Review E*, vol. 72, no. 3, p. 036108, 2005.
- [165] E. N. Saridakis, “Barrow holographic dark energy,” *Physical Review D*, vol. 102, p. 123525, 2020.
- [166] E. N. Saridakis and S. Basilakos, “The generalized second law of thermodynamics with Barrow entropy,” *European Physical Journal C*, vol. 81, p. 644, 2021.
- [167] P. Adhikary, S. Das, S. Basilakos, and E. N. Saridakis, “Barrow holographic dark energy in non-flat universe,” *Physical Review D*, vol. 104, p. 123519, 2021.
- [168] A. Al Mamon, A. Paliathanasis, and S. Saha, “Dynamics of an interacting Barrow holographic dark energy model and its thermodynamic implications,” *The European Physical Journal C*, vol. 136, p. 134, 2021.
- [169] Q. Huang, H. Huang, B. Xu, F. Tu, and J. Chen, “Dynamical analysis and statefinder of Barrow holographic dark energy,” *European Physical Journal C*, vol. 81, p. 686, 2021.

-
- [170] S. Srivastava and U. K. Sharma, “Barrow holographic dark energy with hubble horizon as IR cutoff,” *International Journal of Geometric Methods in Modern Physics*, vol. 18, p. 2150014, 2021.
- [171] G. G. Luciano, “Cosmic evolution and thermal stability of Barrow holographic dark energy in non-flat Friedmann-Robertson-Walker universe,” *Physical Review D*, vol. 106, p. 083530, 2022.
- [172] F. K. Anagnostopoulos, S. Basilakos, and E. N. Saridakis, “Observational constraints on Barrow holographic dark energy,” *European Physical Journal C*, vol. 80, p. 826, 2020.
- [173] J. D. Barrow, “The area of a rough black hole,” *Physics Letters B*, vol. 808, p. 135643, 2020.
- [174] M. Tavayef, A. Sheykhi, K. Bamba, and H. Moradpour, “Tsallis holographic dark energy,” *Physics Letters B*, vol. 781, p. 195, 2018.
- [175] E. N. Saridakis, K. Bamba, R. Myrzakulov, and F. K. Anagnostopoulos, “Holographic dark energy through Tsallis entropy,” *Journal of Cosmology and Astroparticle Physics*, vol. 2018, p. 012, 2018.
- [176] M. Abdollahi Zadeh, A. Sheykhi, H. Moradpour, and K. Bamba, “Note on Tsallis holographic dark energy,” *The European Physical Journal C*, vol. 78, p. 940, 2018.
- [177] H. Moradpour, I. G. Salako, I. P. Lobo, J. P. M. Graça, A. Jawad, and S. A. Moosavi, “Thermodynamic approach to holographic dark energy and the Rényi entropy,” *The European Physical Journal C*, vol. 78, p. 829, 2018.
- [178] C. Tsallis, “Possible generalization of Boltzmann-Gibbs statistics,” *Journal of Statistical Physics*, vol. 52, p. 479, 1988.
- [179] M. L. Lyra and C. Tsallis, “Nonextensivity and multifractality in low-dimensional dissipative systems,” *Physical Review Letters*, vol. 80, p. 53, 1998.
- [180] C. Tsallis, R. S. Mendes, and A. R. Plastino, “The role of constraints within generalized nonextensive statistics,” *Physica A: Statistical Mechanics and its Applications*, vol. 261, p. 534, 1998.

-
- [181] C. Tsallis and L. J. L. Cirto, “Black hole thermodynamical entropy,” *The European Physical Journal C*, vol. 73, p. 2487, 2013.
- [182] M. T. Manoharan, N. Shaji, and T. K. Mathew, “Holographic dark energy from the laws of thermodynamics with Rényi entropy,” *European Physical Journal C*, vol. 83, p. 19, 2023.
- [183] A. Rényi, “*Probability Theory*”. North-Holland, 1970.
- [184] A. Rényi, “On Measures of Information and Entropy,” in *Proceedings of the Fourth Berkeley Symposium on Mathematics, Statistics and Probability, 1960*, vol. 1, (Berkeley, CA), p. 547, University of California Press, 1961.
- [185] C. Tsallis, “*Introduction to Nonextensive Statistical Mechanics: Approaching a Complex World*”. New York: Springer, 2009.
- [186] T. S. Biró and P. Ván, “Zeroth law compatibility of non-additive thermodynamics,” *Physical Review E*, vol. 83, p. 061147, 2011.
- [187] V. G. Czinner and H. Iguchi, “Rényi entropy and the thermodynamic stability of black holes,” *Physics Letters B*, vol. 752, p. 306, 2016.
- [188] T. S. Biró and V. G. Czinner, “A q-parameter bound for particle spectra based on black hole thermodynamics with Rényi entropy,” *Physics Letters B*, vol. 726, p. 861, 2013.
- [189] N. Komatsu, “Cosmological model from the holographic equipartition law with a modified Rényi entropy,” *European Physical Journal C*, vol. 77, 2017.
- [190] H. Moradpour, A. Sheykhi, C. Corda, and I. G. Salako, “Implications of the generalized entropy formalisms on the Newtonian gravity and dynamics,” *Physics Letters B*, vol. 783, p. 82, 2018.
- [191] B. D. Sharma and D. P. Mittal, “New non-additive measures of entropy for discrete probability distributions,” *Journal of Mathematical Sciences*, vol. 10, p. 28, 1975.
- [192] B. D. Sharma and D. P. Mittal, “New non-additive measures of entropy,” *Journal of Combinatorics, Information System Sciences*, vol. 2, p. 122, 1977.

-
- [193] A. S. Jahromi, S. A. Moosavi, H. Moradpour, J. P. M. Graça, I. P. Lobo, I. G. Salako, and A. Jawad, “Generalized entropy formalism and a new holographic dark energy model,” *Physics Letters B*, vol. 780, p. 21, 2018.
- [194] H. Moradpour, A. H. Ziaie, and M. K. Zangeneh, “Generalized entropies and corresponding holographic dark energy models,” *European Physical Journal C*, vol. 80, p. 732, 2020.
- [195] M. Masi, “A step beyond Tsallis and Rényi entropies,” *Physics Letters A*, vol. 338, p. 217, 2005.
- [196] V. Faraoni, E. Gunzig, and P. Nardone, “Conformal transformations in classical gravitational theories and in cosmology,” *Fundamentals of Cosmic Physics*, vol. 20, p. 121, 1999.
- [197] A. Y. Petrov, “*Introduction to modified gravity*”. SpringerBriefs in Physics, 2020.
- [198] K. Hayashi and T. Shirafuji, “New general relativity,” *Phys. Rev. D*, vol. 19, p. 3524, 1979.
- [199] J. W. Maluf, “Hamiltonian formulation of the teleparallel description of general relativity,” *J. Math. Phys.*, vol. 35, p. 335, 1994.
- [200] S. Nojiri and S. D. Odintsov, “Introduction to modified gravity and gravitational alternative for dark energy,” *International Journal of Geometric Methods in Modern Physics*, vol. 4, p. 115, 2007.
- [201] S. Nojiri, S. D. Odintsov, and V. K. Oikonomou, “Modified gravity theories on a nutshell: Inflation, bounce and late-time evolution,” *Physics Reports*, vol. 692, p. 1, 2017.
- [202] M. Braglia, M. Ballardini, F. Finelli, and K. Koyama, “Early modified gravity in light of the H_0 tension and LSS data,” *Physical Review D*, vol. 103, p. 043528, 2021.
- [203] E. N. Saridakis, R. Lazkoz, V. Salzano, P. V. Moniz, S. Capozziello, *et al.*, “*Modified Gravity and Cosmology: An Update by the CANTATA Network*”. Berlin: Springer, 2021.

- [204] R. Ferraro and F. Fiorini, “Modified teleparallel gravity: Inflation without inflaton,” *Phys. Rev. D*, vol. 75, p. 084031, 2007.
- [205] H. A. Buchdahl, “Non-linear lagrangians and cosmological theory,” *Monthly Notices of the Royal Astronomical Society*, vol. 150, p. 1, 1970.
- [206] W. Hu and I. Sawicki, “Models of $f(R)$ cosmic acceleration that evade solar-system tests,” *Phys. Rev. D*, vol. 76, p. 064004, 2007.
- [207] A. A. Starobinsky, “Disappearing cosmological constant in $f(R)$ gravity,” *JETP Lett.*, vol. 86, p. 157, 2007.
- [208] T. P. Sotiriou and V. Faraoni, “ $f(R)$ theories of gravity,” *Reviews of Modern Physics*, vol. 82, p. 451, 2010.
- [209] S. Capozziello, “Curvature quintessence,” *Int. J. Mod. Phys. D*, vol. 11, p. 483, 2002.
- [210] S. Nojiri and S. D. Odintsov, “Modified gravity with negative and positive powers of the curvature: unification of the inflation and of the cosmic acceleration,” *Phys. Rev. D*, vol. 68, p. 123512, 2003.
- [211] T. Harko, F. S. N. Lobo, S. Nojiri, and S. D. Odintsov, “ $f(R, T)$ gravity,” *Phys. Rev. D*, vol. 84, p. 024020, 2011.
- [212] H. Shabani and M. Farhoudi, “Cosmological and solar system consequences of $f(R, T)$ gravity models,” *Physical Review D*, vol. 90, p. 044031, 2014.
- [213] H. Velten and T. R. P. Caramês, “Cosmological inviability of $f(R, T)$ gravity,” *Physical Review D*, vol. 95, p. 123536, 2017.
- [214] M. Xu, T. Harko, and S. Liang, “Quantum cosmology of $f(R, T)$ gravity,” *Eur. Phys. J. C*, vol. 76, p. 449, 2016.
- [215] P. H. R. S. Moraes and P. K. Sahoo, “Modelling wormholes in $f(R, T)$ gravity,” *Phys. Rev. D*, vol. 96, p. 044038, 2017.
- [216] K. Bamba, C. Q. Geng, C. Lee, and L. Luo, “Equation of state for dark energy in $f(T)$ gravity,” *JCAP*, vol. 1101, p. 021, 2011.

- [217] Y.-F. Cai, S. Capozziello, M. D. Laurentis, and E. N. Saridakis, “f(T) teleparallel gravity and cosmology,” *Rept. Prog. Phys.*, vol. 79, p. 106901, 2016.
- [218] C. Q. Geng, C. C. Lee, E. N. Saridakis, and Y. P. Wu, “Teleparallel dark energy,” *Phys. Lett. B*, vol. 704, p. 384, 2011.
- [219] M. Krššák and E. N. Saridakis, “The covariant formulation of f(T) gravity,” *Class. Quant. Grav.*, vol. 33, p. 115009, 2016.
- [220] R. C. Nunes, “Structure formation in f(T) gravity and a solution for H0 tension,” *Journal of Cosmology and Astroparticle Physics*, vol. 2018, p. 052, 2018.
- [221] A. D. Felice and S. Tsujikawa, “Construction of cosmologically viable $f(\mathcal{G})$ gravity models,” *Physics Letters B*, vol. 675, p. 1, 2009.
- [222] B. Li, J. D. Barrow, and D. F. Mota, “The cosmology of Modified Gauss-Bonnet Gravity,” *Physical Review D*, vol. 76, p. 044027, 2007.
- [223] G. Cognola, E. Elizalde, S. Nojiri, S. D. Odintsov, and S. Zerbini, “Dark energy in modified Gauss-Bonnet gravity: Late-time acceleration and the hierarchy problem,” *Physical Review D*, vol. 73, p. 084007, 2006.
- [224] S. Nojiri, S. D. Odintsov, and S. Ogushi, “Cosmological and black hole brane-world universes in higher derivative gravity,” *Phys. Rev. D*, vol. 65, p. 023521, 2001.
- [225] B. M. Leith and I. P. Neupane, “Gauss–Bonnet cosmologies: crossing the phantom divide and the transition from matter dominance to dark energy,” *Journal of Cosmology and Astroparticle Physics*, vol. 2007, p. 019, 2007.
- [226] S. Nojiri and S. D. Odintsov, “Unified cosmic history in modified gravity: from f(R) theory to lorentz non-invariant models,” *Physics Reports*, vol. 505, p. 59, 2011.
- [227] T. Koivisto and D. F. Mota, “Gauss-Bonnet Quintessence: Background Evolution, Large Scale Structure and Cosmological Constraints,” *Physical Review D*, vol. 75, p. 023518, 2007.

-
- [228] S. Nojiri, S. D. Odintsov, and P. V. Tretyakov, “From inflation to dark energy in the non-minimal modified gravity,” *Progress of Theoretical Physics Supplement*, vol. 172, p. 81, 2008.
- [229] S. Nojiri, S. D. Odintsov, and M. Sasaki, “Gauss-Bonnet dark energy,” *Physical Review D*, vol. 71, p. 123509, 2005.
- [230] S.-Y. Zhou, E. J. Copeland, and P. M. Saffin, “Cosmological constraints on $f(\mathcal{G})$ dark energy models,” *Journal of Cosmology and Astroparticle Physics*, vol. 2009, p. 009, 2009.
- [231] J. W. Moffat, “Scalar–tensor–vector gravity theory,” *Journal of Cosmology and Astroparticle Physics*, vol. 2006, p. 004, 2006.
- [232] C. H. Brans, “The roots of scalar-tensor theory: an approximate history,” *arXiv preprint gr-qc/0506063*, 2005.
- [233] T. P. Sotiriou, “ $f(R)$ gravity and scalar tensor theory,” *Classical and Quantum Gravity*, vol. 23, p. 5117, 2006.
- [234] Y. Fujii and K. ichi Maeda, “*The Scalar-Tensor Theory of Gravitation*”. Cambridge University Press, 2003.
- [235] V. Faraoni, “*Cosmology in Scalar-Tensor Gravity*”. Springer, 2004.
- [236] I. Ayuso, R. Lazkoz, and V. Salzano, “Observational constraints on cosmological solutions of $f(Q)$ theories,” *Physical Review D*, vol. 103, p. 063505, 2021.
- [237] N. Frusciante, “Signatures of $f(Q)$ gravity in cosmology,” *Physical Review D*, vol. 103, p. 044021, 2021.
- [238] S. Mandal, D. Wang, and P. K. Sahoo, “Cosmography in $f(Q)$ gravity,” *Phys. Rev. D*, vol. 102, p. 124029, 2020.
- [239] L. Atayde and N. Frusciante, “Can $f(Q)$ gravity challenge Λ CDM?,” *Physical Review D*, vol. 104, no. 6, p. 064052, 2021.
- [240] W. Khyllep, A. Paliathanasis, and J. Dutta, “Cosmological solutions and growth index of matter perturbations in $f(Q)$ gravity,” *Physical Review D*, vol. 103, no. 10, p. 103521, 2021.

- [241] J. Lu, X. Zhao, and G. Chee, “Cosmology in symmetric teleparallel gravity and its dynamical system,” *European Physical Journal C*, vol. 79, p. 530, 2019.
- [242] T. Harko, T. S. Koivisto, F. S. N. Lobo, G. J. Olmo, and D. Rubiera-Garcia, “Coupling matter in modified Q-gravity,” *Phys. Rev. D*, vol. 98, p. 084043, 2018.
- [243] Y. Xu, G. Li, T. Harko, and S.-D. Liang, “ $f(Q, T)$ gravity,” *European Physical Journal C*, vol. 79, p. 708, 2019.
- [244] M. Shiravand, S. Fakhry, and M. Farhoudi, “Cosmological inflation in $f(Q, T)$ gravity,” *Physics of the Dark Universe*, vol. 37, p. 101106, 2022.
- [245] Y. Xu, T. Harko, S. Shahidi, and S.-D. Liang, “Weyl type $f(Q, T)$ gravity, and its cosmological implications,” *European Physical Journal C*, vol. 80, p. 449, 2020.
- [246] A. Nájera and A. Fajardo, “Cosmological perturbation theory in $f(Q, T)$ gravity,” *Journal of Cosmology and Astroparticle Physics*, vol. 03, p. 020, 2022.
- [247] A. D. Felice and S. Tsujikawa, “ $f(R)$ theories,” *Living Rev. Relativity*, vol. 13, p. 3, 2010.
- [248] A. A. Starobinsky, “A new type of isotropic cosmological models without singularity,” *Phys. Lett. B*, vol. 91, p. 99, 1980.
- [249] M. Sharif and M. Zubair, “Thermodynamics in $f(R, T)$ theory of gravity,” *JCAP*, vol. 03, p. 028, 2012.
- [250] M. Jamil, D. Momeni, and R. Myrzakulov, “Violation of the first law of thermodynamics in $f(R, T)$ gravity,” *Chinese Physics Letters*, vol. 29, p. 109801, 2012.
- [251] F. Alvarenga, M. S. Houndjo, A. Monwanou, and J. Chabi Orou, “Testing some $f(R, T)$ gravity models from energy conditions,” *Journal of Modern Physics*, vol. 4, p. 130, 2013.
- [252] P. K. Sahoo, S. Mandal, and S. Arora, “Energy conditions in non-minimally coupled $f(R, T)$ gravity,” *Astronomische Nachrichten*, vol. 342, p. 89, 2021.

- [253] M. K. Kiran, “Non-existence of Bianchi type-III bulk viscous string cosmological model in general relativity,” *Astrophysics and Space Science*, vol. 346, p. 521, 2013.
- [254] P. H. R. S. Moraes and P. K. Sahoo, “The simplest non-minimal matter-geometry coupling in the $f(R, T)$ cosmology,” *The European Physical Journal C*, vol. 77, p. 480, 2017.
- [255] F. G. Alvarenga, M. J. S. Houndjo, A. V. Monwanou, and J. B. C. Orou, “Testing some $f(R, T)$ gravity models from energy conditions,” *Journal of Modern Physics*, vol. 4, p. 130, 2013.
- [256] J. L. Rosa, M. A. Marques, D. Bazeia, and F. S. N. Lobo, “Thick branes in the scalar–tensor representation of $f(R, T)$ gravity,” *European Physical Journal C*, vol. 81, no. 981, p. 1, 2021.
- [257] K. Bamba, S. D. Odintsov, L. Sebastiani, and S. Zerbini, “Finite-time future singularities in modified Gauss–Bonnet and $f(R, \mathcal{G})$ -gravity and singularity avoidance,” *European Physical Journal C*, vol. 67, p. 295, 2010.
- [258] K. Bamba, M. Ilyas, M. Z. Bhatti, and Z. Yousaf, “Energy conditions in modified $f(\mathcal{G})$ gravity,” *General Relativity and Gravitation*, vol. 49, p. 112, 2017.
- [259] C. Brans and R. H. Dicke, “Mach’s principle and a relativistic theory of gravitation,” *Physical review*, vol. 124, p. 925, 1961.
- [260] B. Boisseau, G. Esposito-Farese, D. Polarski, and A. A. Starobinsky, “Reconstruction of a scalar-tensor theory of gravity in an accelerating universe,” *Physical Review Letters*, vol. 85, p. 2236, 2000.
- [261] J. W. Maluf, “The teleparallel equivalent of general relativity,” *Ann. Phys.*, vol. 525, p. 339, 2013.
- [262] R. Aldrovandi and J. G. Pereira, “*Teleparallel gravity: an introduction*”, vol. 173. Springer Science & Business Media, 2012.
- [263] G. R. Bengochea and R. Ferraro, “Dark torsion as the cosmic speed-up,” *Phys. Rev. D*, vol. 79, p. 124019, 2009.

- [264] E. V. Linder, “Einstein’s other gravity and the acceleration of the universe,” *Phys. Rev. D*, vol. 81, p. 127301, 2010.
- [265] J. B. Jimenez, L. Heisenberg, and T. Koivisto, “Coincident general relativity,” *Phys. Rev. D*, vol. 98, p. 044048, 2018.
- [266] J. M. Nester and H. J. Yo, “Symmetric teleparallel general relativity,” *Chinese Journal of Physics*, vol. 37, p. 113, 1999.
- [267] R. Lazkoz, F. S. N. Lobo, M. O. Baños, and V. Salzano, “Observational constraints of $f(Q)$ gravity,” *Physical Review D*, vol. 100, no. 10, p. 104027, 2019.
- [268] L. Järv, M. Rünkla, M. Saal, and O. Vilson, “Nonmetricity formulation of general relativity and its scalar–tensor extension,” *Physical Review D*, vol. 97, p. 124025, 2018.
- [269] J. B. Jiménez, L. Heisenberg, T. S. Koivisto, and S. Pekar, “Cosmology in $f(Q)$ geometry,” *Physical Review D*, vol. 101, p. 103507, 2020.
- [270] J. W. Maluf, “The teleparallel equivalent of general relativity,” *Annalen der Physik*, vol. 525, p. 339, 2013.
- [271] S. Arora and P. K. Sahoo, “Energy conditions in $f(Q, T)$ gravity,” *Physica Scripta*, vol. 95, no. 9, p. 095003, 2020.
- [272] S. A. Narawade, M. Koussour, and B. Mishra, “Constrained $f(Q, T)$ gravity accelerating cosmological model and its dynamical system analysis,” *Nuclear Physics B*, vol. 992, p. 116233, 2023.
- [273] V. Sahni, “The cosmological constant problem and quintessence,” *Classical and Quantum Gravity*, vol. 19, p. 3435, 2002.
- [274] S. Hellerman, N. Kaloper, and L. Susskind, “String theory and quintessence,” *Journal of High Energy Physics*, vol. 2001, p. 003, 2001.
- [275] W. Fischler, A. Kashani-Poor, R. McNees, and S. Paban, “The acceleration of the universe, a challenge for string theory,” *Journal of High Energy Physics*, vol. 2001, p. 003, 2001.

- [276] P. J. Steinhardt, “Quintessential cosmology and cosmic acceleration.” <http://feynman.princeton.edu/steinh/>. Accessed June 2025.
- [277] J. D. Barrow, R. Bean, and J. Magueijo, “Can the universe escape eternal acceleration?,” *Monthly Notices of the Royal Astronomical Society*, vol. 316, p. L41, 2000.
- [278] S. Nojiri, S. D. Odintsov, and S. Tsujikawa, “Properties of singularities in (phantom) dark energy universe,” *Physical Review D*, vol. 71, p. 063004, 2005.
- [279] J. D. Barrow, “More general sudden singularities,” *Classical and Quantum Gravity*, vol. 21, p. 5619, 2004.
- [280] J. D. Barrow, “Sudden future singularities,” *Classical and Quantum Gravity*, vol. 21, p. L79, 2004.
- [281] S. Nesseris and L. Perivolaropoulos, “Fate of bound systems in phantom and quintessence cosmologies,” *Physical Review D*, vol. 70, p. 123529, 2004.
- [282] M. Bouhmadi-López, A. Errahmani, P. Martín-Moruno, T. Ouali, and Y. Tavakoli, “The little sibling of the big rip singularity,” *International Journal of Modern Physics D*, vol. 24, p. 1550078, 2015.
- [283] S. Nojiri and S. D. Odintsov, “The final state and thermodynamics of dark energy universe,” *Physical Review D*, vol. 70, p. 103522, 2004.
- [284] Y. Shtanov and V. Sahni, “Unusual cosmological singularities in brane world models,” *Classical and Quantum Gravity*, vol. 19, p. L101, 2002.
- [285] M. Sami, P. Singh, and S. Tsujikawa, “Avoidance of future singularities in loop quantum cosmology,” *Phys. Rev. D*, vol. 74, p. 043514, 2006.
- [286] E. Elizalde, S. Nojiri, S. D. Odintsov, D. Saez-Gomez, and V. Faraoni, “Reconstructing the universe history, from inflation to acceleration, with phantom and canonical scalar fields,” *Phys. Rev. D*, vol. 77, p. 106005, 2008.
- [287] S. Capozziello, S. Nojiri, and S. D. Odintsov, “Unified phantom cosmology: inflation, dark energy and dark matter under the same standard,” *Phys. Lett. B*, vol. 632, p. 597, 2006.

- [288] M. Belkacemi, M. Bouhmadi-López, A. Errahmani, and T. Ouali, “The holographic induced gravity model with a Ricci dark energy: smoothing the little rip and big rip through Gauss-Bonnet effects,” *Physical Review D*, vol. 85, p. 083503, 2012.
- [289] A. Sheykhi, M. Tavayef, and H. Moradpour, “Revisiting holographic dark energy in cyclic cosmology,” *Canadian Journal of Physics*, vol. 96, p. 1034, 2018.
- [290] K. Bamba, S. Nojiri, and S. D. Odintsov, “Dark energy cosmology: the equivalent description via different theoretical models and cosmography tests,” *Astrophys. Space Sci.*, vol. 342, p. 155, 2012.
- [291] S. Capozziello, M. D. Laurentis, S. Nojiri, and S. D. Odintsov, “Classifying and avoiding singularities in the alternative gravity dark energy models,” *Physical Review D*, vol. 79, p. 124007, 2009.
- [292] K. Bamba, S. D. Odintsov, L. Sebastiani, and S. Zerbini, “Finite-time future singularities in modified Gauss-Bonnet and $F(R, \mathcal{G})$ gravity and singularity avoidance,” *European Physical Journal C*, vol. 67, p. 295, 2010.
- [293] R. Tavakol, “Introduction to dynamical systems,” in *Dynamical Systems in Cosmology* (J. Wainwright and G. F. R. Ellis, eds.), p. 84, Cambridge University Press, 2009.
- [294] C. B. Collins and J. M. Stewart, “Qualitative cosmology,” *Mon. Not. Roy. Astron. Soc.*, vol. 153, p. 419, 1971.
- [295] C. G. Hewitt and J. Wainwright, “Qualitative analysis of a class of inhomogeneous selfsimilar cosmological models,” *Class. Quant. Grav.*, vol. 5, p. 1313, 1988.
- [296] O. I. Bogoyavlensky, “*Methods in the Qualitative Theory of Dynamical Systems in Astrophysics and Gas Dynamics*”. Springer-Verlag, 1985.
- [297] J. Wainwright and G. F. R. Ellis, eds., “*Dynamical Systems in Cosmology*”. Cambridge University Press, 1997.

-
- [298] L. Hsu and J. Wainwright, “Self similar spatially homogeneous cosmologies: Orthogonal perfect fluid and vacuum solutions,” *Class. Quant. Grav.*, vol. 3, p. 1105, 1986.
- [299] A. A. Coley, “*Dynamical Systems and Cosmology*”. Kluwer Academic Publishers, 2003.
- [300] S. Bahamonde, C. G. Böhm, S. Carloni, E. J. Copeland, W. Fang, and N. Tamanini, “Dynamical systems applied to cosmology: Dark energy and modified gravity,” *Physics Reports*, vol. 775, p. 1, 2018.
- [301] D. K. Arrowsmith and C. M. Place, “*An Introduction to Dynamical Systems*”. Cambridge University Press, 1990.
- [302] L. Perko, “*Differential Equations and Dynamical Systems*”, vol. 7 of *Texts in Applied Mathematics*. Springer, 2001.
- [303] S. Wiggins, “*Introduction to Applied Nonlinear Dynamical Systems and Chaos*”. Springer, 2nd ed., 2003.
- [304] D. M. Grobman, “Homeomorphisms of systems of differential equations,” *Doklady Akademii Nauk SSSR*, vol. 128, p. 880, 1959.
- [305] P. Hartman, “A lemma in the theory of structural stability of differential equations,” *Proceedings of the American Mathematical Society*, vol. 11, p. 610, 1960.
- [306] A. M. Lyapunov, “*The General Problem of the Stability of Motion*”. London: Taylor & Francis, 1992. Translated by A. T. Fuller. Originally published in Russian in 1892 as *Obshchaya zadacha ob ustoichivosti dvizheniya*.
- [307] J. Carr, “*Applications of Centre Manifold Theory*”, vol. 35 of *Applied Mathematical Sciences*. New York: Springer, 1981.
- [308] H. Poincaré, “Mémoire sur les courbes définies par une équation différentielle (deuxième partie),” *Journal de Mathématiques Pures et Appliquées*, vol. 8, p. 251, 1882.
- [309] I. O. Bendixson, “Sur les courbes définies par des équations différentielles,” *Acta Mathematica*, vol. 24, no. 1, p. 1, 1901.

- [310] G. D. Birkhoff, “*Dynamical Systems*”. Colloquium Publications, Vol. 9, New York: American Mathematical Society, 1927.
- [311] J. Guckenheimer and P. Holmes, “*Nonlinear Oscillations, Dynamical Systems, and Bifurcations of Vector Fields*”, vol. 42 of *Applied Mathematical Sciences*. Springer-Verlag, 1983.
- [312] J. P. LaSalle, “Some extensions of liapunov’s second method,” *IRE Transactions on Circuit Theory*, vol. 7, no. 4, p. 520, 1960.
- [313] A. G. Riess, L.-G. Strolger, J. Tonry, *et al.*, “Type Ia Supernova Discoveries at $z > 1$ from the Hubble Space Telescope: Evidence for past deceleration and constraints on dark energy evolution,” *Astrophysical Journal*, vol. 607, p. 665, 2004.
- [314] E. Komatsu, K. M. Smith, J. Dunkley, C. L. Bennett, B. Gold, *et al.*, “Seven year wilkinson microwave anisotropy probe (WMAP) observations: Cosmological interpretation,” *The Astrophysical Journal Supplement Series*, vol. 192, no. 2, p. 18, 2011.
- [315] M. Kowalski, D. Rubin, G. Aldering, R. J. Agostinho, A. Amadon, *et al.*, “Improved cosmological constraints from new, old, and combined supernova data sets,” *The Astrophysical Journal*, vol. 686, no. 2, p. 749, 2008.
- [316] M. A. K. Gross, R. S. Somerville, J. R. Primack, J. Holtzman, and A. Klypin, “Cold dark matter variant cosmological models — I. Simulations and preliminary comparisons,” *Monthly Notices of the Royal Astronomical Society*, vol. 301, no. 1, p. 81, 1998.
- [317] P. J. E. Peebles, “Tests of cosmological models constrained by inflation,” *The Astrophysical Journal*, vol. 284, p. 439, 1984.
- [318] A. Blanchard, J. Héloret, S. Ilić, B. Lamine, and I. Tutusaus, “ Λ CDM is alive and well,” *Open Journal of Astrophysics*, vol. 7, 2024.
- [319] L. Lombriser, “On the cosmological constant problem,” *Physics Letters B*, vol. 797, p. 134804, 2019.

-
- [320] A. Silvestri and M. Trodden, “Approaches to understanding cosmic acceleration,” *Reports on Progress in Physics*, vol. 72, no. 9, p. 096901, 2009.
- [321] S. Basilakos, D. Polarski, and J. Solà, “Generalizing the running vacuum energy model and comparing with the entropic-force models,” *Physical Review D*, vol. 86, p. 043010, 2012.
- [322] J. Solà, A. Gómez-Valent, and J. de Cruz Pérez, “Hints of dynamical vacuum energy in the expanding universe,” *The Astrophysical Journal Letters*, vol. 811, no. 1, p. L14, 2015.
- [323] G. Aldering, W. Althouse, R. Amanullah, J. Annis, P. Astier, *et al.*, “Supernova / acceleration probe: A satellite experiment to study the nature of the dark energy,” *arXiv preprint astro-ph/0405232*, 2004.
- [324] B. Guberina, R. Horvat, and H. Nikolić, “Dynamical dark energy with a constant vacuum energy density,” *Physics Letters B*, vol. 636, p. 80, 2006.
- [325] S. Nojiri and S. D. Odintsov, “The new form of the equation of state for dark energy fluid and accelerating universe,” *Physics Letters B*, vol. 639, p. 144, 2006.
- [326] F. Melia, “The cosmic equation of state,” *Astrophysics & Space Science*, vol. 356, p. 393, 2015.
- [327] D. Bertacca, N. Bartolo, and S. Matarrese, “Unified dark matter scalar field models,” *Advances in Astronomy*, vol. 2010, p. 904379, 2010.
- [328] M. Baldi, V. Pettorino, G. Robbers, and V. Springel, “Hydrodynamical N-body simulations of coupled dark energy cosmologies,” *Monthly Notices of the Royal Astronomical Society*, vol. 403, p. 1684, 2010.
- [329] S. Chervon, I. Fomin, V. Yurov, and A. Yurov, “*Scalar Field Cosmology*”, vol. 13 of *Series on the Foundations of Natural Science and Technology*. World Scientific, 2019.
- [330] A. D. Rendall, “Dynamics of k-essence,” *Classical and Quantum Gravity*, vol. 23, p. 1557, 2006.

-
- [331] S. Nojiri and S. D. Odintsov, “Quantum escape of sudden future singularity,” *Physics Letters B*, vol. 595, p. 1, 2004.
- [332] J. de Haro, J. Amoros, and E. Elizalde, “Sudden singularities in semiclassical gravity,” *Physical Review D*, vol. 85, p. 123527, 2012.
- [333] A. Ashtekar, W. Kaminski, and J. Lewandowski, “Quantum field theory on a cosmological, quantum space-time,” *Physical Review D*, vol. 79, p. 064030, 2009.
- [334] H. Calderon and W. A. Hiscock, “Quantum fields and “Big Rip” expansion singularities,” *Classical and Quantum Gravity*, vol. 22, p. L23, 2005.
- [335] B. S. DeWitt, “Quantum Theory of Gravity. I. The Canonical Theory,” *Physical Review*, vol. 160, p. 1113, 1967.
- [336] J. Hwang and H. Noh, “Classical evolution and quantum generation in generalized gravity theories including string corrections and tachyon: Unified analyses,” *Physical Review D*, vol. 71, p. 063536, 2005.
- [337] J. de Haro, J. Amoros, and E. Elizalde, “Fate of the phantom dark energy universe in semiclassical gravity II: Scalar phantom fields,” *Physical Review D*, vol. 86, p. 083528, 2012.
- [338] J. Oppenheim, “A post quantum theory of classical gravity,” *Physical Review X*, vol. 13, p. 041040, 2023.
- [339] L. H. Ford, “Quantum vacuum energy in a closed universe,” *Physical Review D*, vol. 14, p. 3304, 1976.
- [340] M. J. S. Houndjo, “Conformal anomaly around the sudden singularity,” *Europhysics Letters*, vol. 92, p. 10004, 2010.
- [341] T. S. Bunch and P. C. W. Davies, “Stress tensor and conformal anomalies for massless fields in a Robertson-Walker universe,” *Proceedings of the Royal Society of London. Series A, Mathematical and Physical Sciences*, vol. 356, p. 569, 1977.

-
- [342] M. Alves and J. Barcelos-Neto, “On the trace anomaly and the energy-momentum conservation of quantum fields at $d=2$ in classical curved backgrounds,” *Brazilian Journal of Physics*, vol. 34, p. 531, 2004.
- [343] C. Barcelo and M. Visser, “Traversable wormholes from massless conformally coupled scalar fields,” *Physics Letters B*, vol. 466, p. 127, 1999.
- [344] B. C. Xanthopoulos and T. E. Dialynas, “Einstein gravity coupled to a massless conformal scalar field in arbitrary space-time dimensions,” *Journal of Mathematical Physics*, vol. 33, p. 1463, 1992.
- [345] T. S. Bunch, “Stress tensor of massless conformal quantum fields in hyperbolic universes,” *Physical Review D*, vol. 18, p. 1844, 1978.
- [346] P. C. W. Davies, “Singularity avoidance and quantum conformal anomalies,” *Physics Letters B*, vol. 68, p. 402, 1977.
- [347] J. Haro and J. Amorós, “Comment on effects of quantized scalar fields in cosmological spacetimes with big rip singularities,” *Physical Review D*, vol. 84, p. 048501, 2011.
- [348] J. Haro, “Can quantum effects due to a massless conformally coupled field avoid gravitational singularities,” *Theoretical and Mathematical Physics*, vol. 171, p. 563, 2012.
- [349] J. Haro, S. Nojiri, S. D. Odintsov, V. K. Oikonomou, and S. Pan, “Finite-time cosmological singularities and the possible fate of the universe,” *Physics Reports*, vol. 1034, p. 1, 2023.
- [350] F. S. N. Lobo, “The dark side of gravity: Modified theories of gravity,” in *Dark Energy - Current Advances* (R. C. Jr., ed.), p. 173, Research Signpost, 2009.
- [351] S. Capozziello and M. Francaviglia, “Extended theories of gravity and their cosmological and astrophysical applications,” *Gen. Relativ. Gravit.*, vol. 40, p. 357, 2008.
- [352] S. Capozziello and M. D. Laurentis, “Extended theories of gravity,” *Physics Reports*, vol. 509, p. 167, 2011.

- [353] H. I. Arcos and J. G. Pereira, “Torsion gravity: a reappraisal,” *Int. J. Mod. Phys. D*, vol. 13, p. 2193, 2004.
- [354] P. Astier, J. Guy, N. Regnault, R. Pain, E. Aubourg, D. Balam, *et al.*, “The supernova legacy survey: Measurement of Ω_M , Ω_Λ and w from the first year data set,” *Astronomy & Astrophysics*, vol. 447, p. 31, 2006.
- [355] R. M. Wald, “*General Relativity*”. University of Chicago Press, 1984.
- [356] C. G. Böhmmer and E. Jensko, “Modified gravity: A unified approach,” *Physical Review D*, vol. 104, p. 024010, 2021.
- [357] C. P. Singh and V. Singh, “Reconstruction of modified $f(R,T)$ gravity with perfect fluid cosmological models,” *General Relativity and Gravitation*, vol. 46, no. 9, p. 1696, 2014.
- [358] S. Carloni, F. S. N. Lobo, G. Otalora, and E. N. Saridakis, “Dynamical system analysis for a nonminimal torsion-matter coupled gravity,” *Physical Review D*, vol. 93, no. 2, p. 024034, 2016.
- [359] L. P. Chimento and A. Feinstein, “Power-law expansion in k-essence cosmology,” *Modern Physics Letters A*, vol. 19, no. 10, p. 761, 2004.
- [360] V. Sahni, T. D. Saini, A. A. Starobinsky, and U. Alam, “Statefinder – a new geometrical diagnostic of dark energy,” *JETP Letters*, vol. 77, p. 201, 2003.
- [361] V. Sahni, “Dark matter and dark energy,” in *The Physics of the Early Universe* (E. Papantonopoulos, ed.), p. 141, Springer, 2005.
- [362] G. Jungman, M. Kamionkowski, and K. Griest, “Supersymmetric dark matter,” *Physics Reports*, vol. 267, p. 195, 1996.
- [363] I. Zlatev, L. Wang, and P. J. Steinhardt, “Quintessence, cosmic coincidence, and the cosmological constant,” *Physical Review Letters*, vol. 82, p. 896, 1999.
- [364] N. Mahata and S. Chakraborty, “Dynamical system analysis for a phantom model,” *General Relativity and Gravitation*, vol. 46, no. 5, p. 1721, 2014.
- [365] A. Mussatayeva, N. Myrzakulov, and M. Koussour, “Cosmological constraints on dark energy in $f(Q)$ gravity: A parametrized perspective,” *Physics of the Dark Universe*, vol. 42, p. 101276, 2023.

- [366] N. Myrzakulov, M. Koussour, and D. J. Gogoi, “A new $f(Q)$ cosmological model with $H(z)$ quadratic expansion,” *Physics of the Dark Universe*, vol. 42, p. 101268, 2023.
- [367] I. S. Albuquerque and N. Frusciante, “A designer approach to $f(Q)$ gravity and cosmological implications,” *Physics of the Dark Universe*, vol. 35, p. 100980, 2022.
- [368] H. Shabani, A. De, and T. H. Loo, “Phase space analysis of a novel cosmological model in $f(Q)$ theory,” *European Physical Journal C*, vol. 83, p. 535, 2023.
- [369] S. A. Narawade, S. P. Singh, and B. Mishra, “Accelerating cosmological models in $f(Q)$ gravity and the phase space analysis,” *Physics of the Dark Universe*, vol. 42, p. 101282, 2023.
- [370] M. Adak and Ö. Sert, “A solution to symmetric teleparallel gravity,” *Turkish Journal of Physics*, vol. 29, p. 1, 2005.
- [371] K. Flathmann and M. Hohmann, “Post-Newtonian limit of generalized symmetric teleparallel gravity,” *Physical Review D*, vol. 103, p. 044030, 2021.
- [372] R. Ferraro and F. Fiorini, “Modified teleparallel gravity: Inflation without inflaton,” *Physical Review D*, vol. 75, p. 084031, 2007.
- [373] S. A. Narawade, L. Pati, B. Mishra, and S. K. Tripathy, “Dynamical system analysis for accelerating models in non-metricity $f(Q)$ gravity,” *Physics of the Dark Universe*, vol. 36, p. 101020, 2022.
- [374] I. Mol, “The Non-metricity Formulation of General Relativity,” *Advances in Applied Clifford Algebras*, vol. 27, p. 2607, 2017.
- [375] D. M. Scolnic, D. O. Jones, A. Rest, Y. C. Pan, R. Chornock, *et al.*, “The Complete Light-curve Sample of Spectroscopically Confirmed SNe Ia from Pan-STARRS1 and Cosmological Constraints from the Combined Pantheon Sample,” *The Astrophysical Journal*, vol. 859, p. 101, 2018.
- [376] S. Alam, M. Ata, S. Bailey, F. Beutler, D. Bizyaev, *et al.*, “The clustering of galaxies in the completed SDSS-III Baryon Oscillation Spectroscopic Survey:

- Cosmological analysis of the DR12 galaxy sample,” *Monthly Notices of the Royal Astronomical Society*, vol. 470, no. 3, p. 2617, 2017.
- [377] T. M. C. Abbott, S. Allam, P. Andersen, C. Angus, J. Asorey, *et al.*, “First Cosmology Results using Type Ia Supernovae from the Dark Energy Survey: Constraints on Cosmological Parameters,” *The Astrophysical Journal Letters*, vol. 872, p. L30, 2019.
- [378] S. Alam, F. D. Albareti, C. A. Prieto, F. Anders, S. F. Anderson, *et al.*, “The Eleventh and Twelfth Data Releases of the Sloan Digital Sky Survey: Final Data from SDSS-III,” *The Astrophysical Journal Supplement Series*, vol. 219, p. 12, 2015.
- [379] H. F. M. Goenner, “Theories of gravitation with nonminimal coupling of matter and the gravitational field,” *Foundations of Physics*, vol. 14, p. 9, 1984.
- [380] D. Camarena and V. Marra, “Local determination of the hubble constant and the deceleration parameter,” *Physical Review Research*, vol. 2, p. 013028, 2020.
- [381] Y. Li, S. Wang, X. Li, and X. Zhang, “Holographic dark energy in a universe with spatial curvature and massive neutrinos: a full markov chain monte carlo exploration,” *Journal of Cosmology and Astroparticle Physics*, vol. 2013, p. 033, 2013.
- [382] S. del Campo, J. C. Fabris, R. Herrera, and W. Zimdahl, “On holographic dark-energy models,” *Journal of Cosmology and Astroparticle Physics*, vol. 2011, no. 03, p. 006, 2011.
- [383] S. Pourojaghi and M. Malekjani, “A new comparison between holographic dark energy and standard Λ -cosmology in the context of cosmography method,” *European Physical Journal C*, vol. 81, p. 575, 2021.
- [384] E.-K. Li, K. Zhang, and J.-L. Geng, “Generalized holographic Ricci dark energy and generalized second law of thermodynamics in Bianchi Type I universe,” *General Relativity and Gravitation*, vol. 47, no. 7, p. 1, 2015.
- [385] S. Maity and U. Debnath, “Tsallis, Rényi and Sharma–Mittal holographic and new agegraphic dark energy models in d-dimensional fractal universe,” *The European Physical Journal Plus*, vol. 134, p. 514, 2019.

-
- [386] A. Jawad, K. Bamba, M. Younas, S. Qummer, and S. Rani, “Tsallis, Rényi and Sharma–Mittal holographic dark energy models in loop quantum cosmology,” *Symmetry*, vol. 10, p. 635, 2018.
- [387] V. C. Dubey, U. K. Sharma, and A. A. Mamon, “Interacting Rényi holographic dark energy in the Brans–Dicke Theory,” *Advances in High Energy Physics*, vol. 2021, p. 6658862, 2021.
- [388] U. Y. D. Prasanthi and Y. Aditya, “Anisotropic Rényi holographic dark energy models in general relativity,” *Results in Physics*, vol. 17, p. 103101, 2020.
- [389] M. Vijaya Santhi and T. Chinnappalanaidu, “Rényi Holographic Dark Energy Model in a Scalar–Tensor Theory,” *New Astronomy*, vol. 92, p. 101725, 2022.
- [390] B. Jain and J. Khoury, “Cosmological tests of gravity,” *Annals of Physics*, vol. 325, no. 7, p. 1479, 2010.
- [391] C. M. Will, “The confrontation between general relativity and experiment,” *Living Reviews in Relativity*, vol. 17, no. 1, p. 4, 2014.
- [392] T. Clifton, P. G. Ferreira, A. Padilla, and C. Skordis, “Modified gravity and cosmology,” *Physics Reports*, vol. 513, no. 1-3, p. 1, 2012.